INVESTIGATING THE RE-USABILITY CHARACTERISTICS AND LIMITS OF POLYPROPYLENE POWDER IN LASER SINTER ADDITIVE MANUFACTURING

by

Fredrick Mulinge Mwania

Dissertation submitted in fulfilment of the requirements for the degree

MASTER OF ENGINEERING

in

MECHANICAL ENGINEERING

in the

Department of Mechanical and Mechatronics Engineering

Faculty of Engineering, Built Environment, and Information Technology

at

Central University of Technology, Free State

BLOEMFONTEIN

2021

Supervisor: Dr. Maina Maringa, Ph.D.

Co-supervisor: Dr. Kobus van der Walt, D.Tech.

DECLARATION OF INDEPENDENT WORK

DECLARATION WITH REGARD TO INDEPENDENT WORK

I, FREDRICK MULINGE MWANIA, Passport number and student number , do hereby declare that this research project submitted to Central University of Technology, Free State for the degree MASTER OF ENGINEERING IN MECHANICAL ENGINEERING is my own independent work; and complies with the Code of Academic Integrity, as well as other relevant policies, procedures, rules and regulations of Central University of Technology, Free State; and has not been submitted before to any institution by myself of any other person in fulfilment (or partial fulfilment) of the requirements for the attainment of any qualification.

27/02/2021

SIGNATURE OF THE STUDENT **DATE**

ABSTRACT

The aim of this research was to investigate the re-usability characteristics and limits of polypropylene (PP) powder in laser sinter additive manufacturing (AM). Initially, the objective was to analyse Laser PP CP 60 from Diamond Plastics GmbH, and preliminary work was carried out on it, but the focus eventually turned to Laser PP CP 75 after processing difficulties were experienced with the former material. Polymer laser sintering (LS) subjects feed powders to high temperatures, leading to degradation of their thermal, rheological, and physical properties, impeding their recyclability. Therefore, it is imperative to examine the degree of deterioration or aging of polymers before re-using the materials. The recyclability of polymers is measured based on powder particle size, morphology, density, rheological properties, and thermal characteristics. Attempts were made to determine suitable processing parameters of Laser PP CP 60 polypropylene powder grade from Diamond Plastics in the first part of the analysis. This was followed by experiments to characterize the powder after a single print cycle to quantify degradation at this stage using scanning electron microscopy (SEM), differential scanning calorimetry (DSC), thermogravimetric analysis (TGA), and melt flow index testing (MFI). The focus was then turned to the recyclability of Laser PP CP 75 per print cycle by printing a set of test coupons at pre-determined positions in the build volume of an EOSINT P 380 LS machine. The powder remaining in the machine and the cake powder surrounding the coupons after each print cycle was thoroughly mixed using a concrete mixer for about 30 minutes. A sample of the mixed powder was re-introduced into the P 380 machine to print another set of test specimens. In this study, the re-usability of the PP powder was determined by characterizing and comparing the used powder after each cycle with powder from previous cycles and fresh material.

It was established from the preliminary testing of Laser PP CP 60 that slightly different process parameter settings were required to those provided by the supplier to achieve the highest ultimate tensile strength, smoothest surface, and best dimensional accuracy of printed parts. The three characterized batches of Laser PP CP 60 powder (virgin, aged, virgin-aged mixture) exhibited poor (not 100% spherical) but acceptable morphology and particle size distribution. It was also found that the sintering window of virgin Laser PP CP 60 increased significantly (by 28%) after a single cycle of printing, from a value of 21.04 ℃ for the virgin powder to 26.95 ℃ for the recycled powder. The degree of

crystallinity of virgin Laser PP CP 60 decreased from 13.92% to 12.12% after a single printing cycle and then increased to 12.48% after the addition of 50% virgin material. All the three batches, namely virgin powder, used powder, and a 50% virgin:50% used mixture, showed high degradation temperatures of 457.30 ℃, 456.05 ℃, and 455.95 ℃, respectively. Lastly, the three batches of powder showed low MFI values of 6.1, 6.5, and 6.4 g/10 min in the same order.

Turning to Laser PP CP 75, it was concluded that the powder could be re-used for four re-use cycles without having to mix with virgin material because it does not form an "orange peel," as is the case with polyamide-12 (PA 12) (used here as reference material). Besides, the MFI trend indicates that the viscosity of the material is not significantly degraded, which promotes recyclability. The DSC assessment established that the sintering window of Laser PP CP 75 increased with each re-use cycle. The results indicate that the shrinkage rate and curling of the material might reduce with the number of re-use cycles because a wide and sufficient sintering window prevents crystallization of the polymers during processing. From the TGA test, the breakdown temperature of Laser PP CP 75 was seen to increase slightly with the number of re-use cycles, from 455.53 ℃ (virgin material) to 457.53 ℃ after the 4th re-use cycle. Thus, the material does not break down at the temperatures prevailing during printing, making it suitable for LS processing and re-use. The SEM analysis revealed that the average size of Laser PP CP 75 powder particles is not significantly influenced by re-use cycles, making the powder recyclable. Furthermore, the powder did not exhibit signs of agglomeration for the 1st, 2nd, and 3rd re-use cycles. However, this phenomenon was observed in the 4th re-use cycle of printing. Lastly, tensile testing revealed that the material had the highest ultimate tensile strength after the 3rd printing cycle (7.4 MPa), after which the value decreased with recycling. Overall, it can be concluded that PP powder has superior recyclability properties to those of PA 12, which requires mixing with virgin material after every print cycle. Besides, the MFI, particle size and thermal properties are insignificantly altered, which does not hamper the re-use of the material for subsequent printing cycles. Parts printed with virgin Laser PP CP 75 had an average dimensional error of 3.02% and 4.06% after the 4th re-use cycle. Therefore, Laser PP CP 75 might not be commercially suitable because of dimensional accuracy and observed processing difficulties.

ACKNOWLEDGEMENTS

First of all, I thank the almighty God for His mercies. I would also like to extend my gratitude to my supervisors, Dr. Maina Maringa and Dr. Kobus van der Walt, for their steadfast guidance, support, encouragement, and unwavering patience. Their guidance was crucial to the completion of this project. I can truly say they have moulded me into a better researcher and a person. I also extend my gratitude to my family and friends who stood by me during the entire period of these studies. The financial support from the South African Research Chairs Initiative of the Department of Science and Innovation and National Research Foundation of South Africa (Grant № 97994) and the Collaborative Program in Additive Manufacturing (Contract № CSIR-NLC-CPAM-15-MOA-CUT-01) is gratefully acknowledged. Thanks to the Product Development and Technology Station (PDTS) and the Centre for Rapid Prototyping and Manufacturing (CRPM) at CUT for their technical support and the latter for its financial support. I would like to extend my gratitude to the Geology and Chemistry Departments (University of Free State) for their contribution in some of the experiments conducted during the studies.

DEDICATIONS

I dedicate this thesis to my father, mother, siblings, niece, extended family, and friends.

LIST OF PUBLICATIONS ARISING FROM THIS WORK

PEER-REVIEWED JOURNAL PAPERS:

1) Mwania, F. M., Maringa, M., & van der Walt, J. G. (2020). A Review of Methods Used to Reduce the Effects of High Temperature Associated with Polyamide 12 and Polypropylene Laser Sintering. *Advances in Polymer Technology*, *2020*(1), pp.1-11. https://www.hindawi.com/journals/apt/2020/9497158/
2) Mwania, F. M., Maringa, M., & van der Walt, J. G. (2020). Powder Characterization for a New Selective Laser Sintering Polypropylene Material (Laser PP CP 60) after Single Print Cycle Degradation. *International Journal of Engineering Research and Technology*, *13*(11), pp.3342-3358. http://www.irphouse.com/ijert20/ijertv13n11_33.pdf
3) Mwania, F. M., Maringa, M., & van der Walt, J. G. (2020). Mixing and Reuse of Polymer Laser Sintering Powders to Ensure Homogeneity – A Review. *International Journal of Engineering Research and Technology*, *13*(11), pp.3335-3341. http://www.irphouse.com/ijert20/ijertv13n11_32.pdf
4) Mwania, F. M., Maringa, M., & van der Walt, J. G. (2021). Preliminary Testing to Determine the Best Process Parameters for Polymer Laser Sintering of a New Polypropylene Polymeric Material. *Advances in Polymer Technology*, *2021*(1), pp.1-13. https://doi.org/10.1155/2021/667489.
5) Mwania, F. M., Maringa, M., & van der Walt, J. G. (2021). A Review of the Techniques Used to Characterize Laser Sintering of Polymeric Powders for Use and Re-use in Additive Manufacturing. *Manufacturing Review*, *8*(14), pp.1-17. http://dx.doi.org/10.1051/mfreview/2021012

Peer-reviewed Conference Papers:

1) Mwania, F. M., Maringa, M., & van der Walt, J. G. Recycling of Polypropylene Powder Used in Laser Sinter Additive Manufacturing – A Literature Review. *RAPDASA Conference, Emoya Estate, Bloemfontein, South Africa*, 20(1), pp.315-330. https://site.rapdasa.org/wp-content/uploads/2020/04/315-Mwania.pdf

Authored Book Chapters:

1) Fredrick M. Mwania, Maina Maringa, Kobus van der Walt. A Review of Methods Used to Reduce the Effects of High Temperature Associated with Polyamide 12 and Polypropylene Laser Sintering. In: Monica Trif, Alexandru Vasile Rusu, editors. *Prime Archives in Polymer Technology*. Hyderabad, India: Vide Leaf. 2020. https://videleaf.com/wp-content/uploads/2020/12/A-Review-of-Methods-Used-to-Reduce-the-Effects-of-High-Temperature-Associated-with-Polyamide-12-and-Polypropylene-Laser-Sintering.pdf

Read Conference Papers

1) Mwania, F. M., Maringa, M., & van der Walt, J. G. How 3D and 4D Manufacturing Technologies are Driving Societal Transformation Towards Improved Productivity and Efficiency. *1st Free State Joint Provincial Summit on the Industry 4.0 on the theme, Leveraging the Youth Dividend for the Social-Economic Advancement of the Free State, Free State Provincial Government and Central University of Technology, Bloemfontein, Free State*, 28th–29th November 2019. https://freestate4irsummMwania
2) Mwania, F. M., Maringa, M., & van der Walt, J. G. A review of Methods to Ameliorate the Effects of High Temperature on Polymers and in Particular Polypropylene in Laser Sinter Additive Manufacturing. *10th International Conference of the African Materials Research Society*, Arusha City, Tanzania, 10th–13th December 2019. https://africanmrs.net/tanzania-2019/

Pending Conference Paper

1) A conference paper submitted to RAPDASA 2021 Conference entitled, "Fractography of Polypropylene Laser Sintered Tensile Test Specimens." The paper has been accepted for presentation at the conference and recommended for possible publication in the *South African Journal of Industrial Engineers* (*SAJIE*).

Table of Contents

DECLARATION OF INDEPENDENT WORK ii
ABSTRACT iii
ACKNOWLEDGEMENTS v
DEDICATIONS vi
LIST OF PUBLICATIONS ARISING FROM THIS WORK vii
NOMENCLATURE AND ABBREVIATIONS xvii
CHAPTER 1 - INTRODUCTION 1
1.0 Background 1
1.1 Problem Statement 5
1.2 Aim of the Study 6
1.2.1 Objectives of the Study 6
1.3 Thesis Outline 7
CHAPTER 2 - LITERATURE REVIEW 8
2.0 Summary 8
2.1 POLYMERS 9
2.1.1 Identification and Classification of Polymers 10
2.1.1.1 Classification based on origin 11
2.1.1.2 Classification based on structure 12
2.1.1.3 Classification based on molecular forces 13
2.1.1.4 Classification based on the mode of polymerization 14
2.2 POLYPROPYLENE 15
2.2.1 Chemical Composition of Polypropylene 15
2.2.2 Production of Polypropylene 15
2.2.3 Physical Properties of Polypropylene 16
2.2.4 Uses of Polypropylene 18
2.3 ADDITIVE MANUFACTURING PROCESSES 18
2.3.1 Evolution of AM Technology 19
2.3.2 Classification of AM Processes 20
2.4 LASER SINTERING OF POLYMERS 21
2.4.1 Comparison between PP and PA 12 used in Laser-Sintering AM 23
2.4.2 Properties of Suitable Polymer Powders for Use in Laser Sintering 23
2.4.2.1 Particle size distribution and morphology 24
2.4.2.2 Thermal properties 25

2.4.2.3 Rheological properties 25
2.4.2.4 Optical properties 26
2.4.3 Process Parameters for Laser-Sintering Materials 26
2.4.4 The Effect of Heating on Polymers 28
2.4.4.1 Chemical deterioration of PA 12 and PP due to high temperatures 32
2.4.4.2 Deterioration of polymers due to high temperatures 33
2.4.5 Analysis of the Recycling of Polymeric Powders for AM 34
2.4.6 Mixing of Laser-Sintering Powders in Rotating Cylinders 36
2.4.6.1 Sampling and assessment of the homogeneity of mixed powder 37
2.4.6.2 Selection of a mixer for polymer laser sintering 38
2.4.7 Other Methods to Address the Effects of Heating on Polymer 40
2.4.7.1 Adding flow and antistatic agents 40
2.4.7.2 Low-temperature laser sintering 42
2.4.8 Techniques Employed to Characterize Laser-Sintering Polymers 44
2.4.8.1 Laser diffraction technique 44
2.4.8.2 Scanning electron microscopy 46
2.4.8.3 Gas pycnometry 47
2.4.8.4 Melt flow test 48
2.4.8.5 Differential scanning calorimetry and thermal gravimetric analysis 48
2.4.8.5.1 Differential scanning calorimetry 48
2.4.8.5.2 Thermogravimetric analysis 50
2.4.8.6 Characterization of the mechanical and surface properties 51
2.4.8.6.1 Elongation at break, tensile strength, and elastic modulus 51
2.4.8.6.2 Determination of surface roughness 53
2.4.8.7 Dynamic mechanical analyzer 55
2.4.8.8 Other tests 57
2.5 Conclusion 59
CHAPTER 3 - RESEARCH METHODOLOGY 60
3.0 RESEARCH FLOW 60
3.1 SUITABLE PROCESS PARAMETERS FOR LASER PP CP 60 61
3.1.1 Determining the Best Removal and Building Chamber Temperatures 62
3.1.2 Determining the Mechanical Properties of Built Parts 64
3.1.3 Determining the Physical Property of Surface Roughness 65
3.1.4 Determining the Dimensional Accuracy of the Printed Parts 66

3.2 CHARACTERIZATION OF LASER PP CP 60 AFTER SINGLE PRINT 67
3.2.1 Scanning Electron Microscopy 67
3.2.2 Differential Scanning Calorimetry Testing 68
3.2.3 Thermogravimetric Analysis 69
3.2.4 Melt Flow Index Testing 69
3.3 DETERMINING THE RECYCLABILITY OF LASER PP CP 75 70
CHAPTER 4 - RESULTS AND ANALYSIS 72
4.0 SUMMARY 72
4.1 SUITABLE PROCESS PARAMETERS FOR LASER PP CP 60 73
4.1.1 Determining the Best Building and Removal Chamber Temperatures 73
4.1.2 Mechanical Properties of Built Test Specimens 75
4.1.3 Surface Roughness of Built Test Specimens 79
4.1.4 Dimensional Accuracy of the Printed Parts 82
4.1.5 Further Testing to Optimize the Process Parameters of Laser PP CP 60 85
4.2 CHARACTERIZING LASER PP CP 60 AFTER SINGLE PRINT 88
4.2.1 Powder Morphology from the Results of Scanning Electron Microscopy 88
4.2.2 Distribution of Particle Sizes from the Results of SEM 92
4.2.3 Differential Scanning Calorimetry Testing 95
4.2.4 Thermogravimetric Analysis 100
4.2.5 Melt Flow Index Testing 102
4.3 Recyclability of Laser PP CP 75 powder 104
4.3.1 Physical Inspection 104
4.3.2 Characterization to Establish Recyclability of Laser PP CP 75 106
4.3.2.1 Melt flow testing of Laser PP CP 75 after 100% re-use 107
4.3.2.2 Results of DSC for Laser PP CP 75 after 100% re-use 109
4.3.2.3 Results of TGA for Laser PP CP 75 after 100% re-use 114
4.3.2.4 Results of SEM for Laser PP CP 75 after 100% re-use 115
4.3.3 Part Characterization to Establish Recyclability of Laser PP CP 75 118
4.3.3.1 Uniaxial tensile test for Laser PP CP 75 after 100% re-use 118
4.3.3.2 Dimensional accuracy of parts printed using Laser PP CP 75 122
CHAPTER 5 – CONCLUSION AND RECOMMENDATIONS 124
5.0 CONCLUSIONS 124
5.1 RECOMMENDATIONS 127

LIST OF FIGURES

Figure 1.1 Summary of the AM process (Ligon et al., 2017) 3
Figure 1.2 Selective laser sintering (Lambert, 2014) 4
Figure 2.1. Outline for chapter 2 8
Figure 2.2 Classification of polymers (Bassam, 2014) 11
Figure 2.3 Polymer classification based on structure (Polymerization, n.d.) 12
Figure 2.4 Chemical structure of polypropylene (Maddah, 2016) 15
Figure 2.5 Polypropylene manufacturing process (Langhauser et al., 1994) 16
Figure 2.6 Polymer laser-sintering materials (Schmid & Wegener, 2016) 22
Figure 2.7. Extrinsic and intrinsic properties of AM powders (Lanza, 2015) 24
Figure 2.8 Temperature deformability of polymers (Beyler & Hirschler, 2002) 28
Figure 2.9 Three-step thermal degradation process for polymers (Zeus, 2005) 29
Figure 2.10 The heating profile of polymers during LS (Drummer et al., 2019) 31
Figure 2.11 Recycling process of polymers in LS (Dotchev & Yusoff, 2009) 35
Figure 2.12 Flow chart for the selection of a mixer (Deveswaran et al., 2009) 38
Figure 2.13 Concrete mixer used at CRPM 39
Figure 2.14 Operating process of a tilting drum concrete mixer (Ferraris, 2001) 40
Figure 2.15 Dry particle coating process (Lexow & Drummer, 2016) 41
Figure 2.16 The effect of flow and antistatic agents (Lexow & Drummer, 2016) 42
Figure 2.17 Effect of low- and high-temperature LS (Kigure & Niino, 2017) 43
Figure 2.18 A rigid plate used in low-temperature LS (Kigure & Niino, 2017) 43
Figure 2.19 A beam striking a particle (Bodycomb, 2012) 44
Figure 2.20 Scanning electron microscope (Seyforth, 2015) 46
Figure 2.21 An extrusion plastometer (ISO, 2010) 48
Figure 2.22 A DSC experimental setup (Schick, 2009) 49
Figure 2.23 Typical example of a DSC result (Marin, 2017) 49
Figure 2.24 Experimental setup for TGA (Xi et al., 2004) 50
Figure 2.25 An example of TGA thermal curve (Xi et al., 2004) 51
Figure 2.26 A typical stress-strain curve (Tension Test, 2009) 52
Figure 2.27 Types of tensile test specimens (Tension Test, 2009) 52
Figure 2.28 Tensile testing machine (ASM, 2004) 53
Figure 2.29 Representation of surface roughness (Chapter 8, n.d.) 54
Figure 2.30 Schematic of a laser profilometer (Mital' et al., 2019) 54
Figure 2.31 A skid and stylus profilometer 55

Figure 2.32 An example of a DMA, model 242 EArtemis (Menard, 2015) 56
Figure 2.33 DMA sinusoidal stress and strain curves (Menard & Menard, 2015) 56
Figure 2.34 The transition points of a polymer from the DMA test (Elmer, 2012) 57
Figure 2.35 Molecular weight of fresh and aged PA 12 (Rüsenberg et al., 2012) 58
Figure 3.1. Research flow diagram 61
Figure 3.2 Test coupons to determine building and removal chamber temperatures ...63
Figure 3.3 Orientation of the labelled test specimens (ASTM D 638) 64
Figure 3.4 Standard tensile test specimen (ASTM D 638) (ASTM).....66
Figure 3.5 Carbon coater.....67
Figure 3.6 JEOL JSM-6610LV scanning electron microscope 68
Figure 3.7 Mettler Toledo DSC (821e/700) equipment 68
Figure 3.8 Mettler Toledo (TGA/SDTA851) TGA apparatus 69
Figure 3.9. MFI Tester from Ametex Ltd. 70
Figure 3.10 The set of test coupons at pre-determined positions 71
Figure 4.1. Flow diagram of results and analysis.....73
Figure 4.2 Printed parts showing minimal curling and dislodged components 74
Figure 4.3 Comparison of the elastic modulus for the printed specimens 77
Figure 4.4 Comparison of the percentage elongation % for the printed specimens 77
Figure 4.5 Comparison of the ultimate tensile strength for the printed specimens.....78
Figure 4.6 The mean arithmetic deviation (Ra) of the top surface of the specimens ...80
Figure 4.7 The mean arithmetic deviation (Ra) of the bottom surface 80
Figure 4.8 Partially baked cake powder (Laser PP CP 60).....87
Figure 4.9 Damaged edges of the test specimen printed using Laser PP CP 60.....87
Figure 4.10 Powder morphology of virgin Laser PP CP 60.....88
Figure 4.11 Powder morphology of used (1 cycle) Laser PP CP 60.....88
Figure 4.12 Powder morphology of used-virgin Laser PP CP 60 89
Figure 4.13 Ideally ordered and perfectly random mixtures (Poux et al., 1991) 90
Figure 4.14 An example of an ordered mixture (Saharan et al., 2008) 91
Figure 4.15 Distribution of particle sizes of the virgin Laser PP CP 60 93
Figure 4.16 Distribution of particle sizes of the used (1 cycle) Laser PP CP 60 94
Figure 4.17 Distribution of particle sizes of the used-virgin Laser PP CP 60.....94
Figure 4.18 DSC thermogram of the virgin powder 95
Figure 4.19 DSC thermogram of the used (1 cycle) powder.....96
Figure 4.20 DSC thermogram of the used-virgin powder mixture 96

Figure 4.21 Sintering windows for virgin, used, and used-virgin powders 98
Figure 4.22. Degree of crystallinity of the virgin, used, and used-virgin powders.....99
Figure 4.23 TGA thermogram of the virgin Laser PP CP 60.....100
Figure 4.24 TGA thermogram of the used (1 cycle) Laser PP CP 60.....101
Figure 4.25 TGA thermogram of the used-virgin Laser PP CP 60 mixture.....101
Figure 4.26 Degradation temperature of the virgin, used, and used-virgin powder..102
Figure 4.27 MFI of the virgin, used, and used-virgin mixture.....103
Figure 4.28 Test specimen printed with re-used Laser PP CP 75 (2nd cycle) 105
Figure 4.29 Test specimen printed with re-used Laser PP CP 75 (3rd cycle).....105
Figure 4.30 Test specimen printed with re-used Laser PP CP 75 (4th cycle).....106
Figure 4.31 Test specimen printed with re-used Laser PP CP 75 (5th cycle).....106
Figure 4.32 Trend of the MFI values for up to four re-use cycles 108
Figure 4.33 MFR of PA 12 with re-use cycles (Gornet et al., 2002) 109
Figure 4.34 Melting points of Laser PP CP 75 for a number of re-use cycles.....110
Figure 4.35 Melting points of PA 12 for 7-re-use cycles (Gornet et al., 2002) 111
Figure 4.36 Sintering window of Laser PP CP 75 versus re-use cycles 112
Figure 4.37 DSC thermogram for virgin, aged and mixed PA 12 powder.....113
Figure 4.38 Degradation temperature of Laser PP CP 75 versus re-use cycles 114
Figure 4.39. Powder morphology for Laser PP CP 75.....117
Figure 4.40 Ultimate tensile strengths of parts printed using Laser PP CP 75 118
Figure 4.41 Young's modulus of parts printed using Laser PP CP 75.....119
Figure 4.42 Percentage elongation at break of Laser PP CP 75 printed parts.....120
Figure 4.43 Effects of re-use cycles on the mechanical properties of PP 121
Figure 4.44 Average dimensional error for parts printed using Laser PP CP 75.....123

LIST OF TABLES

Table 2.1 IUPAC prefixes for organic compounds 10
Table 2.2 Physical properties of propylene (Maddah, 2016; Mark, 2007) 16
Table 2.3 Advantages and disadvantages of AM 19
Table 2.4 The historical background of AM (Bourell et al., 2009) 19
Table 2.5 Properties of PA 12 and PP (Fiedler et al., 2007) 23
Table 3.1 Determining the best removal and building chamber temperatures 63
Table 3.2 The process parameters used for different standard tensile specimens 65
Table 3.3 Dimensions of the standard tensile test specimen (ASTM D 638) 66
Table 3.4 Parameters for recyclability of Laser PP CP 75 71
Table 3.5 Mass of the cake, overflow and supply powders 71
Table 4.1 Observations for removal and building chamber temperature test 74
Table 4.2 Some mechanical properties of built test specimens 75
Table 4.3 Experimental and supplier's process parameters for Laser PP CP 60 79
Table 4.4 Surface roughness of built test specimens 79
Table 4.5 Best process parameters for Laser PP CP 60 based on surface roughness 81
Table 4.6 Length (*LO*) of the test specimens 82
Table 4.7 Width (*W*) of the gauge length of the test specimens 83
Table 4.8 Overall width (*WO*) of the test specimens 83
Table 4.9 Process parameters for Laser PP CP 60 based on dimensional accuracy 85
Table 4.10 Process and removal chamber temperatures for Laser PP CP 60 86
Table 4.11 Particle size distribution for the three batches of powders 92
Table 4.12 DSC results of virgin, used, and used-virgin mixture Laser PP CP 60 97
Table 4.13 Sintering window values for the different batches of Laser PP CP 60 98
Table 4.14 Degree of crystallization for the different batches of Laser PP CP 60 99
Table 4.15 Degradation temperature for the different batches of Laser PP CP 60 102
Table 4.16 MFI for the virgin, used, and used-virgin mixture 103
Table 4.17 MFI values for the five batches of powder considered in the analysis 107
Table 4.18 Changes in melting point of Laser PP CP 75 after four re-use cycles 110
Table 4.19 Calculated sintering window of Laser PP CP 75 after four re-use cycles 112
Table 4.20 TGA results for Laser PP CP 75 after 100% re-use 114
Table 4.21 Particle size distribution 115
Table 4.22 Ultimate tensile strength of printed parts after 100% re-use 118
Table 4.23 Young's modulus of printed parts after 100% re-use 119

Table 4.24 Percentage of elongation at break of printed parts after 100% re-use.....120
Table 4.25 Dimensional errors of LS printed parts 122

NOMENCLATURE AND ABBREVIATIONS

AM	Additive Manufacturing
SLS	Selective Laser Sintering
LS	Laser Sintering
2D	Two Dimensional
3D	Three Dimensional
PP	Polypropylene
PA 12	Polyamide 12
CAD	Computer-Aided Design
DP	Degree of Polymerization
DSC	Differential Scanning Calorimetry
SEM	Scanning Electron Microscopy
MFI	Melting Flow Index
MVR	Melt Volume Rate
PA 2200	Polyamide 2200
n.d.	Note Dated
℃	Degrees Celsius
µm	Micron
mm	Millimetre
mm/s	Millimetre per second
W	Watts

Min	Minute
g	Gram

CHAPTER 1 - INTRODUCTION

1.0 Background

Material science is an essential branch of the engineering discipline and entails the study of the properties of various materials that are used in engineering applications (Callister & Rethwisch, 2007). Engineers use the knowledge acquired in this field to determine the suitability of the materials used in different engineering applications. These materials include metals, wood, ceramics, composites, and polymers (Callister & Rethwisch, 2007). This study focused on polymers, and in particular polypropylene.

Polymers are extensively used to produce both engineering and other products for day-to-day use. These materials have a vast range of applications, such as in the development of packaging, building and construction, transportation, electrical and agricultural products. Their comprehensive utilization is based on their physical and chemical properties that can be tailored to a wide range of uses (Ebewele, 2000). The extensive applications of polymers create a need to study their properties and behaviour under different conditions.

Polymers are classified as either thermosetting or thermoplastic polymers (Bassam, 2014). Thermoplastics melt and become viscous when heated, whereas thermosets disintegrate (Gotro & Prime, 2002). Polypropylene (PP), the focus of this study, is a thermoplastic polymer made up of propylene monomers. It is one of the most commonly used polymers due to its excellent chemical and physical properties and affordability, and ease of manufacture (Vogl, 1999). PP, whose monomer is called propene, is a colourless, flammable, and odourless, gaseous hydrocarbon extracted from petroleum (Vogl, 1999). The polymer is produced through the addition polymerization of propene.

Polymer products can be processed either via conventional or additive manufacturing (AM) technologies. Conventional methods involve moulding and removal of material to make components. There are different traditional manufacturing methods for the development of components using thermoplastic and thermosetting polymers. The processes used to transform thermoplastics into finished products include extrusion, sintering, thermoforming, calendering, vacuum forming, and injection moulding, while thermosets are formed via compression, injection and transfer moulding processes (Ebewele, 2000; Kumar & Gupta, 2003).

On the other hand, additive manufacturing (AM) refers to producing parts by joining successive layers of a particular material using a bonding technique (Wong & Hernandez, 2012). It is a key component of the 4th industrial revolution (Dilberoglu et al., 2017). The method differs from the conventional processes in that it involves the addition of materials instead of removing materials that result in wastage. AM technology has become widespread due to its ability for mass customization of products, as well as the ability to develop complex components at zero or little additional cost (Wong & Hernandez, 2012). The technology is so versatile that the complexity of the products manufactured through the technology is only limited by imagination. Additive manufacturing was referred to as rapid prototyping because the technology was initially used to develop prototypes. However, it has gradually matured and is presently capable of printing functional parts. The technology was invented in the 1980s and has continued to grow through the introduction of new manufacturing techniques and materials (Matos et al., 2019). Furthermore, 3D printing techniques have today metamorphosed into 4D printing. The 4D printing technology involves the use of smart materials, that is, materials that respond to stimuli such as temperature, humidity, pressure, light, or pH (Dilberoglu et al., 2017).

Additive manufacturing is considered a major component of the fourth industry revolution due to its ability to manufacture intricate and customized products. However, the shift from conventional manufacturing to AM has been limited by amongst other factors, low manufacturing speeds and high production costs (Dilberoglu et al., 2017). Therefore, AM can be made a manufacturing method of choice in the future by introducing some improvements. One of the improvements proposed by Dilberoglu et al. (2017), is the decentralization of work through distribution of workload to different workshops or machines by use of cloud services. This process will allow some processes to be undertaken in tandem and in turn reduce manufacturing time. Another possible future trend for AM is reduction of waste resources and energy by implementing the just-in-time manufacturing technique. Other forecasted prospects for AM include transformative and innovative products, such as, clothes that adapt to weather changes, furniture that will be able to self-assemble and disassemble, pipes that alter shape based on the flow, and biomimicry devices that adapt to growth and disintegrate when they are no longer in use (4D printing, n.d).

The AM processes commence by developing product ideas that are then transformed into digital data using computer-aided design (CAD) software or 3D scanning. The digital information is then sliced into layered data, the support structures are adjusted, and the manufacturing path planned. The layered data is then transferred to a 3D printer where the parts are printed (Ligon et al., 2017). Lastly, post-processing is done to remove support structures, improve the surface finish or modify the mechanical properties of the components (Ligon et al., 2017). The process of AM is described in Figure 1.1.

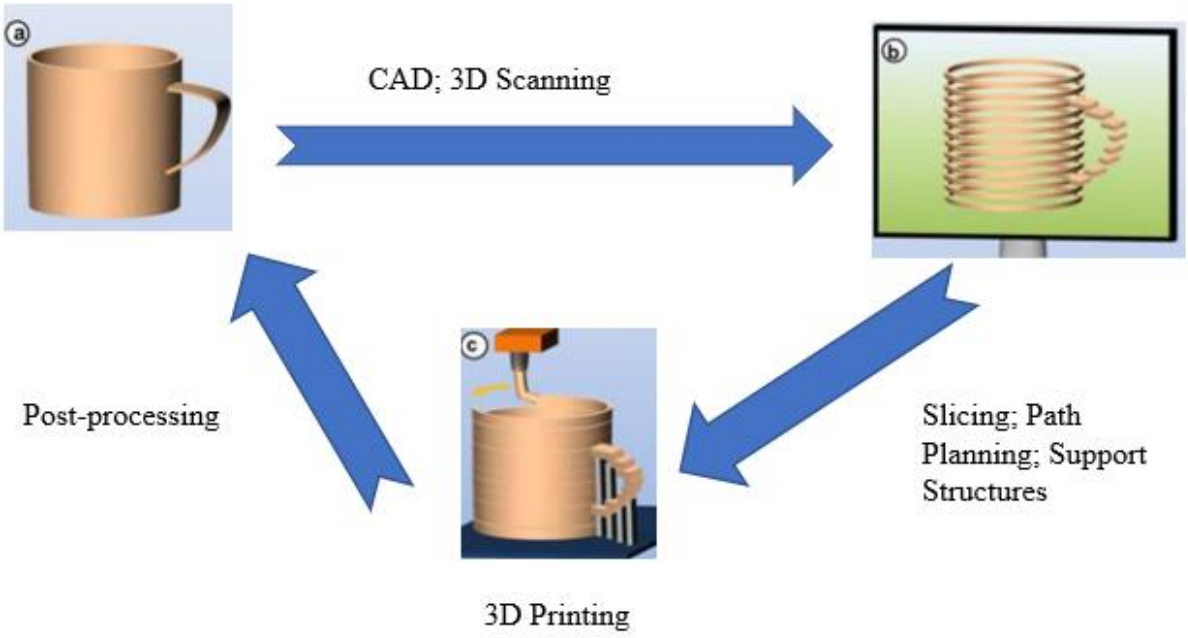

Figure 1.1 Summary of the AM process (Ligon et al., 2017)

AM processes have evolved over the years from merely being used for prototyping components to the manufacturing of functional parts with complex geometries that are impossible to produce using conventional manufacturing methods (Goodridge et al., 2012; Wong & Hernandez, 2012). Currently, AM processes are used to develop products in many sectors, including but not limited to aerospace, medical and bio-medical, automotive, sports and leisure, and architecture. AM technologies include selective laser sintering, fused deposition modelling, solid ground curing, stereolithography, laminated object manufacturing, and foil polymerization (Wong & Hernandez, 2012; Berman, 2012).

Selective laser sintering (SLS) is one of the major AM technologies (Goodridge et al., 2012; Wudy et al., 2014). The process involves fusing powder by means of ultraviolet or carbon dioxide laser beams (Goodridge et al., 2012; Wudy et al., 2014). The choice of the

laser beam is a function of the material being processed. The process is referred to as laser sintering (LS) when applied to polymeric materials (Bourell et al., 2014). The LS process starts by heating the build chamber to a temperature just below the melting point of the material being processed for semi-crystalline polymers. Prior to this, the powder particles are prepared using the ball milling technique, amongst other methods, to break the powder particles into smaller sizes (Goodridge et al., 2012; Wudy et al., 2014). The ready-to-use powder is then fed onto the laser bed in the build chamber, and a laser scans over the powder, melting it and building a thin layer of material. The process continues, whereby layer after layer is built from bottom to top until the component is complete (Goodridge et al., 2012; Wudy et al., 2014). Figure 1.2 shows a 2D schematic representation of this process used to manufacture parts with different polymeric materials, such as nylon (polyamide 12), polypropylene, polystyrene, elastomers, and composites.

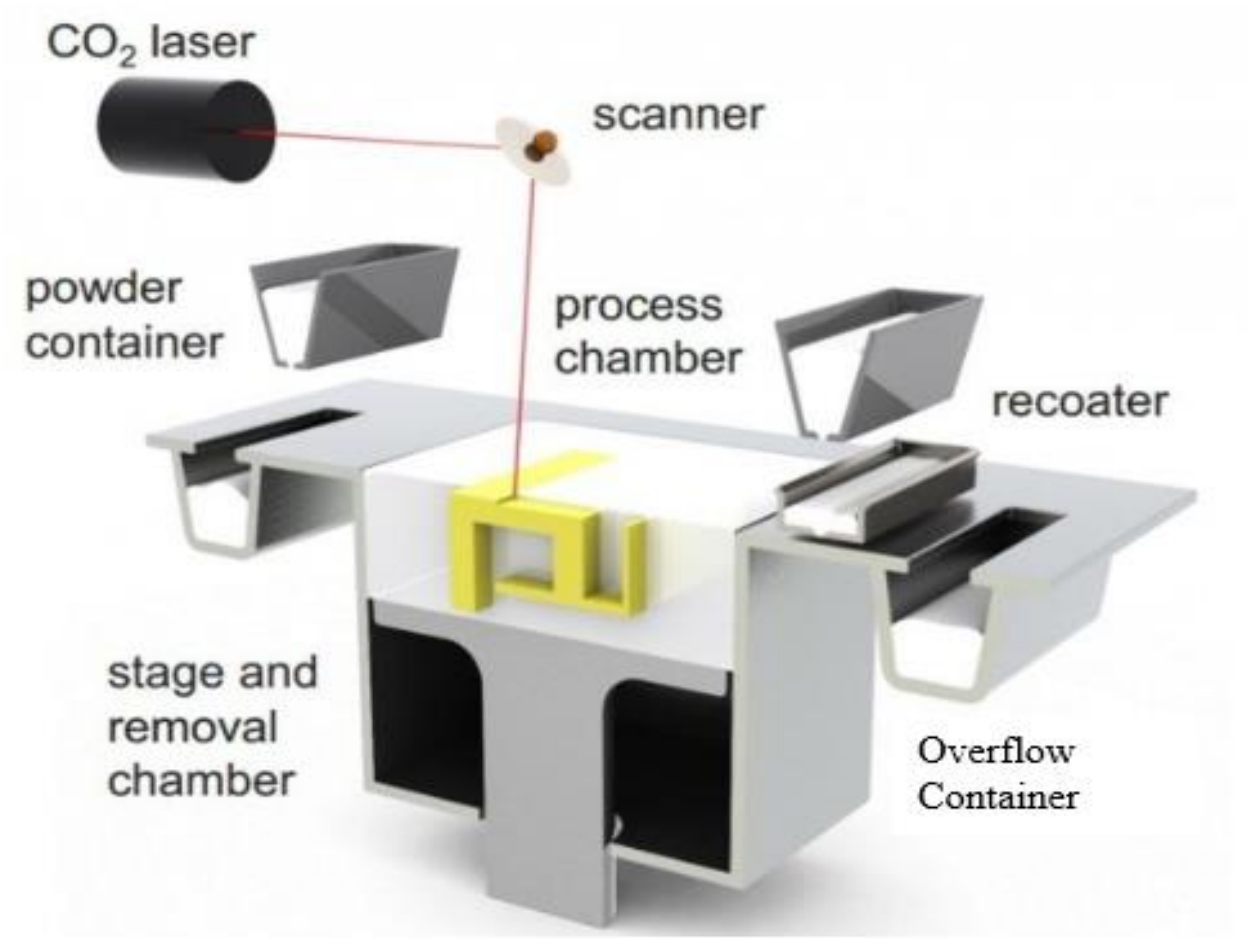

Figure 1.2 Selective laser sintering (Lambert, 2014)

1.1 Problem Statement

Over the past two decades, the popularity of AM has increased significantly, and the technology has matured from prototyping to the manufacture of functional parts (Flores Ituarte et al., 2018). AM technology and its applications are increasingly being used because it enables the development of components with intricate internal and external shapes and features, has reduced the lead time compared to conventional methods, permits mass customization of products, and can be used for a wide range of materials (Goodridge et al., 2012). However, only a limited number of polymers can be utilized in AM because most of them do not have suitable properties, and there is limited study on the polymers that can be used in AM. Polyamide and its blends make about 95% of all the polymers used in AM because of their suitable particle size and shape, density, thermal, optical, and rheological properties (Wudy & Drummer, 2016). Other polymers have been introduced in AM, such as PP, polyether ether ketone (PEEK), and polybutylene (PB), especially in LS (Hesse et al., 2019). PP is among the most widely used plastics due to its comparatively better properties than other polymers, such as high impact strength, high tensile strength, low cost, lightweight, and good chemical resistance (Kumar & Gupta 2003; Bassam, 2014). However, due to the limited availability of PP for LS, the cost of the powder is significantly higher. One kilogram of PP powder from Diamond Plastics costs about 60 Euros compared to the feedstock of the same material used in conventional manufacturing, such as injection moulding, which is 20 times less expensive (Goodridge et al., 2012). Therefore, it is necessary to recycle the powder used in LS to reduce manufacturing costs and reduce wastage, mainly since only 10–20% of the feedstock material is used to develop components (Kigure & Niino, 2017).

The LS process is one of the most promising AM technologies for polymers because of its ability to produce parts with good surface finish, high dimensional accuracy and good mechanical properties (Bourell et al., 2014; Ligon et al., 2017). Furthermore, the LS process does not require supporting components during the manufacturing process, as is the case in other processes, such as material extrusion (MEX), also referred to as fusion deposition modelling (FDM). LS has challenges because the physical, mechanical and chemical properties of the polymeric powder deteriorate due to high processing temperatures, which in turn, reduces re-usability of the powder after several cycles

(Goodridge et al., 2012; Wudy et al., 2014; Wudy & Drummer, 2016; Flores Ituarte et al., 2018; Hesse et al., 2019).

Previous studies show that used PA 12 cannot be recycled without mixing it with fresh material due to the "orange peel" effect, which compromises the surface roughness and dimensional accuracy of the manufactured parts (Dotchev & Yusoff, 2009; Yamauchi et al., 2016; Kigure & Niino, 2017). It has also been shown that after the 5th to 7th cycles of re-use, PA 12 cannot be recycled further due to extreme deterioration of its properties as a result of thermal aging (Wudy & Drummer, 2016; Hesse et al., 2019). Using the existing body of knowledge of PA 12, it can be argued that the properties of all polymeric materials deteriorate after LS, which affects the physical and mechanical integrity of manufactured products. Hence, there is a re-use limit for polymers that are utilized in LS. However, manufacturers of PP powder, such as Diamond Plastics, suggest that PP can be fully re-used, which raises questions on the recyclability of PP. Therefore, there is a need to determine whether PP can be re-used in LS without mixing it with fresh material. This study investigated the re-usability characteristics and limits of PP in laser sintered AM.

1.2 Aim of the Study

The aim of this research was to investigate the re-usability characteristics and limits of PP powder in LS.

1.2.1 Objectives of the Study

The objectives of this study were:

1. To determine the characteristics of fresh PP powder from Diamond Plastics (Laser PP CP 60 and Laser PP CP 75).
2. To determine the characteristics of PP powder grade from Diamond Plastics after exposure to heat in the LS process.
3. To determine the aging trends of PP powder grade from Diamond Plastics after exposure to heat in the LS process.
4. To determine the number of cycles laser-sintered PP powder grade from Diamond Plastics can be recycled before reaching an aging cut-off.

1.3 Thesis Outline

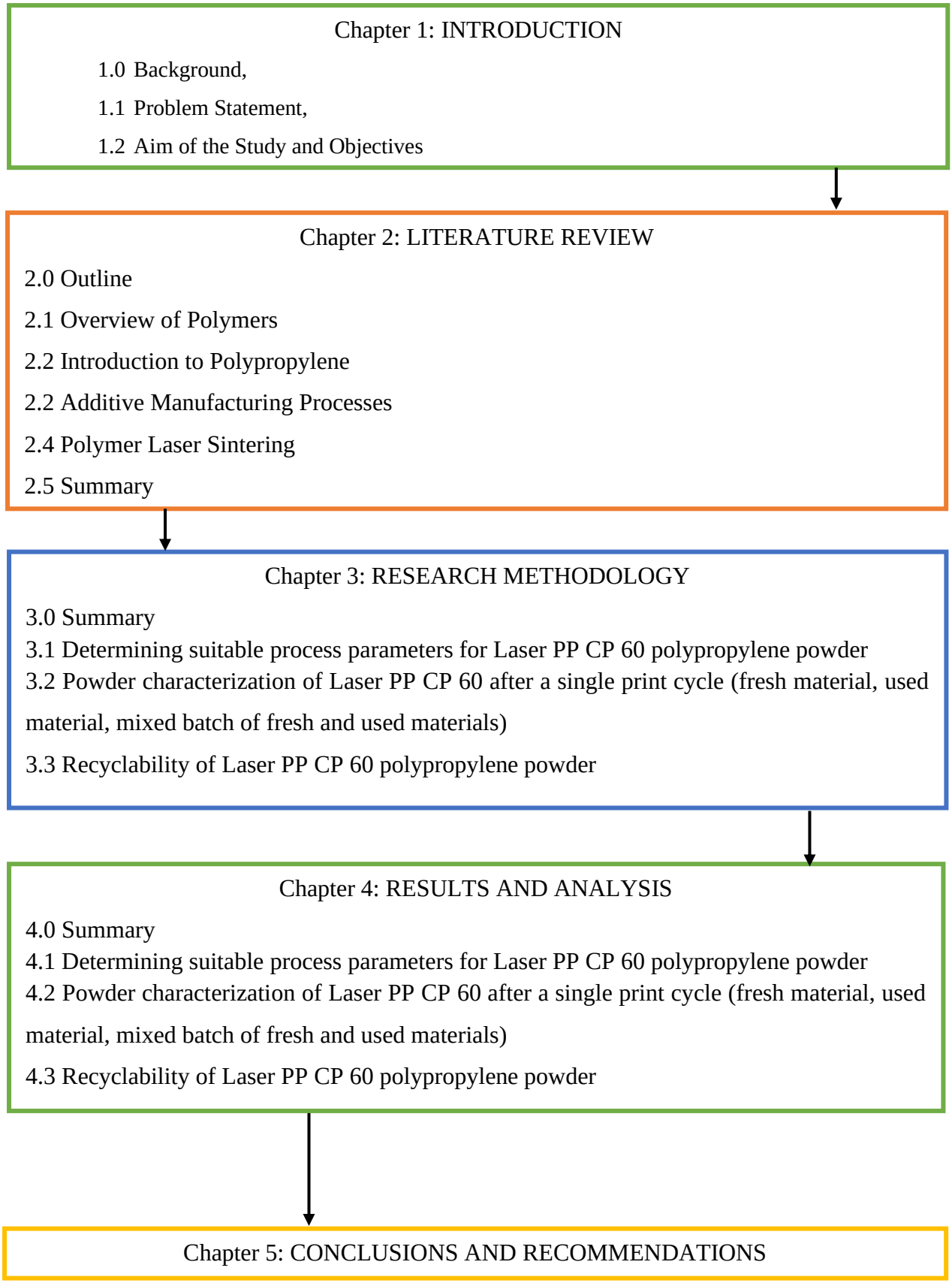

CHAPTER 2 - LITERATURE REVIEW

The material presented in this chapter has been published in expanded form in peer-reviewed journals and conference proceedings with the details:

1) Mwania, F. M., Maringa, M., & van der Walt, J. G. (2020). A Review of Methods Used to Reduce the Effects of High Temperature Associated with Polyamide 12 and Polypropylene Laser Sintering. *Advances in Polymer Technology*, 2020(1), pp.1-11. https://www.hindawi.com/journals/apt/2020/9497158/
2) Mwania, F. M., Maringa, M., & van der Walt, J. G. (2020). Mixing and Reuse of Polymer Laser Sintering Powders to Ensure Homogeneity – A Review. *International Journal of Engineering Research and Technology*, 13(11), pp.3335-3341. http://www.irphouse.com/ijert20/ijertv13n11_32.pdf
3) Mwania, F. M., Maringa, M., & van der Walt, J. G. Recycling of Polypropylene Powder Used in Laser Sinter Additive Manufacturing – A Literature Review. *RAPDASA Conference, Emoya Estate, Bloemfontein, South Africa*, 20(1), pp.315-330. https://site.rapdasa.org/wp-content/uploads/2020/04/315-Mwania.pdf

2.0 Summary

This chapter gives an overview of polymers, and in particular, polypropylene (PP). The general properties and classification of polymers are outlined. The chapter also delves into the properties, production processes and uses of PP. In addition, AM processing technologies for polymers are presented. Finally, the chapter provides an overview of laser sintering of polymers in AM in which the process, aging and recycling aspects are discussed.

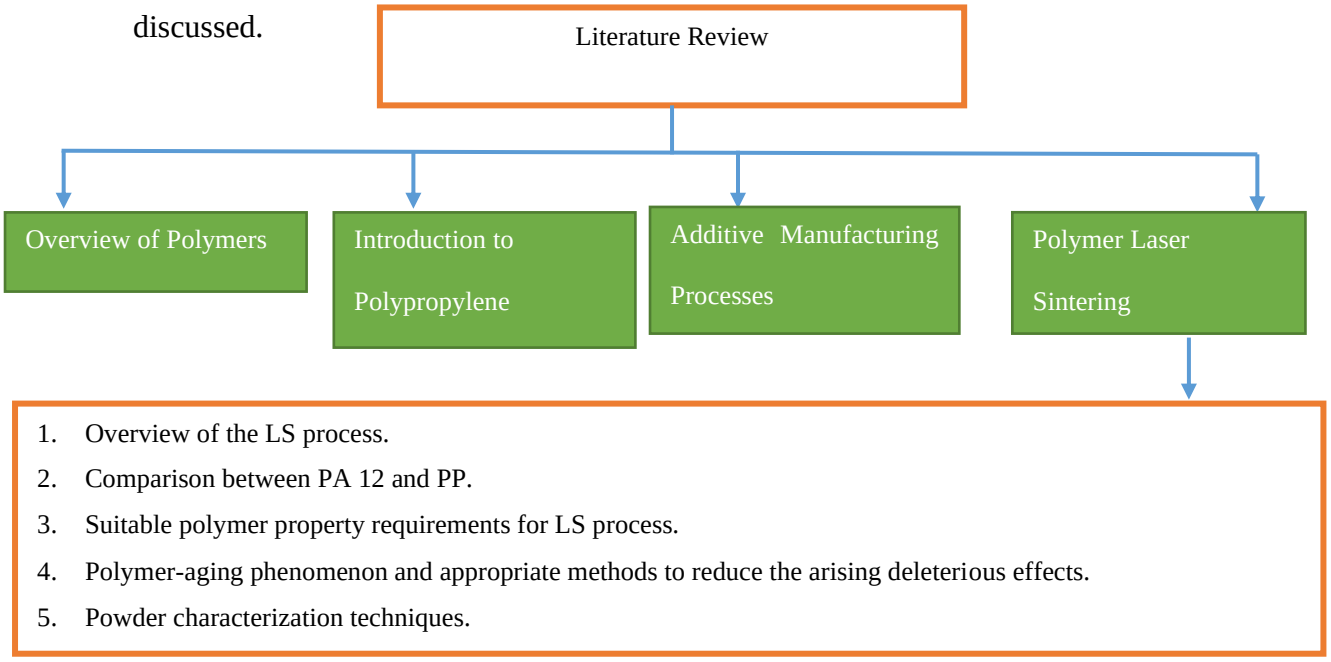

Figure 2.1. Outline for chapter 2

2.1 POLYMERS

The word “polymer” is derived from the two Greek words, “poly” and “meros”. The latter word means parts, while “poly” refers to “many” (Bassam, 2014). The name was inspired by the fact that a polymer consists of many repeating units, referred to as monomers, linked together by covalent bonds (ECHA, 2012). A monomer is defined as a simple chemical unit capable of joining other similar or dissimilar units through covalent bonds via a process of polymerization (ECHA, 2012) to form polymers. A polymer differs from macromolecules in that the latter comprises different monomers and therefore have molar masses that vary from one type of macromolecule to another (Hiorns et al., 2013). To determine the average molecular weight of a polymer, the degree of polymerization (DP), which is a statement of the number of monomers in a given polymer, must be established (Hiorns et al., 2013). Equation 2.1 is used to obtain the average molecular weight of a polymer (Hiorns et al., 2013).

$$Average\ molecular\ weight\ of\ a\ polymer = DP \times weight\ of\ the\ monomer \quad (2.1)$$

It is important to note that polymers differ from oligomers in that the latter contains fewer individual units, typically five, compared to the former. Furthermore, removing one monomer from an oligomer leads to a change in its chemical properties, unlike the case of a polymer (Kratochvíl & Suter, 1990).

The study of polymers is of great importance since this class of materials forms a crucial part of the daily lives of people. These materials find vast applications, such as in the development of packaging, building and construction, transportation, electrical and agricultural materials (ECHA, 2012). Moreover, their physical and chemical properties can be tailored to a broad range of uses. The general properties of polymers are (Ebewele, 2000):

i. Relatively low densities compared to metals and ceramics.
ii. High corrosion resistance.
iii. Low electrical and thermal conductivities.
iv. Relatively good strength-to-weight ratios but low values of strength compared to metals and ceramics.
v. Low moduli of elasticity.
vi. Degrade when exposed to sunlight and other forms of radiation.

2.1.1 Identification and Classification of Polymers

In order to facilitate easy identification of the many types of existing polymers, the following approaches are utilized (Vohlídal, 2009; Hiorns et al., 2013; Bassam, 2014):

i. Sub-unit-based naming – this method involves using the prefix "poly", followed by the name of the monomer, for example, polystyrene, polyethylene, polypropylene, polycarbonate, and polyamide.

ii. Structure-based – this form of naming involves the use of International Union for Pure and Applied Chemistry (IUPAC) names in accordance with the details given in Table 2.1.

Table 2.1 IUPAC prefixes for organic compounds

Prefix	Number of carbon atoms	Alkyl group
meth-	1	methyl
eth-	2	ethyl
prop-	3	propyl
but-	4	butyl

Examples include poly (1-phenylethyle); 1,4-phenylene; butane-1, 4-diyl; ethane-1,2-diyl; 1-bromoethane-1, 2-diyl; and methylmethylene, 1-oxopropane-1, 3-diyl.

iii) Bond-based – this method involves using the prefix "poly" and the addition of the type of bond of the compound. For instance, polysiloxane for the –O-Si- bond and fluoropolymer for the C-F bond.

iv) Abbreviations – the strategy here involves the use of capital letters. For example, PS refers to polystyrene, PMMA refers to polymethylmethacrylate, EP refers to epoxy resin, PP – polypropylene, PA – polyamide, and PEEK refers to polyether ether ketone.

v) Use of trade names – this strategy involves using common names for the different polymers, such as Plexiglas for PMMA, Styrofoam for polystyrene, Viton for fluoropolymer elastomer, and Saran for polyvinylidene chloride.

As mentioned earlier, a polymer is a generic name that refers to a wide array of compounds with high molecular weights. Polymers are mainly categorized based on either one of the following factors (Vohlídal, 2009; Hiorns et al., 2013; Bassam, 2014):

i. Source or origin of the polymer.
ii. Structure of the polymer.
iii. Molecular forces.
iv. Mode of polymerization.

The classification of polymers is summarized in Figure 2.2.

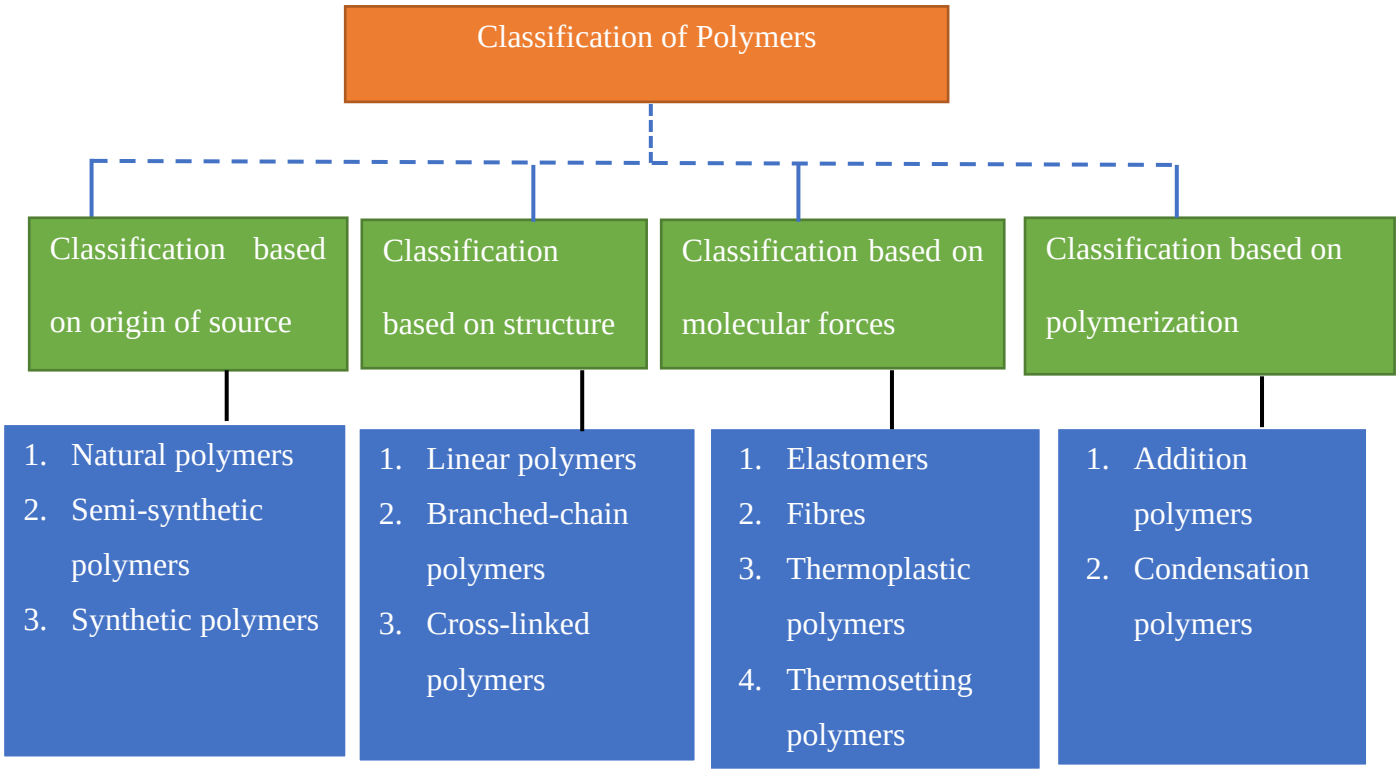

Figure 2.2 Classification of polymers (Bassam, 2014)

2.1.1.1 Classification based on origin

In this approach, polymers are classified based on their origin. This classification has three major sub-categories: natural polymers, semi-synthetic polymers, and synthetic polymers (Bassam, 2014). The polymers are obtained from natural sources such as plants and animals, including cellulose, resins, rubber, proteins, and starch (Bassam, 2014). Semi-synthetic polymers are generated from simple changes to natural polymers, and they

include silicones and starch. Lastly, synthetic polymers are obtained through artificial polymerization processes and include nylon, synthetic rubber, Teflon, polystyrene, terylene, nylon, polypropylene, polybutadiene, formaldehyde-resins, silicones, polyvinyl chloride, Bakelite, and polythene (Bassam, 2014).

2.1.1.2 Classification based on structure

This form of classification considers the arrangement of the monomers and how they are connected. There are three main categories of polymers based on their structure: linear, branched, and cross-linked polymers (Bassam, 2014). In linear polymers, monomers are linked to each other to form long straight chains. Branched-chain polymers have straight chains with side chains. Lastly, cross-linked polymers have many straight chains that are linked together by covalent bonds. Figure 2.3 gives a schematic illustration of these three categories of polymers.

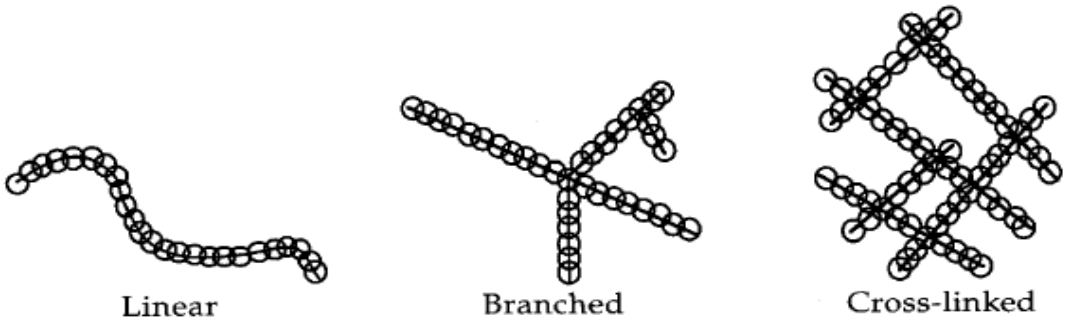

Figure 2.3 Polymer classification based on structure (Polymerization, n.d.)

In this class, polymers can be sub-divided further into either homopolymers or copolymers. Homopolymers are composed of similar monomer units, while copolymer polymers comprise two or more different monomer units (Hiorns et al., 2013). Examples of common polymers falling in these three categories include:

1. Linear polymers – polythene, nylon, polyester, and polyvinyl chloride.
2. Branched-chain polymers – polypropylene, glycogen, and amylopectin.
3. Cross-linked polymers – melamine, Bakelite, formaldehyde and vulcanized rubber.

2.1.1.3 Classification based on molecular forces

The molecular forces that hold the monomers together determine the physical and chemical properties of the polymers. Based on this classification, there are four main sub-classes: elastomers, fibres, thermoplastics polymers, and thermosetting polymers (Klein, 2011).

Elastomers are types of plastics with netlike cross-linking. They degrade when melted. They are elastic at temperatures above the glass point but become brittle at temperatures below the glass transition temperature. They include styrene-butadiene rubber, butadiene resin, styrene-butadiene resin and polyurethane resin (Klein, 2011).

Fibres are polymers that possess high tensile strength and high modulus of elasticity due to strong intermolecular forces. They are crystalline in nature because of the close packing of their chains due to intermolecular forces. Examples of polymer fibres include polyesters (terylene), aramid, glass, Kevlar, Nomex, polyvinyl fibre, polyolefins, polyurethanes, and polyacrylonitrile (Klein, 2011).

Thermoplastic polymers are re-formable. Thus, when heated, they become viscous, and when cooled, they return to their original form (Vohlídal, 2009). Therefore, they can be recycled. They include polypropylene, polyethene, polystyrene, polyvinyl chloride, polyesters, polyamide, polycarbonate, polyimide, polysulphone, linear polyurethane, chlorinated polyethers, polyacetate, polyacrylnitrile, polyethylene, polymethyl-methacrylate, polyvinyl acetate, and fluoropolymers (Kumar & Gupta, 2003).

Thermosetting polymers have a smaller percentage of cross-linked molecular chains than elastomers which makes them less rigid. Unlike thermoplastics, these polymers do not melt or flow when exposed to heat but instead break down (Klein, 2011). Thermosetting polymers cannot, therefore, be recycled. Thermosetting polymers, also commonly referred to as thermosets, include epoxy resin (EP), phenolic resin (PF), vulcanized rubber, Bakelite, epoxy resins, cross-linked polyurethane, alkyd resin, allyl resin, urea resin, melamine resin, phenolic resin, polyamide, silicone, and polyester resin (UP) (Prime, 2009). Thermosetting polymers have good dimensional, chemical and thermal stability and are used to make aerospace components, countertops, floor and dental materials, fishing rods, cutlery, golf clubs and tennis racquets (Prime, 2009).

2.1.1.4 Classification based on the mode of polymerization

The two sub-classes within this classification include addition polymers and condensation polymers (Kumar & Gupta, 2003). Addition polymers are formed by joining monomers to one another without the removal of any product. The linking occurs on the carbon atoms and is also referred to as chain-growth polymerization, which takes place in three phases: chain initiation, chain propagation and chain termination. Most linear polymers are addition polymers and include polyethylene, polypropylene, poly (vinyl chloride), Saran, styrene-butadiene rubber, Viton, butyl rubber, nitrile rubber and polystyrene (Kumar & Gupta, 2003; Klein, 2011). Condensation polymers are produced by the addition of monomers and the concurrent removal of compounds such as water, alcohol or ammonia (Kumar & Gupta, 2003). The process gives rise to by-products such as water. These polymers are also referred to as step-growth polymers and include polyester, polyamide, cellulose, polypeptide, and poly (β-hydroxybutyric acid) (Kumar & Gupta, 2003; Klein, 2011).

Polymerization that involves different monomers results in the formation of what is referred to as copolymers, which are categorized as statistical copolymers, alternating copolymers, block copolymers, and graft copolymers (Hiorns et al., 2013). Statistical copolymers are also known as random polymers and are constituted of randomly distributed monomers. Alternating copolymers consist of alternating monomers. Block copolymers are characterized by long sequences of monomers that are joined to other sequences of different monomers. Lastly, grafted copolymers have side chains linked to the main chains. Examples of copolymers include poly (vinylidene chloride) food wrap (Saran), nitrile rubber, butyl rubber, and synthetic rubber and fluoropolymer elastomer (Viton) (Kasser, 2007; Hiorns et al., 2013). The preceding four types of polymers are represented as follows, where the letters (A) and (B) represent different monomers (Kasser, 2007).

i. Statistical/random copolymers - ~ABBAAABAABBBABAABA~.
ii. Alternating copolymers - ~ABABABABABABABAB~
iii. Block copolymers - ~AAAAA-BBBBBBB~AAAAAAA~BBB~.
iv. Graft copolymer - ~AAAAAAA(BBBBBBB~) AAAAAAA(BBBB~) AAA~

2.2 POLYPROPYLENE

Polypropylene (PP) is a thermoplastic polymer made up of propylene monomers and is one of the most commonly used polymers due to its excellent chemical and physical properties, cost and ease of manufacture (Vogl, 1999). The polymer is a colourless, flammable, and odourless, gaseous hydrocarbon extracted from petroleum (Vogl, 1999).

2.2.1 Chemical Composition of Polypropylene

PP is produced through addition polymerization of propene, which makes up about 85% of the polymer (Karger, 2012). The chemical structure of PP is shown in Figure 2.4.

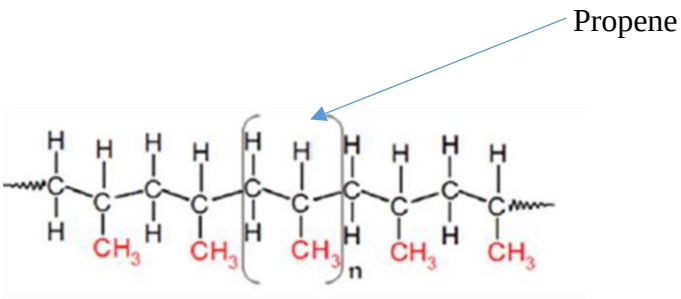

Figure 2.4 Chemical structure of polypropylene (Maddah, 2016)

Additives are usually added when manufacturing polymers to improve their physical and chemical properties. These additives include clarifiers, nucleators, slip additives, ultraviolet (UV) stabilizers, silica, talc, and calcium carbonate (Yordem et al., 2011). Slip additives are used to reduce friction during the processing phase. UV stabilizers are chemical compounds used for absorbing UV radiation and then dissipate the energy to prevent degradation of the plastics. Silica, talc, and calcium carbonate alter the mechanical and chemical properties of PP while also providing bulking to ease the handling of the polymer (Katz & Milesk, 1987).

2.2.2 Production of Polypropylene

PP is a chain-growth polymer that is manufactured through addition polymerization. Two catalysts may be used to produce PP: Ziegler-Natta and metallocene catalyst (Langhauser et al., 1994). The polymerisation process involves the use of titanium (IV) and aluminium alkyl (triethyl aluminium). During the process of polymerization, a mixture of propene and

hydrogen gases are passed over a Ziegler-Natta catalyst at 320–360 ^{0}C and a pressure of 8–35 atmospheres (Langhauser et al., 1994). The PP produced is then separated from the gaseous propene and hydrogen using cyclones. Figure 2.5 shows a schematic of the production process for PP.

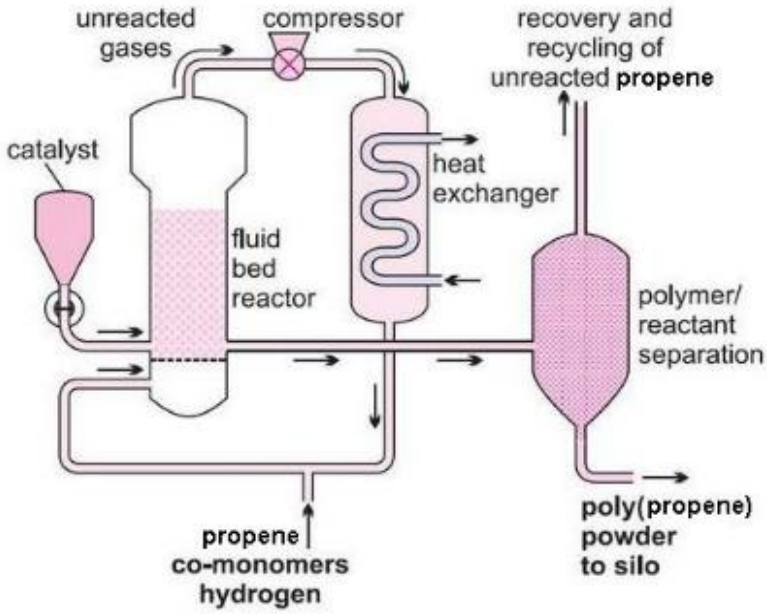

Figure 2.5 Polypropylene manufacturing process (Langhauser et al., 1994)

Metallocene catalysts are increasingly being employed in the production of PP. Metallocenes are chemical compounds comprising a transition metal atom bonded to two cyclopentadienyl ligands (a radical with the formula C_5H_5). Examples of metallocenes include ferrocene and zirconium (Ogawa, 2009).

2.2.3 Physical Properties of Polypropylene

The physical properties of PP are summarized in Table 2.2.

Table 2.2 Physical properties of propylene (Maddah, 2016; Mark, 2007)

Parameters	**Value**
Melting point	130 ^{0}C
Tensile strength	32 MPa
Flexural strength	41 MPa

Specific gravity	0.91
Shrink rate	1.5–2.0%
Crystallinity	50–60%
Glass transition temperature	-10 ^{0}C
Amorphous density at 25 ^{0}C	0.85 g/cm^3

Polypropylenes are also characterized by the following properties (Landel, 1993):

1. Low density.
2. Excellent heat resistance.
3. Easily processed.
4. Good chemical stability.
5. Outstanding impact strength.
6. Low water absorption properties.
7. Low dielectric and dissipation factor.
8. UV radiation and high temperatures affect them.
9. Good transparency.
10. Recyclability.

These chemical and physical properties of PP make it a suitable replacement for other materials such as wood, glass and other polymers. The mechanical and chemical characteristics of PP are subject to temperature. High temperatures, above 250 ^{0}C, damage PP products by weakening their hydrogen-carbon bonds (Wilkie & McKinney, 2004). Notably, these properties differ between homopolymers and copolymers. PP is a polymer with (Kumar & Gupta; 2003):

1. High flexural strength.
2. Relatively slippery surface.
3. Water resistance.
4. Good chemical resistance.
5. Good fatigue resistance.
6. Excellent electrical insulation.
7. Good impact strength.

Moreover, PP is known to (Landel, 1993; Kumar & Gupta; 2003):

1. Have a high thermal expansion coefficient.

2. Be susceptible to ultraviolet degradation.
3. Have poor resistance to chlorinated solvents.
4. Have high flammability.
5. Be susceptible to oxidation.

2.2.4 Uses of Polypropylene

As previously mentioned, PP is one of the most widely used polymers due to its versatility, availability, recyclability, low cost, transparency, and lightweight. Some of the uses for PP include (Kumar & Gupta, 2003; Klein, 2011; Jagtap & Mandave, 2015):

1. Packaging for the food sector.
2. Dashboards, PP film cushioning, car bumpers, and other interior components for the automotive industry.
3. Consumer products include kitchenware, furniture, toys, battery cases, thermal shirts for the military, loudspeaker housings, carpets, ropes, reusable containers, and appliances.
4. Sewage pipes, drainpipes, returnable transport packaging, and electric cables.

2.3 ADDITIVE MANUFACTURING PROCESSES

According to the ISO ASTM 52900:2015, AM is defined as a process of joining materials to make parts from 3D model data, usually layer upon layer, as opposed to subtractive manufacturing and formative manufacturing methodologies. Other authors have provided different etymologies. For instance, Aydin (2015) defines AM as the production of parts by joining successive layers of a particular material using a bonding technique (Aydin, 2015). Additive Manufacturing can also be defined as a collection of technologies utilized in manufacturing 3D-printed products by adding layers of the raw material, such as polymers, glass or metal (Shashi et al., 2017; Ford, 2014). The method differs from the conventional methods in that it involves the addition of materials instead of subtraction of materials that result in wastage. AM facilitates the production of net-shaped components with complex shapes; it is more flexible and has higher precision and shorter lead time than conventional manufacturing processes (Wong & Hernandez, 2012). These advantages imply that AM is likely to grow as a method of production in the industrial sector. The following advantages and limitations characterize AM.

Table 2.3 Advantages and disadvantages of AM

Advantages	Disadvantages
Allows the production of intricate components.	High costs of processing.
Suitable for mass customization.	Post-processing is often necessary
No need for tools.	A limited number of materials are available.
There is minimal wastage of materials.	The low speed of production makes it unsuitable for mass production.
Efficient use of energy.	The size of components that can be laser sintered presently is under 1 x 1 x 0.3 metres.
Permits design flexibility.	
Environmentally friendly.	
Reduced lead time.	

Several types of AM processes have been developed since the 1980s. It is worth noting that most AM processes adhere to the following steps: drawing of CAD models, conversion of the CAD models into acceptable AM machine format, machine setup, part production, part removal, and post-processing (Shashi et al., 2017). This literature provides a brief overview of various additive AM processes that are presently in use.

2.3.1 Evolution of AM Technology

AM technology has transformed since its invention, as summarized in Table 2.4. An extensive history of AM was presented by Wohlers & Gornet (2014).

Table 2.4 The historical background of AM (Bourell et al., 2009)

Year	Activity
1987–1989	Invention of the rapid prototyping process of stereolithography and its commercialization.

1990	Binder jetting process developed at the Massachusetts Institute of Technology.
1998	Optomec manufactures the first commercial directed energy deposition machine.
2002	Advent of the Arcam commercialized electron beam technology.
2005	Introduction of laser-based powder bed fusion machines.
2011	Introduction of AM in the medical field, mainly in dentistry.
2013	Introduction of the first powder bed fusing 4-laser concept machine.
2015	Utilization of AM processes to manufacture jet engine parts.
Today	Use of four lasers to simultaneously generate a single component and increment of build-up area up to 800 mm in length.

2.3.2 Classification of AM Processes

AM methods can also be classified based on the ISO/ASTM 52900:2015 Standard Terminology for Additive Manufacturing – General Principles – Terminology into vat photopolymerization (VPP), material jetting (MJT), binder jetting (BJT), material extrusion (MEX), powder bed fusion (PBF), sheet lamination (SHL), and directed energy deposition (DED). The technologies mentioned above differ on procedure and materials, as described in the following discussion (ISO/ASTM 52900:2015).

- Material Extrusion (MEX) – an AM technique in which material is selectively dispensed from a nozzle or orifice.
- Vat Photopolymerization (VPP) - an AM technology in which liquid photopolymer in a vat is selectively cured using a light-activated polymerization.
- Powder Bed Fusion (PBF) – an AM process in which thermal energy is used to selectively fuse regions of a powder bed.

- Binder Jetting (BJT) – an AM strategy in which a liquid bonding agent is selectively deposited to join powder materials.
- Material Jetting (MJT) – an AM method in which droplets of build material are selectively deposited.
- Directed energy Deposition (DED) – an AM technique in which focused thermal energy is utilized to fuse materials by melting as they are being deposited.
- Sheet Lamination (SHL) – an AM process in which sheets of materials are coalesced to form a component.

2.4 LASER SINTERING OF POLYMERS

Many polymers have been studied and patented for application in AM. Examples of these polymers include polypropylene, polyesters, thermoplastic polyurethanes, olefin block copolymers, and styrene-butadiene-styrene (Drummer et al., 2010). Some of these polymers, such as PA 12 and PP, are commonly used in LS. The LS process of polymers can be divided into three phases in the following generic order.

1. The process commences by spreading polymeric powder on the building platform in the building chamber, which is then preheated before using the laser beam to melt the material (Wudy et al., 2014). For the semi-crystalline polymers, the building chamber is preheated to temperatures just below their melting point and above their recrystallization temperature (Goodridge et al., 2012). The preheating process is performed to ensure that the laser beam is used to tip the material into a molten state to avoid using excessive laser energy that would otherwise promote degradation of the powder (Wudy et al., 2014).
2. The powder is then heated selectively using a laser beam to fuse the particles. The build platform inside the building chamber is then lowered by one layer, and a new layer of powder material applied, followed by selective heating of the new layer with a laser beam. This process continues until a component is fully built.
3. Once the part has been completed, the chamber and the parts are cooled to room temperature in a controlled manner to prevent curling of the parts, which would arise if cooling was rapid (Wudy et al., 2014).

The LS process is one of the most widely used AM technologies for polymeric materials because of its ability to develop parts with good surface finish, high dimensional accuracy,

sufficient geometrical accuracy, and good mechanical properties (Hesse et al., 2019; Liverani et al., 2017). The process does not require support structures, as is the case with FDM, as the powder surrounding the built component serves this purpose, a fact that reduces post-processing production time and cost (Goodridge et al., 2012). Besides, applying LS 3D printing to manufacture different pore structures, shapes and components is much easier than for other AM technologies such as FDM, which is limited due to the use of filaments (Maconachie et al., 2019). Meshed structures are lighter in weight and require less material which helps reduce costs of production (Maconachie et al., 2019). Maconachie et al. further noted that lattice structures possess better acoustic, dielectric, and mechanical properties than their parent materials, making them attractive for aerospace applications (Liverani et al., 2017). Besides, Liverani et al. illustrated that internal lattice structures have high specific strength and stiffness.

Polyamide and its blends are the most commonly used polymers in LS due to their suitable properties (Flores et al., 2018). However, the limited variety of polymeric materials applicable to LS has been a significant hindrance in advancing LS of polymers. Figure 2.6 provides details of the commercial polymers available for LS regarding usage, price and market share.

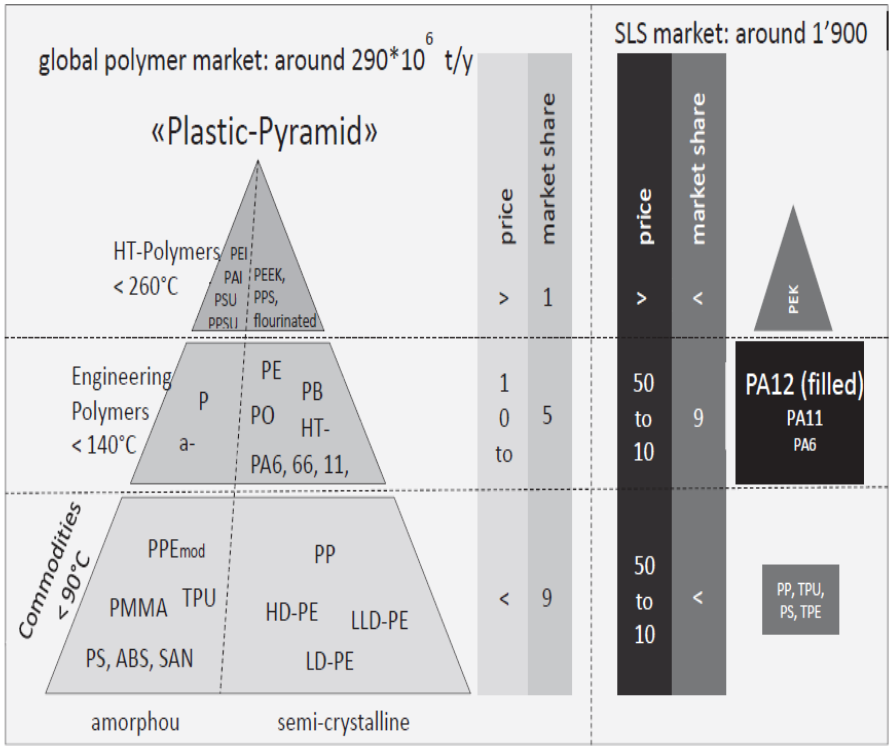

Figure 2.6 Polymer laser-sintering materials (Schmid & Wegener, 2016)

The diagram shows the limited variety of semi-crystalline polymer materials available in LS, which include: polyether ether ketone (PEEK), polyphenylene sulfide (PPS), polyethylene (PE), polybutylene (PB), polyamide (PA), and polypropylene (PP).

2.4.1 Comparison between PP and PA 12 used in Laser-Sintering AM

The use of PP in laser sintering does not yield results as satisfying as those of PA polymers, because of factors such as crystallinity, capacity to absorb laser energy, extended shrinkage, blocking of the powder bed, cracking of the upper powder layer during preheating, and particle size distribution (Fiedler et al., 2007). As this research focuses on the recyclability of PP, with PA 12 as reference material, a comparative analysis of some properties of the two LS polymers is presented in Table 2.5.

Table 2.5 Properties of PA 12 and PP (Fiedler et al., 2007)

Parameter	**PP**	**PA 12**
Window of sintering	Smaller than for PA	Larger than for PP
Crystallinity	More crystalline	Less crystalline
Thermal degradation	Degrades at about 450 ℃ in nitrogen	Degrades at about 430 ℃ in nitrogen
Particle size	Not spherical	Almost spherical
CO_2 laser beam absorbance	About 15%	About 25%

The information in this table indicates that PA 12 has better properties than PP at various levels. Firstly, its particles are almost spherical, which facilitates spreading (Schmid et al., 2015). In addition, its larger window of sintering reduces the chances of curling from the effect of rapid cooling (Goodridge et al., 2012). The material is expected to portray better fusion than PP because of its higher absorbance of laser beams resulting in more compact products (Goodridge et al., 2012). Finally, it is noted that high crystallinity is associated with higher shrinkage, which hampers the printing of complex components (Marin, 2017).

2.4.2 Properties of Suitable Polymer Powders for Use in Laser Sintering

Polymers applicable to the LS process should possess suitable intrinsic and extrinsic properties (Amado et al., 2011), as shown in Figure 2.7. Extrinsic properties, in this case, describe the physical characteristics of polymers, including powder density, as well as

particle size distribution and morphology. The intrinsic properties of polymers consist of thermal, rheological and optical properties (Schmid et al., 2015). The parameters used to describe the thermal behaviour of polymeric powders include melting point, sintering window and temperature degradation point. The rheological properties of polymers include viscosity and surface tension, while the optical characteristics of polymers determine the absorbing behaviour for laser energy (Marin, 2017; Wudy et al., 2014). The techniques for characterization of polymer powders are based on the abovementioned intrinsic and extrinsic properties.

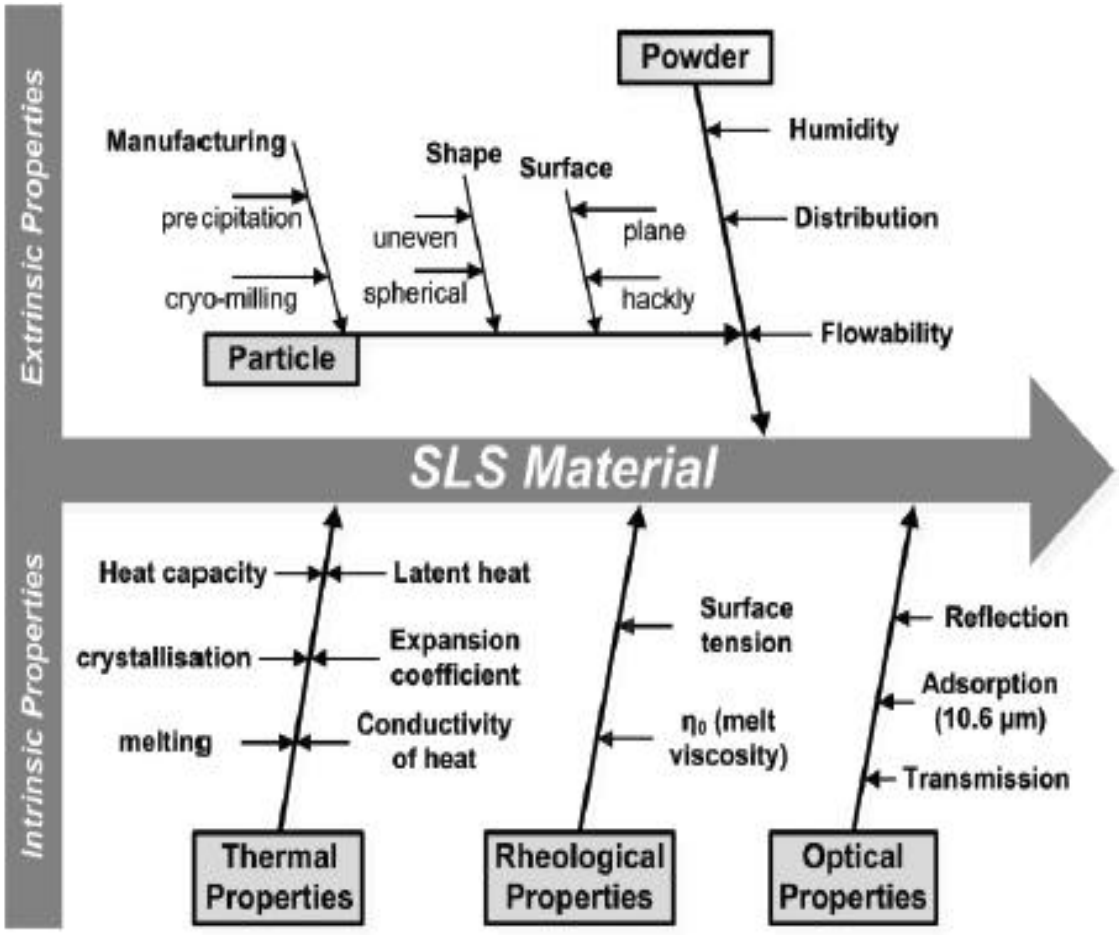

Figure 2.7. Extrinsic and intrinsic properties of AM powders (Lanza, 2015)

2.4.2.1 Particle size distribution and morphology

Particle size distribution and morphology need to be optimized for LS powders. Polymeric powder particles suitable for LS should be nearly spherical to encourage flowability (Schmid et al., 2015). Moreover, the powders should have an approximate powder

distribution of between 20 µm and 80 µm (Schmid et al., 2015; Mys et al., 2018). Extremely small particles induce stickiness which reduces flowability (Schmid et al., 2015). On the other hand, extremely large particles affect the spreading of the powder by a roller or blade. Large particles also discourage fusion which introduces porosity and reduces the mechanical integrity of printed parts (Schmid & Wegener, 2016). Nearly spherical powder particles are recommended for LS materials to encourage flowability and powder spread across the building chamber.

2.4.2.2 Thermal properties

Appropriate thermal properties are essential for the successful processing of semi-crystalline polymers using LS. Polymers should have a high-temperature degradation point as LS occurs under high temperatures (Marin, 2017). The processing temperatures should be maintained between the melting- and crystallization points of polymeric materials to prevent uneven solidification of the printed parts, which is likely to affect the geometrical accuracy and the surface finish of the components. The difference between the melting- and crystallization points of a polymeric material is referred to as the sintering window. Suitable polymers are characterized by a wide and sufficient sintering window, preventing crystallization of the polymers during processing (Goodridge et al., 2012; Marin, 2017). Rapid crystallization of printed components is a significant hurdle in LS because it encourages curling, which affects the surface finish and dimensional accuracy of the produced parts (Schmid et al., 2015).

Furthermore, suitable polymers should have a narrow melting point region to avoid the use of high laser energy to fuse particles of powder (Goodridge et al., 2012). High laser energy leads to greater degradation of the powder supporting the components being printed, limiting the recyclability of the powder (Marin, 2017). Thermal properties do, therefore, significantly determine acceptable polymers for the LS process.

2.4.2.3 Rheological properties

Viscosity and surface tension also determine the applicability of polymers in the LS process. The rheological properties are described in terms of polymer power and melt viscosity. In this regard, a suitable polymeric melt should have low viscosity and low surface tension to ensure adequate coalescence of the particles of powder (Schmid et al.,

2015; Drummer et al., 2010; Craft, 2018). It should be noted that extremely low melt viscosity compromises the surface roughness of printed components because the melt seeps into the surrounding support powder (Goodridge et al., 2012). Unlike injection moulding, LS does not provide additional compacting. It is, therefore, essential that the powder has low melt viscosity with low shear stress (Schmid et al., 2015). Low-power particle surface tension encourages better flowability of the material. Viscosity, surface tension and shear stress thus form crucial material-property requirements for LS polymers.

2.4.2.4 Optical properties

Optical properties influence the LS process in that a suitable polymeric material should absorb sufficient laser energy to ensure the satisfactory fusion of the powder particles. Most polymers absorb the commonly utilized CO2 laser energy with a wavelength of about 10 µm sufficiently (Schmid et al., 2015).

However, most polymeric materials do not meet the requirements for LS, which is the reason for the small number of polymers used in this type of AM. According to Marin (2017), suitable LS polymers should have:

1. A low melt viscosity at low shear stresses.
2. A wide temperature range between melting and degradation temperatures.
3. An appropriate temperature range between melting and crystallization point.
4. Adequate dry-flow and melt-flow characteristics.
5. Low moisture sensitivity.
6. No significant emission of volatiles during processing.
7. Suitable thermal properties.
8. Nearly spherical particles that preferably are less than 100 µm in size, and
9. Not fuse or segregate during storage.

2.4.3 Process Parameters for Laser-Sintering Materials

Process parameters can be classified into laser-related factors, scan-related- and temperature-related parameters (Marin, 2017). Some of the laser-related factors include wavelength, laser power, hatch distance, vector length, ratio of length to width, point overlapping, beam spatial distribution, continuous or pulsed laser operation, and beam diameter (Zhang & LeBlanc, 2018). Some of the scan-related factors include scanning

speed, scanning pattern and scanning angle. The temperature-related parameters comprise the build chamber temperature and the removal chamber temperature (Marin, 2017).

Process parameters influence the mechanical properties, density, hardness, porosity, surface roughness, and dimensional accuracy of printed parts (Zhang & LeBlanc, 2018). Therefore, optimizing the process parameters is crucial in meeting part requirements. Moreover, most of these process parameters are related to each other (Marin, 2017). For example, a low powder bed temperature requires high laser power and vice versa. In addition, a combination of high powder bed temperature and laser power results in dense parts. However, it compromises the recyclability of the unsintered powder due to over-baking of the powder. Conversely, low power and powder bed temperature result in components with better dimensional accuracy but with low density and delamination of layers (Marin, 2017). Furthermore, low powder bed temperatures and removal chamber temperatures promote part curling, thus affecting the dimensional accuracy of components and might, in extreme cases, halt the printing process as the recoater blade dislodges parts from the powder bed (Kleijnen et al., 2019). Low laser power requires low scanning speeds, while high laser power requires high scanning speeds to ensure the complete fusion of the powder particles. Improper bonding of powder particles encourages porosity, undermining the mechanical strength of printed articles (Marin, 2017).

The laser power, scanning speed, hatch distance, and layer thickness are the most easily adjustable process parameters in LS. The four parameters determine the amount of laser energy transferred to the powder and are related to one another, as shown by Equations 2.2 and 2.3 (Zhang & LeBlanc, 2018).

$$E = \frac{P}{V \times H} \tag{2.2}$$

where, E = laser energy density (J/mm^2), P = laser power (J/s), V = laser scanning speed (mm/s), and H = hatch distance (mm)

$$V = \frac{P}{V \times H \times D} \tag{2.3}$$

where, V = volumetric laser energy density (J/mm^3), P = laser power (J/s), V = laser scan speed (mm/s), H = hatch distance (mm), and D = layer thickness (mm).

Previous studies have shown that increasing laser energy density increases part density and mechanical properties, but in turn, introduces curling, which affects the dimensional accuracy of printed components (Marin, 2017).

2.4.4 The Effect of Heating on Polymers

Polymers undergo physical and chemical alterations when subjected to heat in a process called thermal decomposition. These changes might be positive or negative depending on the end-use of the polymer. When the changes are negative, the process is termed thermal degradation (Beyler & Hirschler, 2002). It is worth noting that the various physical processes that occur during thermal decomposition are subject to the nature of the material. For instance, simple phase changes for thermosetting polymers are not possible since they are infusible and insoluble upon heating, whereas thermoplastics undergo changes of phase when heated (Beyler & Hirschler, 2002). The deformability of thermoplastics increases with temperature, as shown in Figure 2.8.

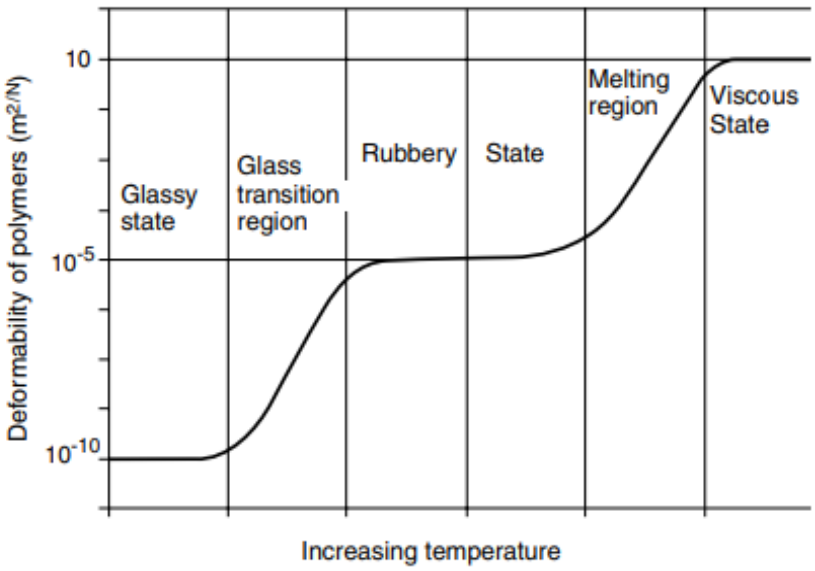

Figure 2.8 Temperature deformability of polymers (Beyler & Hirschler, 2002)

In the glassy state, thermoplastic polymers are rigid and in solid form. As the temperature rises, the polymers transit to the glass transition region, where they become rubbery. Further heating of the polymers results in melting, and they become viscous.

Thermal degradation of polymers can be represented using a three-step conventional model, including initiation, propagation, and termination (Zeus, 2005). During the initiation phase, the polymer (R) loses hydrogen atoms (H), leading to the formation of free radicals, which react with oxygen (O_2) during the propagation phase to form peroxy radicals (ROO^*) (Zeus, 2005). These radicals are, in turn, capable of removing hydrogen atoms from other polymer chains leading to the formation of hydroperoxides (ROOH) and other free radicals (R^*) (Zeus, 2005). The hydroperoxides split into two free radicals (RO^*) and ($^*OH$), which continue to propagate the reaction (Zeus, 2005). This process is terminated when the free radicals react to form inert products. The process is illustrated in Figure 2.9.

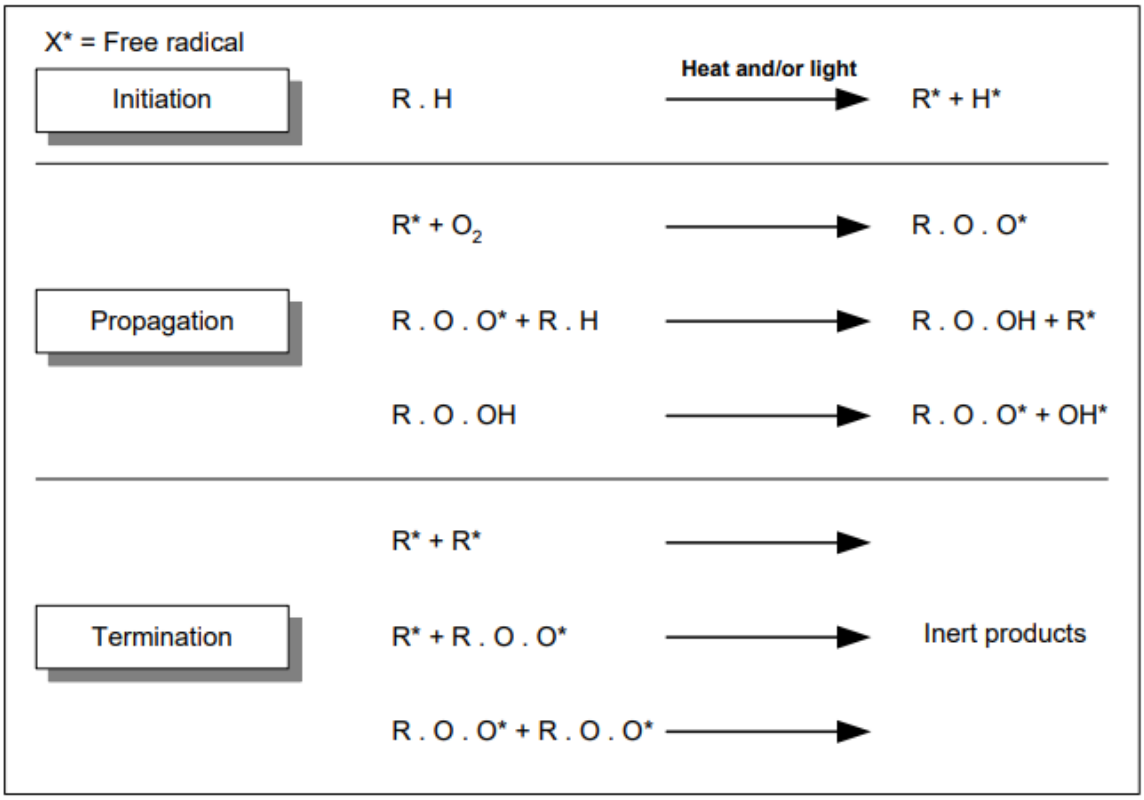

Figure 2.9 Three-step thermal degradation process for polymers (Zeus, 2005)

Different polymers degrade at different temperatures. Comparing the cases of polyethylene and PP systems, the degradation of polyethylene and PP in a nitrogen atmosphere does not commence until the temperatures reach above 400 ℃ and 350 ℃, respectively. However, complete volatilization of both is achieved at 500 ℃ (Wilkie & McKinney, 2004). By contrast, the degradation of polyethylene in the air starts at 235 ℃, while that of PP starts

below 235 °C. PP is more likely to degrade thermally at lower temperatures than PE or PA, as shown by Wilkie & McKinney (2004). From this discussion, it is evident that processing temperatures should be regulated when laser sintering PP powder. However, the powder will inevitably be exposed to high temperatures for a certain amount of time during processing. Therefore, the physical and chemical properties of the powder will change during the LS process.

Polymers degrade by the following mechanisms: random-chain scission, end-chain scission, chain-stripping, and cross-linking (Wilkie & McKinney, 2004). The scission process involves breaking the carbon-carbon bond in the polymer backbone, resulting in the formation of two radicals. The process might occur at any position throughout the polymer or occur at the ends of the polymer. When the scission process occurs at any position, it is referred to as random scission, leading to the formation of a monomer and oligomers. When the process occurs at the end of the polymer chain, it is known as end-chain scission, resulting in the formation of a monomer. Chain stripping occurs when molecules such as hydrochloric acid (HCl) or acetic acid (HC3OOH) are removed from the polymer. Lastly, cross-linking occurs when various chains in a polymer become entangled with each other. The degree of cross-linking is subject to the percentage of polymer chains connected to the backbone of the polymer. Under controlled conditions, cross-linking improves the properties of various thermoplastics such as (Aly, 2015):

1. Better heat and dimensional stability.
2. Improved impact resistance.
3. Higher tensile strength and stiffness.
4. Improved solvent resistance.
5. Improved electrical and dielectric properties.
6. Better resistance to corrosion.

On the other hand, uncontrolled cross-linking reduces chain lengths and leads to a decrease in molecular weight, which causes changes in mechanical properties, such as reduction in ductility (Davis et al., 1962). In LS, although heating is controlled, the polymeric materials are subjected to high temperatures for long durations, which alter their properties and, in turn, influence their recyclability.

According to Goodridge et al. (2012), during LS, the temperature of the building chamber is kept constant to prevent shrinkage of the polymer, which would lead to distortion of the

built components. For semi-crystalline polymers, the temperature of the process chamber should be maintained between crystallization and melting points. The difference between the two temperatures is known as the sintering window. Furthermore, the authors state that the sintering window for a suitable LS polymeric material should be sufficient to promote gradual cooling of the printed components before the advent of crystallization to prevent curling and shrinkage. Marin (2017) established that the sintering window for PP powders from Adanc3d Materials and Diamond Plastics lies between 35.1 ℃ and 28.8 ℃, respectively. The same researcher found that the sintering window for PA 12 from EOS lies between 32 to 34 ℃. Figure 2.10 provides a summary of the heating profile of polymeric materials during LS. In the diagram, the symbol *Ts* is the starting temperature, T_B the building temperature, T_E the extraction temperature, and t_{BC} the combined building and cooling times. The combined building and cooling times are subject to the distribution, volume and height of the parts being printed (Drummer et al., 2019). The curves in Figure 2.10 show that polymers are subjected to high temperatures during the entire LS process. This exposure alters the properties of the polymers, which influences the recyclability of the unsintered powder (Marin, 2017).

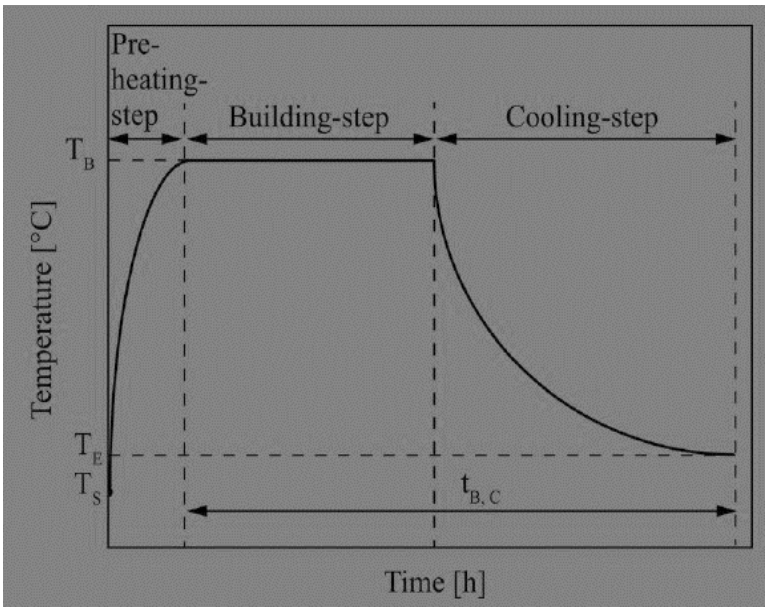

Figure 2.10 The heating profile of polymers during LS (Drummer et al., 2019)

The processability and part properties of LS polymer components are considerably influenced by the viscosity of the material (Wegner et al., 2014). This occurs at two levels; firstly, the effect of the viscosity of powder on its flowability, which influences its

spreading on the powder bed. Secondly, the viscosity of the powder-melt determines the degree of powder particle fusion, which then determines the mechanical strength of printed parts (Goodridge et al., 2012). A closer look at the aging of PA 12 and PP regarding viscosity is therefore necessary.

Lamberti et al. (2007) established that the viscosity of polymers is subject to their crystallinity. The researchers expressed the viscosity of polymer melts at a particular temperature as shown by Equation 2.4, where the symbols η stands for viscosity, T temperature, η_{ref} magnitude of reference viscosity, and a_T degree of crystallinity, at specific temperatures. Considering η_{ref} as a constant, it can be concluded from this equation that the viscosity of polymers at a particular temperature is directly proportional to the degree of crystallinity of the material at the same temperature.

$$\eta(T) = \eta_{ref}.a_T \tag{2.4}$$

2.4.4.1 Chemical deterioration of PA 12 and PP due to high temperatures

Polyamide 12 and PP undergo aging from exposure to high temperatures through several mechanisms: random-chain scission, end-chain scission, chain-stripping, and cross-linking (Wilkie & McKinney, 2004). Studies by Wegner & Ünlü (2016) and Wudy, Drummer & Drexler (2014) indicated that the behaviour of PP and PA 12, when subjected to LS, are almost similar.

High melt viscosity lowers the coalescence of powder particles, thus leading to porosity and, in turn, undermines the mechanical strength of printed parts (Berretta et al., 2016). Experiments by Wudy, Drummer & Drexler (2014) illustrated that the melt flow rate (MFR) of PA 12 decreases with increasing building time, build chamber temperature and the number of processing cycles. Similarly, the MFR of PP (ROWAK Rolaserit PP) decreases with the number of re-use cycles of the powder (Wegner & Ünlü, 2016). This is because high temperatures cause cross-linking of hydrocarbon chains, which increase the molecular weight of the polymers and leads to an increase in their melt viscosity (Pham et al., 2008). Moreover, Wegner & Ünlü (2016) established that the melt volume rate (MVR) of PP decreases with each re-use cycle. MVR measures the ease of flow of melted polymer, and it determines the viscosity of a material (Wegner & Ünlü, 2016). The authors found the Hausner number increased from about 1.15 to about 1.25 for the 3rd re-use cycle and

concluded that the viscosity of powder and melt increased with re-use cycles and would affect the recyclability of the material.

High processing temperatures increase the viscosity of both PA 12 and PP powders, thus reducing their flowability. Goodridge et al. (2012) found that powder with low flowability negatively impacts powder spreading and enhances coalescence of the powder particles during LS. The flowability of the polymeric powders is also influenced by the action of the recoater blade, which introduces electrostatic charges to the powder, and hence encourages agglomeration, thus negatively influencing its spread (Hesse et al., 2019). Therefore, high temperatures during LS limits the recyclability of polymeric materials such as PA 12 and PP.

2.4.4.2 Deterioration of polymers due to high temperatures

Polymeric powders used in the LS process must exhibit a certain level of melt flowability as this determines the homogeneity of the fusion of the powder particles, which establishes the density and the mechanical strength of manufactured parts (Goodridge et al., 2012). Various studies have shown that both the powder and melt flowability of polymers, such as PA 12 and PP, decrease with increasing build time and powder bed temperature during LS, impacting the quality of printed parts (Goodridge et al., 2012, Hesse et al., 2019).

In this regard, an increase in building time and temperatures leads to an increase in the crystallinity of PA 12, which affects the built parts (Dadbakhsh et al., 2017). A high degree of crystallinity is associated with higher shrinkage of printed components and lower ductility, which affects the dimensional and geometrical accuracy and surface finish of printed parts (Marin, 2017). However, the phenomenon reduces the chances of porosity forming, resulting in better tensile characteristics of printed parts (Marin, 2017). High crystallinity affects the LS of polymers as it leads to an increase in molecular weight of polymers (Lamberti et al., 2007, Josupeit et al., 2015) and an increase of viscosity with an undesirable attendant reduction in flowability. Therefore, it can be concluded that depending on the final use of printed components, high processing temperatures and their relationship with crystallinity might either be advantageous or detrimental.

A study by Wudy et al. (2014) showed that PA 6 and 66 experienced a higher rate of cross-linking at high temperatures, increasing their molecular weight, and as a result, the

viscosity of the materials, which in turn reduces their flowability. The consequence of this is the inhomogeneous spreading of powder, causing porosity inside printed parts, thus reducing the mechanical integrity and quality of the surface finish of printed components (Berretta et al., 2014). Dotchev et al. (2009) found that when PA 2200 from EOS is recycled five times, with or without small quantities of new material, the parts produced have a rough surface finish; a phenomenon referred to as “orange peel”.

Furthermore, the apparent density of PA 12 and PP decreases with increasing temperature, while the relative density of the manufactured components decreases with the number of re-use cycles (Wegner & Ünlü 2016; Pham et al., 2008). This phenomenon might be attributed to increased viscosity, which causes the introduction of pores and lower particle-packing due to the poor coalescence of powder (Berretta et al., 2017). Therefore, the mechanical properties of parts printed using PP decreases with increasing processing temperature and re-use cycles.

2.4.5 Analysis of the Recycling of Polymeric Powders for AM

As previously mentioned, sintering of any polymer powder results in degradation of the material, giving rise to a powder with changed properties that cannot provide sintered parts with the same quality as those manufactured using virgin powder. When polymers such as PA 2200 are recycled several times (five times) with or without small quantities of new material, the parts produced have a rough surface finish (Dotchev & Yusoff, 2009). This phenomenon is referred to as “orange peel”. Hence, such powder must be mixed with unused powder to restore its flowability, MFR and thermal properties. The cost of polymer for LS is very high at approximately $100 per kilogram (Duddleston, 2015). The LS process has a low conversion rate, with only about 15% of the powder charge being consumed directly in the production of parts (Yamauchi et al., 2016). Therefore, it is necessary to recycle the unused powder. Most of the sintering polymer powders are not recycled alone. Typically, 30–70% of the recycled powder is blended with virgin material and then reprocessed (Dotchev & Yusoff, 2009; Yamauchi et al., 2016; Kigure & Niino, 2017).

The most common technique utilized in restoring the properties of polymeric powder for LS involves mixing the used powder with fresh polymer powder. After sintering, the used powder is sieved and stored for re-use in the next cycle. Before re-using the powder, quick

and simple tests should be performed on the used powder to quantify the level of degradation after every cycle. The most commonly used tests, in this case, include MFR testing and differential scanning calorimetry (DSC). The latter method highlights changes in the thermal properties of materials, whereas the former shows changes in the rheological behaviour of powder. After testing, the data is applied to determine the ratio of virgin to used powder that should be mixed. The ratio of the cake powder (unused powder obtained from around the built parts) to the mixture is referred to as the recyclability of the powder (Yamauchi, Kigure & Niino, 2016).

Most 3D part manufacturers recycle polymeric powders following recommendations from the manufacturers of the powder. Examples include 3D Systems' recommendation to mix PA 12 powder with fresh powder in a 1:1 ratio, whereas EOS proposes a 30–50% fresh PA 2200 powder ratio with 70–50% used powder. The polymeric powder recycling process followed currently in LS is summarized in Figure 2.11.

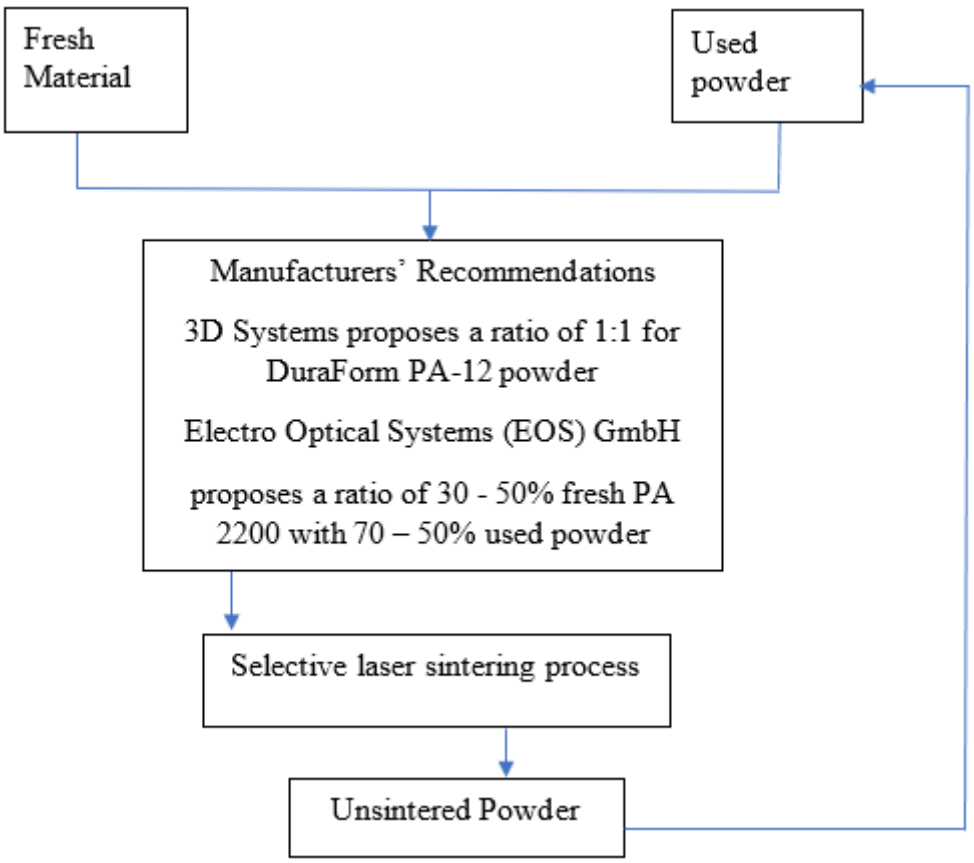

Figure 2.11 Recycling process of polymers in LS (Dotchev & Yusoff, 2009)

Experiments conducted by Dotchev & Yusoff (2009) resulted in a flowchart to determine the percentage of used powder and fresh powder to be used for LS of PA 12. They concluded that the current powder recycling practices do not consider the variation of the properties of used and fresh powders, which is likely to affect the properties of the printed parts. In addition, the redundant powder (completely degraded powder) limits the number of re-use cycles for the polymeric powder.

There is limited research on the re-usability of PP powder; however, some manufacturers, such as Diamond Plastics, suggest 100% re-usability, which broaches questions since a study by Wegner & Ünlü (2016) showed that the MFR and density of PP are reduced with each re-use cycle. Therefore, more research is needed to determine the re-use limit of PP and the most suitable ratio between used and fresh PP after each LS cycle.

2.4.6 Mixing of Laser-Sintering Powders in Rotating Cylinders

Rotating cylinders are commonly used for mixing powders used in LS, and the process can take place in either vertical, horizontal or inclined positions. Studies show that for non-segregating powders and powders with the same size, shape, and density, vertical mixing is diffusive, whereas horizontal mixing is a combination of convective and diffusive (Hogg, 2009). In the horizontal position, the powder batch is divided into two regions; the static region, where there is no mixing since the particles follow the motion of the cylinder, and the shear zone, where the actual mixing takes place (Hogg, 2009). To ensure that the powder batch behaves like a single entity, the Froude number of the mixture must be equal to 2.5 (Hogg, 2009). The Froude number describes the conditions in the shear zone and is calculated using the expression (Hogg, 2009):

$$Fr = R\omega^2/g \tag{2.5}$$

where, the symbol *Fr* stands for Froude number, *R* radius of the cylinder, ω angular velocity of the cylinder, and *g* acceleration due to gravity.

The Froude number becomes unity when critical speed is attained. Critical speed is calculated, as shown in Equation 2.6 (Hogg, 2009).

$$\omega_c = \sqrt{g/R} \tag{2.6}$$

where, ω_c stands for critical speed, g acceleration due to gravity, and R radius of the cylinder.

Only diffusive mixing takes place with reference to vertical mixing. Notably, the diffusion coefficient is subject to the volume of the powder, particle size, and rotational speed. According to Hogg (2009), the diffusion coefficient decreases with an increase in powder volume in the cylinder and an increase in the size of particles. The diffusion coefficient also increases with an increase in the rotational speed.

2.4.6.1 Sampling and assessment of the homogeneity of mixed powder

The two most commonly used methods in powder sampling are stratified and nested sampling (Deveswaran et al., 2009). The latter method involves selecting samples from a single point within a batch, whereas the stratified sampling method involves selecting samples from different locations in any given batch of powder (Deveswaran et al., 2009). Samples must be taken when the powder is in motion and within short time intervals to ensure an accurate representation of the powder (Deveswaran et al., 2009).

It is essential to take five samples from different locations in the mixer to ensure an accurate representation of the powder (Maynard, 2007). For a horizontal mixer, samples should be taken from each corner and one from the middle of the batch. In addition, one sample should be taken at the discharge of the mixer (Maynard, 2007). Samples are mainly collected using a thief probe, a metal rod with recessed cavities along its length. The rod is inserted into a batch of powder and samples collected in its cavities. The effectiveness of the technique depends on the operator's experience and other factors such as the insertion angle, penetration rate, and twisting effect (Maynard, 2007). Overall, the sampling process is crucial since it determines the accuracy of the samples.

The homogeneity of a batch of powder can be determined by taking several samples at random and then obtaining the variance of the composition of each sample (Hogg, 2009). Different technologies can determine the effectiveness of a mixing process. These technologies include a standard granulometric analyzer to determine the average size of particles for a given sample (Bauman et al., 2008). A laser particle analyzer and SEM determine the distribution of particles in each sample. The results are analyzed statistically

to determine the variation. A homogenous powder batch should have zero standard deviation for all the samples considered (Bauman et al., 2008).

2.4.6.2 Selection of a mixer for polymer laser sintering

The efficiency of mixing polymeric powders used in LS is dependent on the mixer used. In this regard, a suitable mixer should have the following characteristics (Deveswaran et al., 2009):

1. Be capable of producing a homogenous powder within a reasonable timeframe and without damaging it.
2. Be dust-tight.
3. Require low maintenance and energy.
4. Be easy to discharge and clean.
5. Be flexible for various batch sizes.

A flow chart for the selection of a mixer is summarized in Figure 2.12.

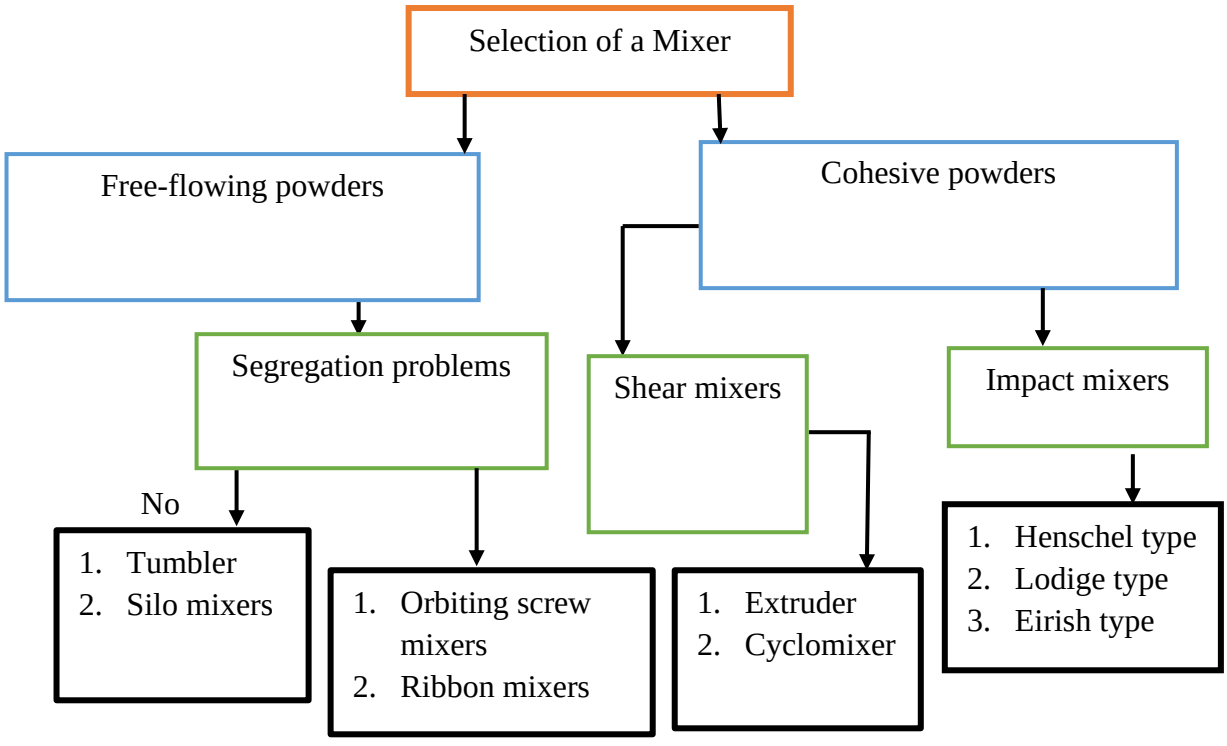

Figure 2.12 Flow chart for the selection of a mixer (Deveswaran et al., 2009)

Most mixers have limitations such as loss of product, abrasion of the particles of powder, contamination of powder, and inflexibility to different batch sizes of powder (Mikhaiel,

2013). Some low-shear mixers, such as tumblers, might not effectively mix powders in an agglomerated state since they must be broken up first and then redistributed (Hogg, 2009). However, tumbler mixers continue to be used in the industry because of their effective convective and diffusive mechanisms of blending, close quality control, and gentle mixing of powders (Maynard, 2007). The speed of most tumblers ranges between 5 and 25 revolutions per minute, with a fill level range of 50 to 75% (Maynard, 2007). The shape of most tumblers is asymmetrical to reduce the effects of centripetal force (which is prevalent in circular shaped mixers) and hence ensure homogeneity of the mixed powder. Polymer LS powders are mixed using the tumbler type of mixers, in particular, concrete mixers. Most AM centres, such as the Centre for Rapid Prototyping and Manufacturing (CRPM) at Central University of Technology, Free State (South Africa), use tilting drum mixers, such as the one shown in Figure 2.13.

Figure 2.13 Concrete mixer used at CRPM

The powder mixture is loaded into the drum, set to a suitable axis of rotation, preferably inclined at 15^0 to the horizontal, as shown in Figure 2.21 (Ferraris, 2001). The powder is then mixed by rotating the mixer for an appropriate period and then discharged, as shown in Figure 2.14. Poux et al. (1991) proposed that the most suitable mixing time lies between 2 to 10 minutes.

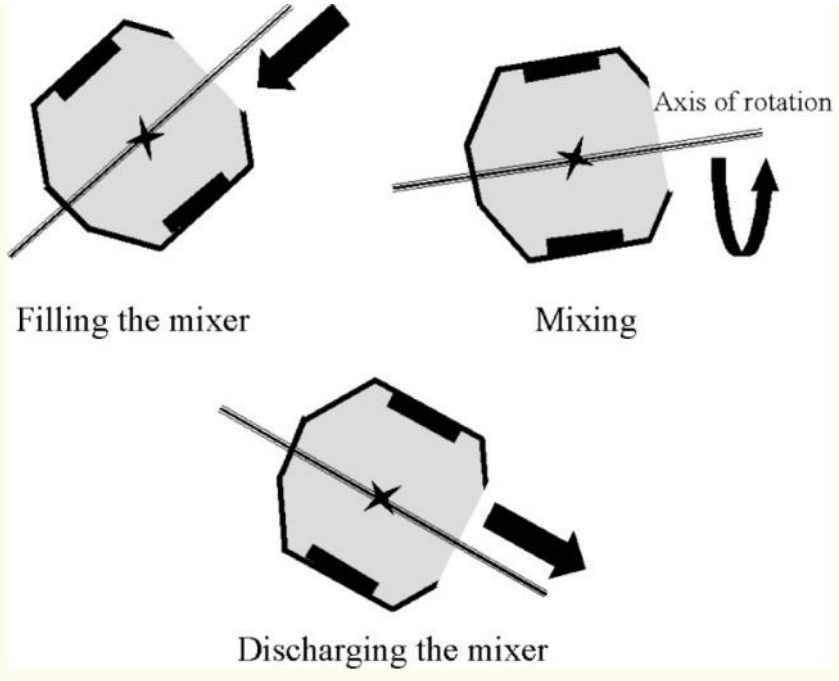

Figure 2.14 Operating process of a tilting drum concrete mixer (Ferraris, 2001)

Drum concrete mixers are preferred for mixing polymer powders because they are easy to use and maintain. Moreover, they are relatively inexpensive and easy to install. Furthermore, their speed is between 5 and 25 revolutions per minute, which reduces the chances of centripetal and centrifugal forces (Ferraris, 2001). Besides, these types of mixers can handle relatively large amounts of powder.

2.4.7 Other Methods to Address the Effects of Heating on Polymer

Apart from mixing aged polymer powder with virgin material, the deleterious effects of heating polymers can be addressed through either enhancement of the powder or process modification approaches. Some other techniques include mixing used powder with flow and antistatic agents and adopting low-temperature LS processes.

2.4.7.1 Adding flow and antistatic agents

The flowability of polymer powders for LS can be improved by using fillers and additives, such as flow and antistatic agents. Flow agents less than 1 µm in size are commonly used to this end and include fumed silica, glassy oxides, metallic stearates, or fluoroplastics (Lexow & Drummer, 2016). Axalta Product Systems, for instance, recommends that their commercial PP powder be mixed with at least 0.25 wt% fumed nano-silica composite

(SiO_2) from the same supplier (Lexow & Drummer, 2016). These flow agents are added to powder particles through a dry particle coating process, as illustrated in Figure 2.15. The flow agents reduce the contact surface area of the powder particles, which then reduces the adhesion force between the powder particles and promotes smooth powder flow.

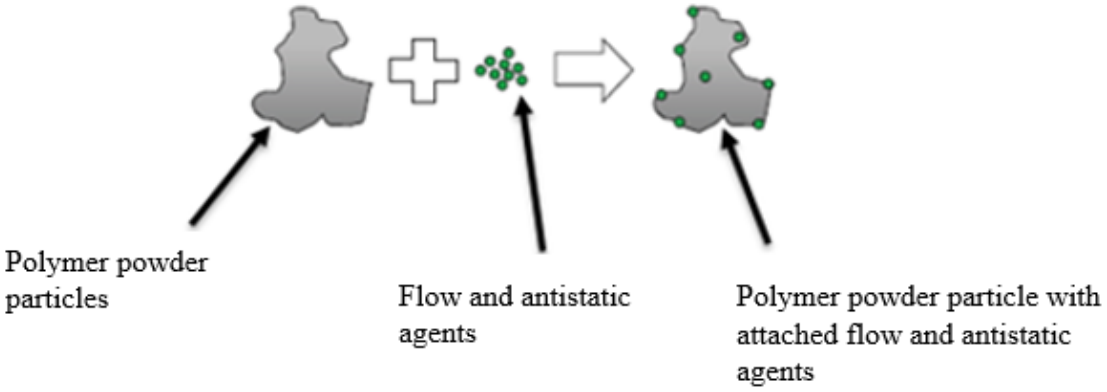

Figure 2.15 Dry particle coating process (Lexow & Drummer, 2016)

Antistatic agents eliminate static charge in plastics, reducing the agglomeration of the powder particles, which encourages free-flowing characteristics of the polymer powder (Lexow & Drummer, 2016). There are various antistatic agents available for polymers, including ethylated alkylamines and fatty acid esters, the most commonly used antistatic agents in polyolefins. Antistatic agents can be used in percentages of 0.05 to 1.5% by weight depending on the application of the powder. Both flow and antistatic agents affect the properties of the primary material, which reduces the mechanical integrity of the printed parts (Goodridge et al., 2012).

Lexow & Drummer (2016) conducted a study on PP and found that the flowability of the powder was increased by the addition of both flow and antistatic agents. Besides, they determined that flow agents increased the bulk density of PP. Details of these two phenomena are presented in Figure 2.16. However, more research is required to determine the optimum ratio of PP powder to flow and antistatic agents for the number of re-use cycles of the powder and mixing ratios of fresh to used powder.

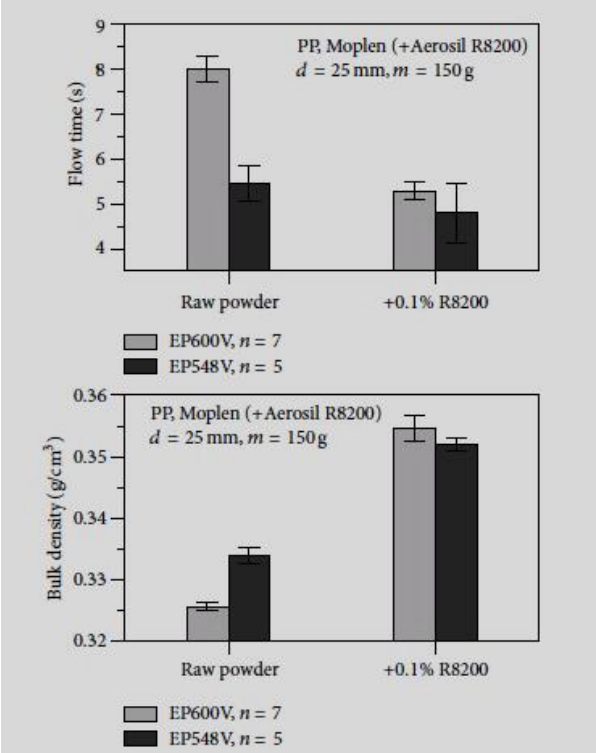

Figure 2.16 The effect of flow and antistatic agents (Lexow & Drummer, 2016)

The process of using both flow and antistatic agents has both advantages and disadvantages. The technique is easy to apply and effectively improves the flowability of used polymeric materials. However, the technique fails to enhance the mechanical properties of printed parts significantly. The method is also sensitive to the ratio between powder and the flow and antistatic agents, influencing the percentage elongation at the breakpoint.

2.4.7.2 Low-temperature laser sintering

LS requires the powder bed and powder temperatures to be maintained between the recrystallization and melting point of the polymer to prevent the components from curling (Schmid et al., 2014). These conditions are the dominant factors that lead to the deterioration of polymeric powders in LS. Yamauchi et al. (2017) proposed low-temperature LS as an alternative. Such a process does not require the powder bed to be maintained at high temperatures. For example, in low-temperature LS, the powder bed temperature of PA 12 is maintained at 130 ℃, as opposed to the normal process where temperatures are maintained at about 170 ℃ (Goodridge et al., 2012; Kigure & Niino, 2017). A comparative analysis between high- and low-temperature LS for PA 12 is shown

in Figure 2.17. The rate of deterioration of powder is lower for low-temperature sintering than for high-temperature LS, as shown by changes of powder relative density and MFR with each build cycle in the two cases.

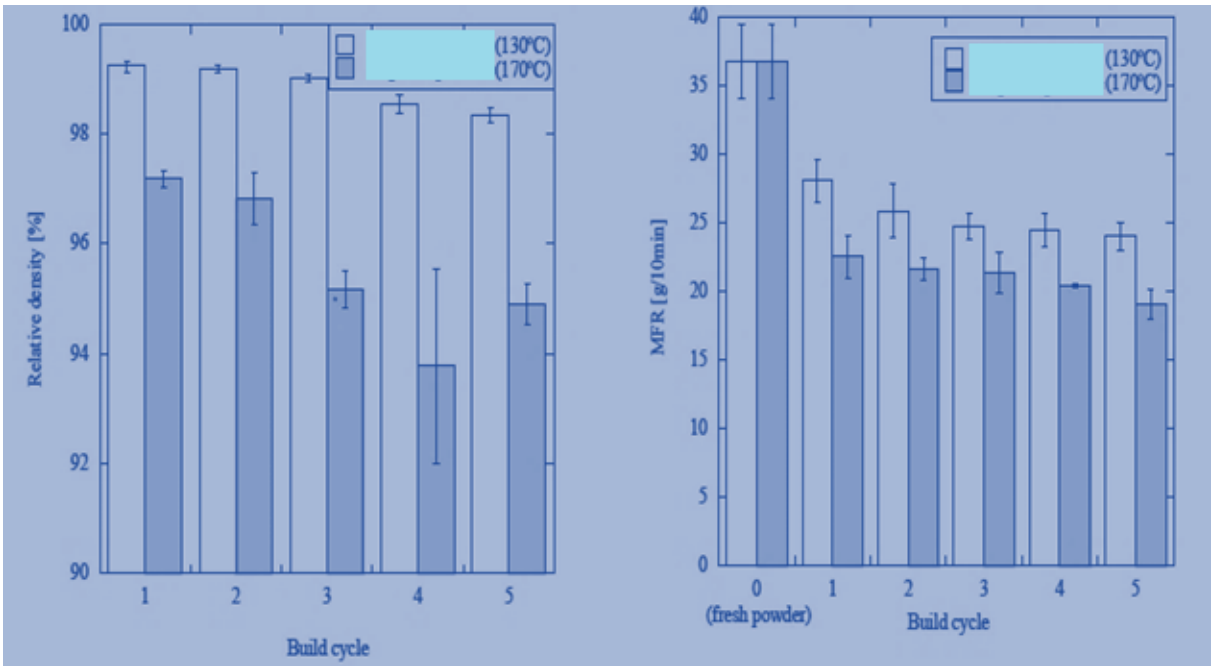

Figure 2.17 Effect of low- and high-temperature LS (Kigure & Niino, 2017)

The proposed low-temperature LS method involves binding the parts to a rigid base, as shown in Figure 2.18, to reduce the effect of curling. The base plate is made from the same material as the build, which is PA 12.

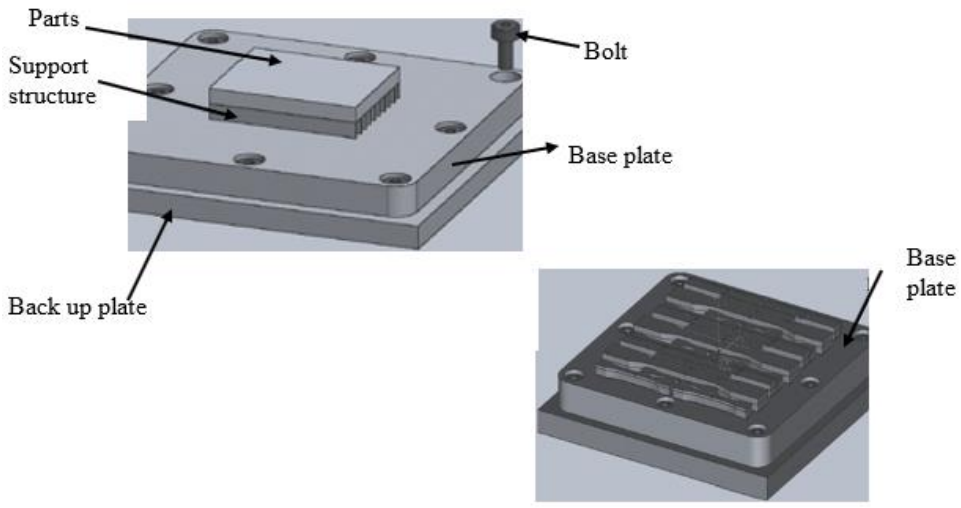

Figure 2.18 A rigid plate used in low-temperature LS (Kigure & Niino, 2017)

Low-temperature LS increases the recyclability of polymeric materials at the expense of lower mechanical and physical properties of the parts due to reduced viscosity and less coalescence of the powder particles. Low-temperature LS also reduces the design flexibility since the part is held down on a rigid base. Moreover, different bases need to be constructed for various parts, which is time-consuming and may not be feasible. Post-treatment is required to prevent the parts from curling once removed from the base plate.

2.4.8 Techniques Employed to Characterize Laser-Sintering Polymers

The standard techniques employed to characterize the suitability of polymeric powders for use and re-use in the LS process include laser diffraction, SEM, MFI testing, DSC, and TGA. Characterization can also be performed on the printed components. The standard part-testing techniques include mechanical part testing (elongation at break, tensile strength, and elastic modulus), surface roughness, hardness tests, and part density testing.

2.4.8.1 Laser diffraction technique

Theory: When a beam of light strikes a particle, it undergoes diffraction, reflection, absorption or refraction, as shown in Figure 2.19.

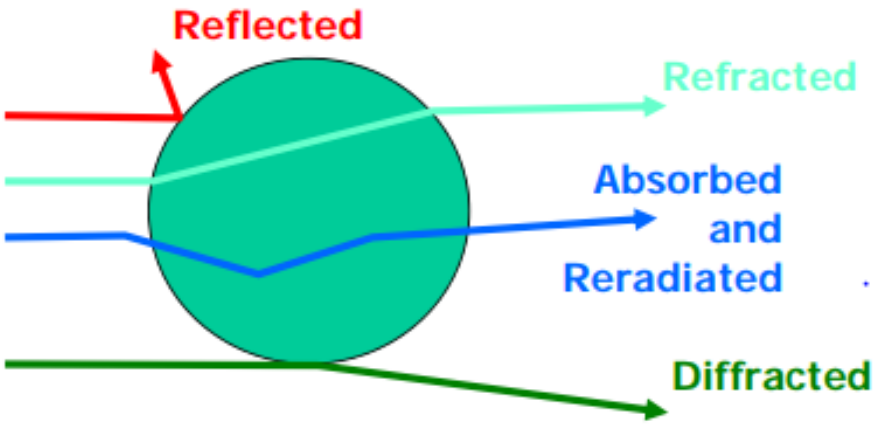

Figure 2.19 A beam striking a particle (Bodycomb, 2012)

Laser diffraction techniques use diffraction of light to determine the size of the particle, where the software provides results by using Fraunhofer and Mie models. The Fraunhofer theory assumes that all the particles are much larger than the light wavelength. The particle should be at least 40 times the wavelength of the laser beam (Bodycomb, 2012). Therefore, only scattering at the contour of the particles is considered, and the scattering pattern is

similar to that of thin 2D circular disks. When using the Fraunhofer model, only the scattering in the near forward is considered. The Mie theory is used when the particles are much smaller.

The following parameters should be captured when performing a laser diffraction experiment:

1. Make and model of the equipment.
2. Make of dispersant.
3. Run time of the instrument.
4. Refractive index of the sample.
5. Refractive index of the dispersant.
6. Volume mean diameter of the specimen.
7. Volume percent versus diameter of the test specimen.
8. Cumulative volume percent versus diameter of the specimen.

The following are the standard operating conditions for a laser diffraction experiment:

1. The area of operation should be free of electrical noise, mechanical vibration, high or low temperatures, high or low humidity, and excessive light.
2. The technique is suitable for particles in the range of 0.1 microns to 3 millimetres.
3. Proper sampling should be used to ensure that the samples give an accurate representation of the bulk material.
4. The materials and dispersant should be examined before the test to ensure there is no attrition of the particles.
5. The dispersant used in the experiment should have the following properties: it should be transparent, its refractive index should differ from that of the material being tested, it should be compatible with the test equipment, and should not modify the sample specimen through solubility or recrystallization.
6. The test sample concentration should be appropriate to ensure that the machine and the operating conditions are met.

The following factors should be reported:

1. Density distribution by volume.
2. Cumulative distribution finer.
3. $X_{10.}$
4. $X_{50.}$

5. X_{90}.
6. Information on sample and preparation.
7. Dispersant used.
8. Equipment used.

2.4.8.2 Scanning electron microscopy

Theory: Scanning electron microscopy (SEM) operates by focusing a beam of electrons from an electron gun onto the test sample using a system of electromagnetic lenses. The SEM equipment consists of an optical column under a vacuum to ensure that the stream of electrons propagates efficiently to the sample and back to the detector (Seyforth, 2015). A schematic of a SEM is shown in Figure 2.20. Tungsten electron guns are commonly used and produce electron beams with high energy (Zhou et al., 2007). The electron lenses that focus the beam of electrons consist of coils of wires that form electromagnets to produce magnetic fields that direct the electron beam. The lenses can also be used to alter the beam's diameter (Zhou et al., 2007). Once the beam of electrons hits the specimen, the secondary electrons, backscattered electrons, transmitted electrons or the specimen current are used to provide signals for SEM observation (Zhou et al., 2007). The magnification of the SEM is subject to the amount of current supplied.

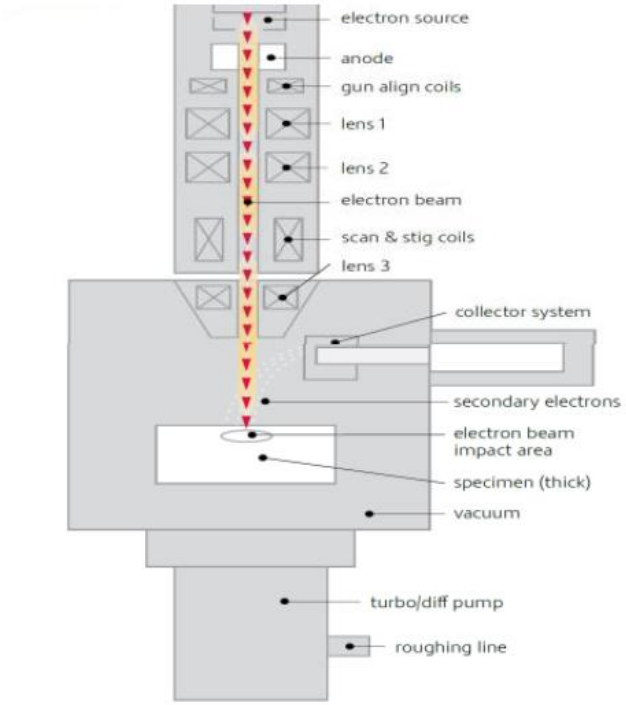

Figure 2.20 Scanning electron microscope (Seyforth, 2015)

The resolution of a SEM is obtained using Equation 2.7.

$$2d = \frac{\lambda}{nsin\theta} = \frac{\lambda}{NA} \quad (2.7)$$

where,

d = size of the smallest resolvable feature in metres

n = refractive index of the medium

NA = numerical aperture

θ = half the angle subtended by the objective lens

λ = wavelength of the incident beam in metres

2.4.8.3 Gas pycnometry

Theory: A gas pycnometer is an instrument that uses a gas such as nitrogen or helium to determine the volume of a particular specimen. Helium gas is preferred because it exhibits ideal gas characteristics. The standard test procedure for pycnomerty include:

1. Weighing and recording the weight of a clean empty sample cell.
2. Filling the sample cell with the specimen up to ¾ of the cell total volume. Weigh and record the weight of the specimen and the sample cell.
3. Following the manufacturer's instructions, determine the density of the sample: a sample of known weight is placed in one of the two chambers of known volume. The temperature of the system is kept constant. After adding the test material, helium is added to the equipment. Run the machine after entering the recommended parameters.

The following information should be captured in pycnometry measurement:

1. Sample ID.
2. Measured skeletal volume and associated statistics.
3. Calculated skeletal densities.
4. Sample mass.
5. Gas used.

The true density of the PP can be determined using the formula presented in Equation 2.8:

$$density\ \left(\frac{kg}{m^2}\right) = \frac{mass\ (kg)}{volume\ (m^3)} \quad (2.8)$$

2.4.8.4 Melt flow test

This process uses a melt flow index (MFI) tester consisting of a 2.16 kg test load, charging rod, cleaning rod and a die ejector. The tungsten carbide die has a diameter of 2.095 mm. The testing process begins by cleaning the die using the cleaning tool and a special cleaning paper. After cleaning, about 6 grams of the powder sample is loaded into the barrel. The piston with a mounted test load is inserted in the barrel and the powder in the barrel is preheated for about 6 minutes at 230 ℃. The time taken for the piston to move between two marked points is measured (International Organisation for Standard (ISO), 2010). The mass of the ejected polymer material is also determined using an electronic weighing machine, and the value of MFI calculated using Equation 2.9.

$$\text{MFI} = \frac{600 \times \textit{measured mass of the ejected polyamide material}}{\textit{time taken to eject the polyamide material between the marked points of the ejector}} \quad (2.9)$$

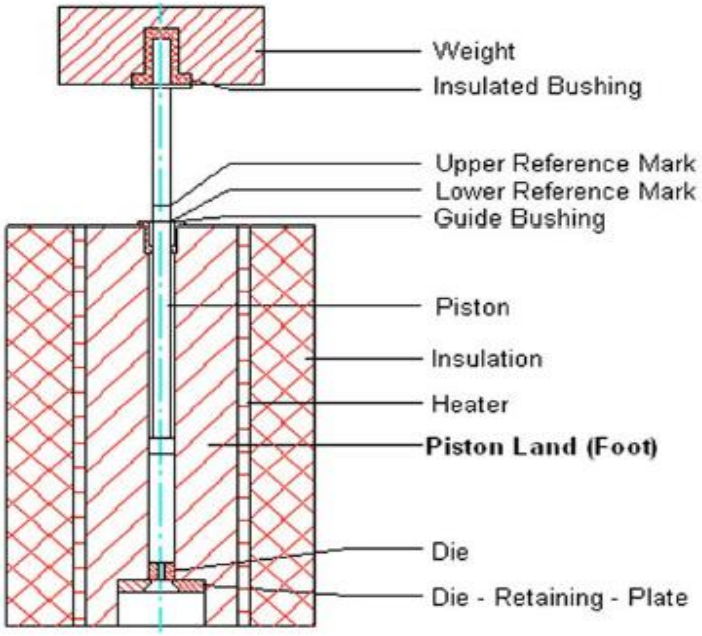

Figure 2.21 An extrusion plastometer (ISO, 2010)

2.4.8.5 Differential scanning calorimetry and thermal gravimetric analysis

2.4.8.5.1 Differential scanning calorimetry

Differential scanning calorimetry (DSC) is a thermal analysis tool used to monitor the changes in heat capacity of a material with temperature changes. A DSC apparatus is illustrated in Figure 2.22. During the process, a sample of known mass is heated or cooled,

and the alterations in heat capacity of the material concerning changes in heat flow are tracked. Therefore, the technique allows for identifying transitions such as melting point, crystallization point, glass transition, and phases changes.

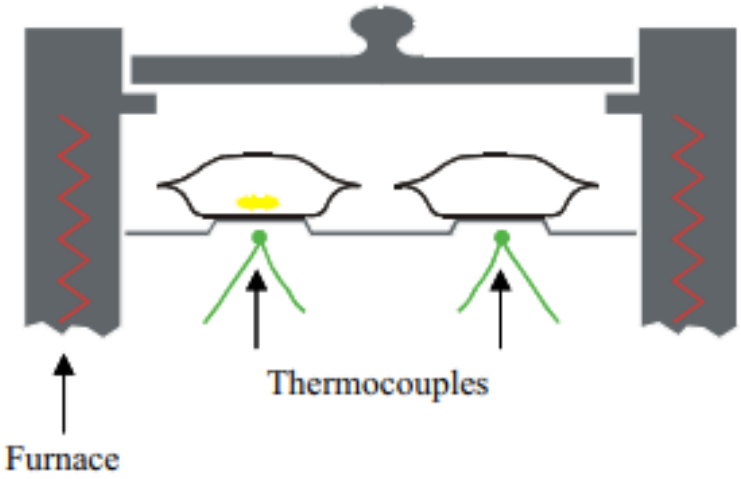

Figure 2.22 A DSC experimental setup (Schick, 2009)

Interpreting DSC data

A typical DSC curve is shown in Figure 2.23.

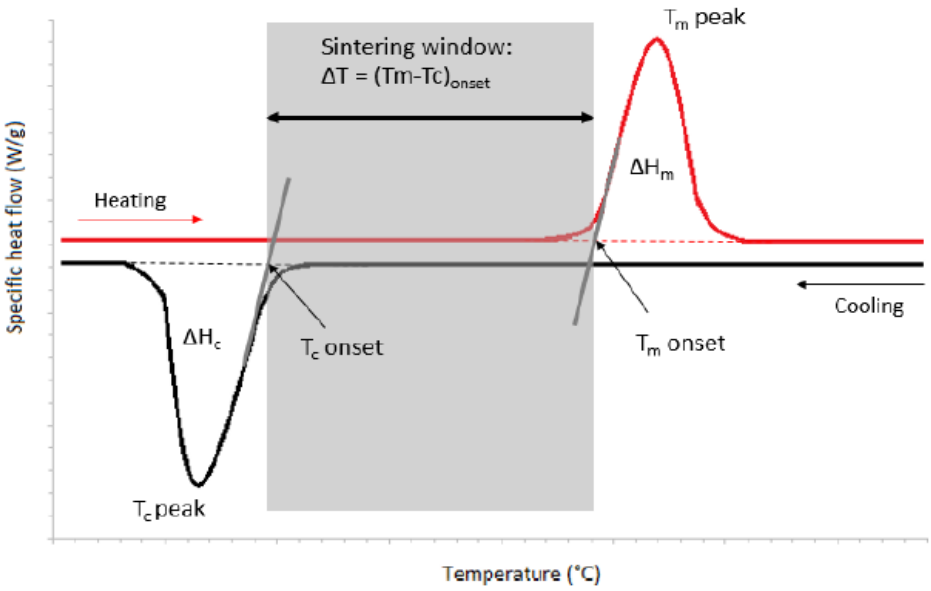

Figure 2.23 Typical example of a DSC result (Marin, 2017)

From Figure 2.23, the following parameters can be obtained: onset of melting and crystallization points, peak melting and crystallization points, sintering window, and degree of crystallization. The sintering window for powders is defined by Equation 2.10.

$$Sintering\ window = (T_m - T_c)_{\text{onset}} \quad (2.10)$$

where,

Tm = onset melting point

Tc = onset crystallization point

The degree of crystallization (C%) is defined as:

$$(C\%) = (\Delta H_m / \Delta H_m^0) \times 100\% \quad (2.11)$$

where,

ΔH_m = experimental melting enthalpy

ΔH^0_m = theoretical melting enthalpy of the material

The theoretical melting enthalpy of 100% crystalline PP = 209 J/g (Wypych, 2012).

2.4.8.5.2 Thermogravimetric analysis

Theory: Thermogravimetric analysis (TGA) is a tool used to determine the state of a compound by monitoring the mass of the substance as a function of temperature or time (Xi et al., 2004). The apparatus comprises a pan supported by a precision balance, temperature programmer, a recorder, and a furnace, as shown in Figure 2.24. During the experiment, the mass of a sample is monitored when heating or cooling. The exercise should be conducted in the presence of an inert gas.

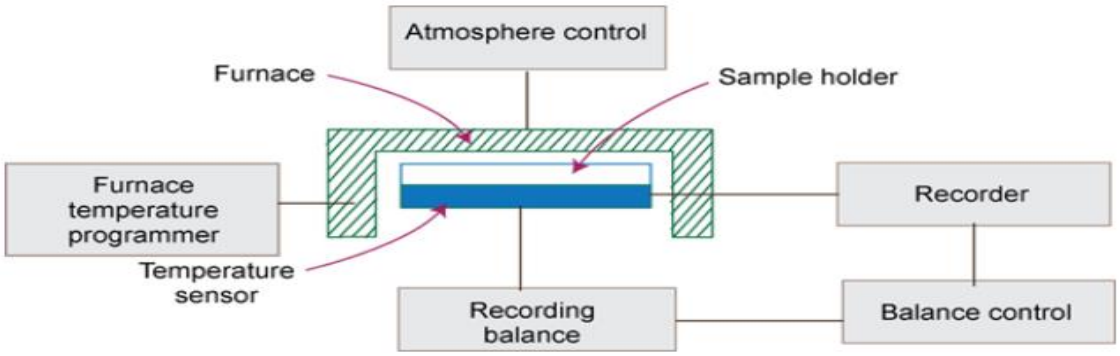

Figure 2.24 Experimental setup for TGA (Xi et al., 2004)

The typical analysis is displayed in a TGA thermal curve shown in Figure 2.25. From the TGA results, the temperature at which a polymer degrades is determined.

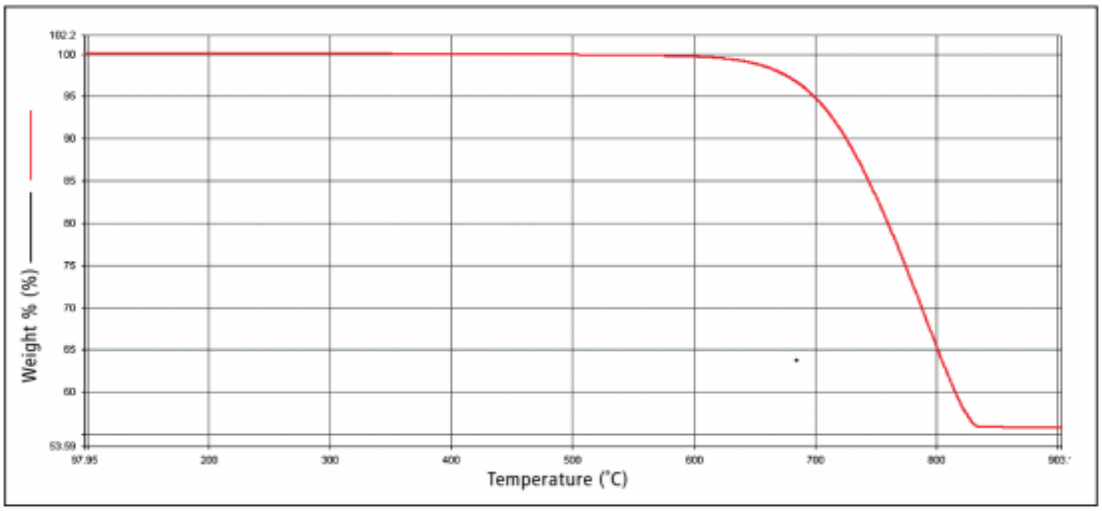

Figure 2.25 An example of TGA thermal curve (Xi et al., 2004)

2.4.8.6 Characterization of the mechanical and surface properties

2.4.8.6.1 Elongation at break, tensile strength, and elastic modulus

Theory: The tensile test is conducted to determine the strength of materials when subjected to a stretching force (Zaborski, n.d.). During this process, samples of standard dimensions are pulled slowly and at a uniform rate to provide information on the strength of the material. The results obtained in a tensile test are usually in the form of stress-strain curves, as shown in Figure 2.26 that provide information such as ultimate tensile strength, yield point, elastic modulus, elongation at break, and reduction in area (Tension Test, 2009). Other characteristics of the material, such as toughness, resilience, and Poisson's ratio, can be determined from tensile testing. Either round or rectangular specimens can be used in this testing.

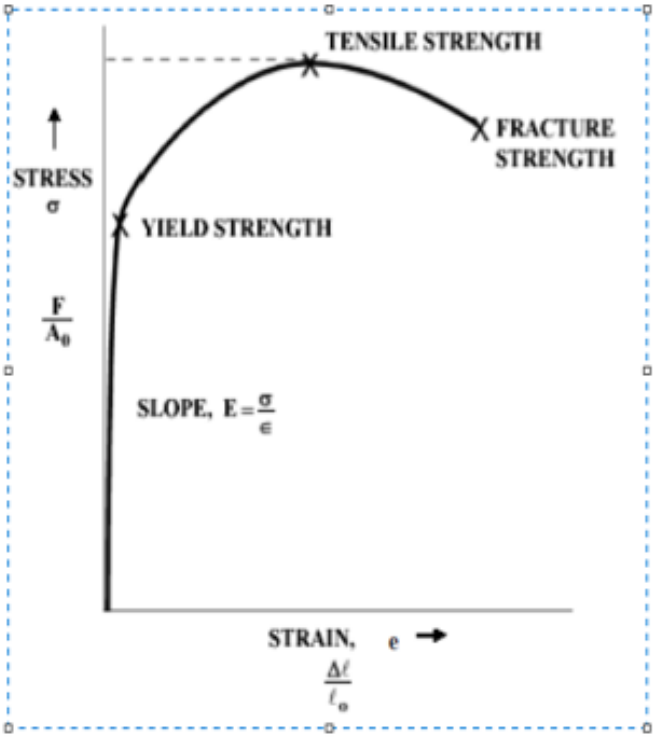

Figure 2.26 A typical stress-strain curve (Tension Test, 2009)

δ = Stress

e = Strain

F = Applied load

A_0 = Initial cross-sectional area of the specimen

l_o = Initial length of the specimen

Δl_o = Change in length of the specimen

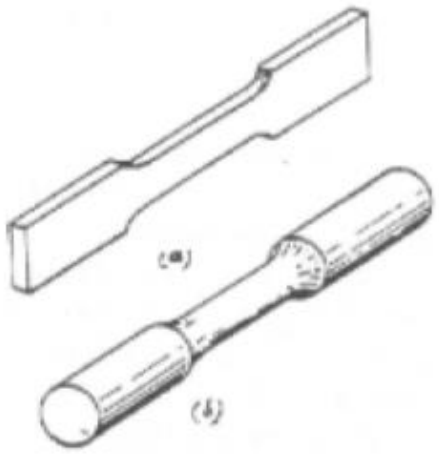

Figure 2.27 Types of tensile test specimens (Tension Test, 2009)

Many machines are used in tensile testing: the most commonly used being the universal testing machine shown in Figure 2.28.

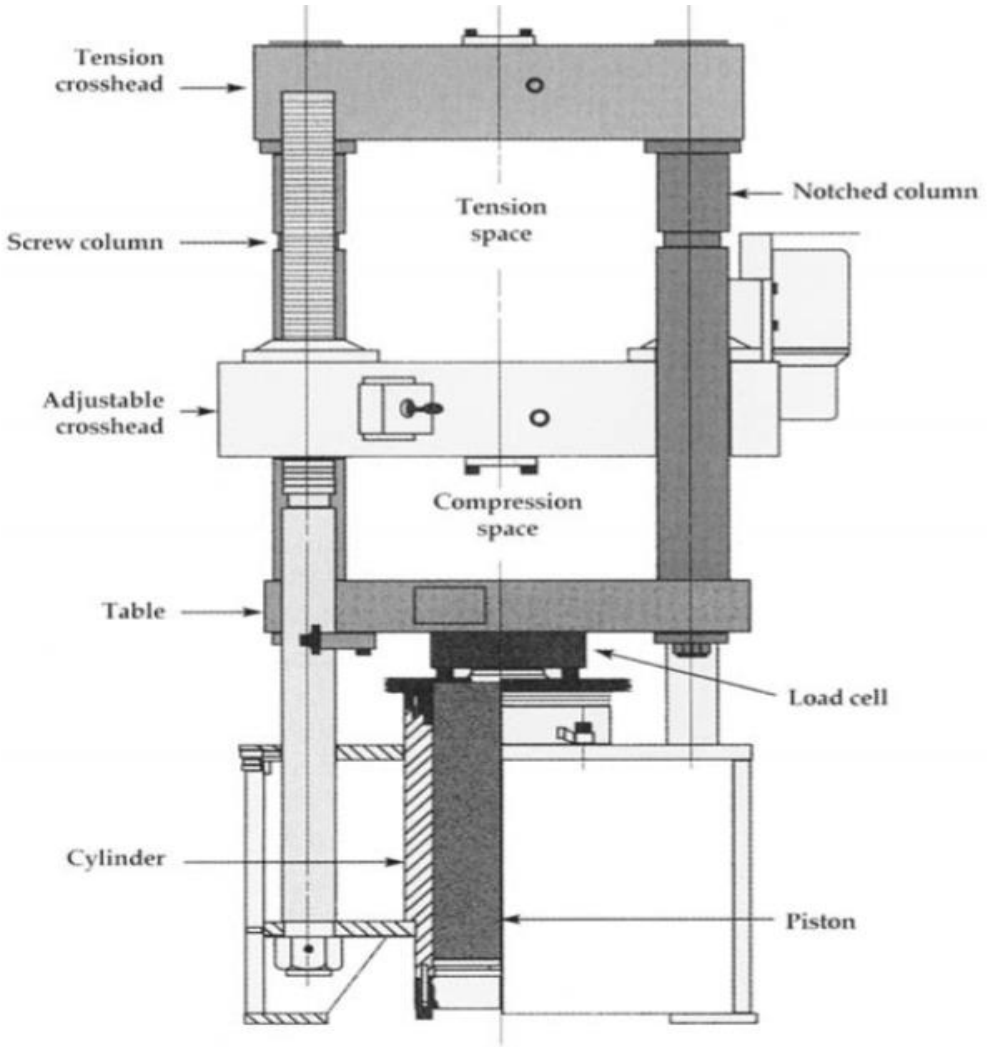

Figure 2.28 Tensile testing machine (ASM, 2004)

2.4.8.6.2 Determination of surface roughness

Theory: Surface roughness defines the surface texture, which embodies tiny scratches and grooved structures, and it represents the height difference between an ideally smooth surface and the actual surface, as illustrated in Figure 2.29 (Chapter 8, n.d). Surface irregularities affect the dimensional accuracy of manufactured components and increase frictional forces for objects that slide over each other (Farkas & Drégelyi-Kiss, 2018). In addition, surface roughness represents the quality of the manufacturing method used. Surface irregularities of manufactured components are characterized using either the contact stylus or laser surface tests (Farkas & Drégelyi-Kiss, 2018).

The contact stylus technique uses a configured probe that slides over the surface to be measured, while laser surface testing uses a laser beam to scan the surface of the component, as shown in Figures 2.30 and 2.31, respectively. The collected data is converted to electric signals, which generate a profile of the surface on a display monitor. The following parameters are determined in a surface roughness test:

Ra – the mean arithmetic deviation of the examined profile
Rz – the greatest height of the profile unevenness
Rp – the height of the largest profile projection
Rq – the depth of the largest profile depression

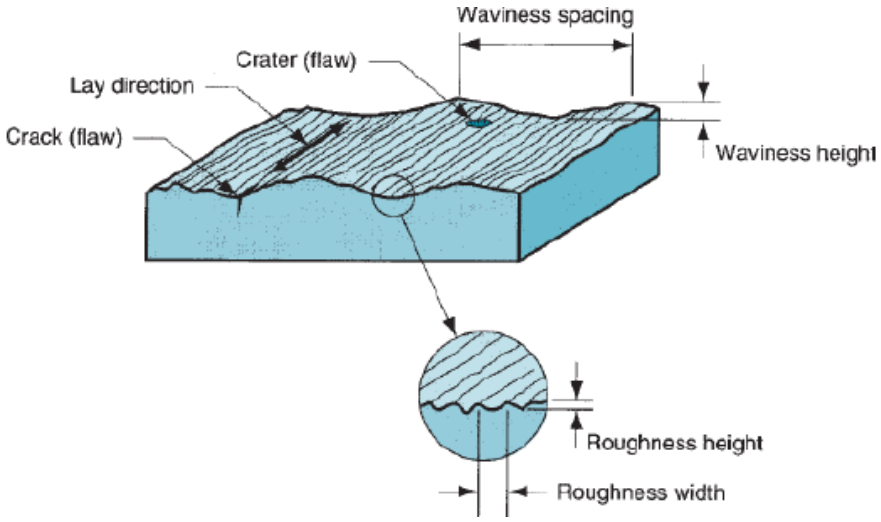

Figure 2.29 Representation of surface roughness (Chapter 8, n.d.)

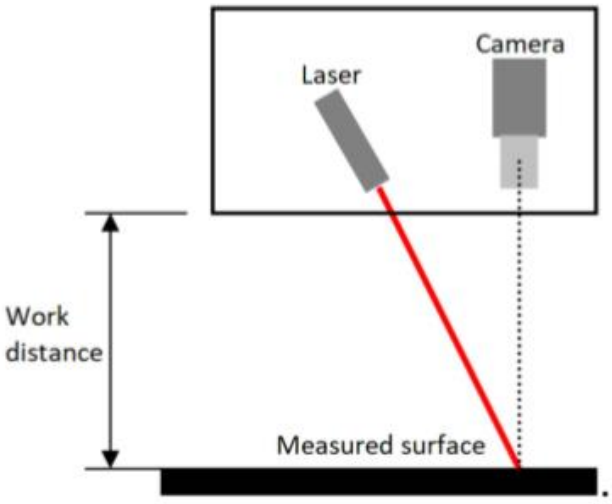

Figure 2.30 Schematic of a laser profilometer (Mital' et al., 2019)

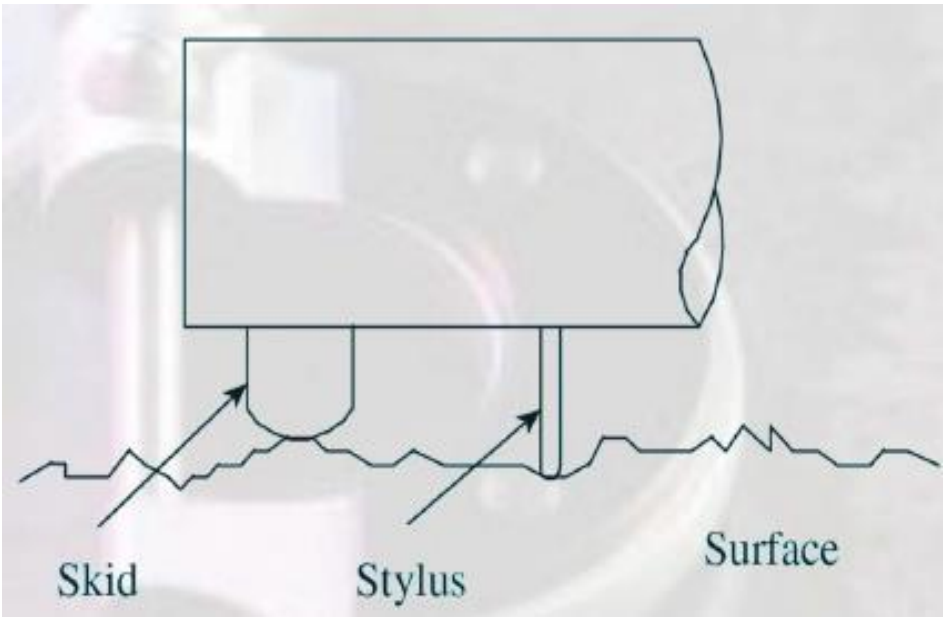

Figure 2.31 A skid and stylus profilometer

2.4.8.7 Dynamic mechanical analyzer

Theory: The dynamic mechanical analyzer (DMA) is the equipment used to determine the properties of polymeric materials as a function of factors such as temperature, time, stress, frequency, or a combination of all these factors (Elmer, 2012). Moreover, the DMA is used to determine the viscoelastic properties of polymers. The elastic response of polymers measures the shape recovery of materials, whereas the viscous response determines the ability of a material to disperse mechanical energy and prevent breakage (Dunson, 2017). The elastic response is measured in terms of storage modulus (E'), while the viscous response is measured using loss modulus (E'').

The DMA involves applying sinusoidal force to a material and provides information on the modulus and the transition phases (Elmer, 2012). A typical DMA consists of a force motor that generates a sinusoidal wave transmitted via a driveshaft to the test material. The sinusoidal stress applied to the test material generates a sinusoidal strain. Other material properties, such as modulus, viscosity, and damping, can be calculated by considering the amplitude of the sine waves and the lag between the stress and strain waves.

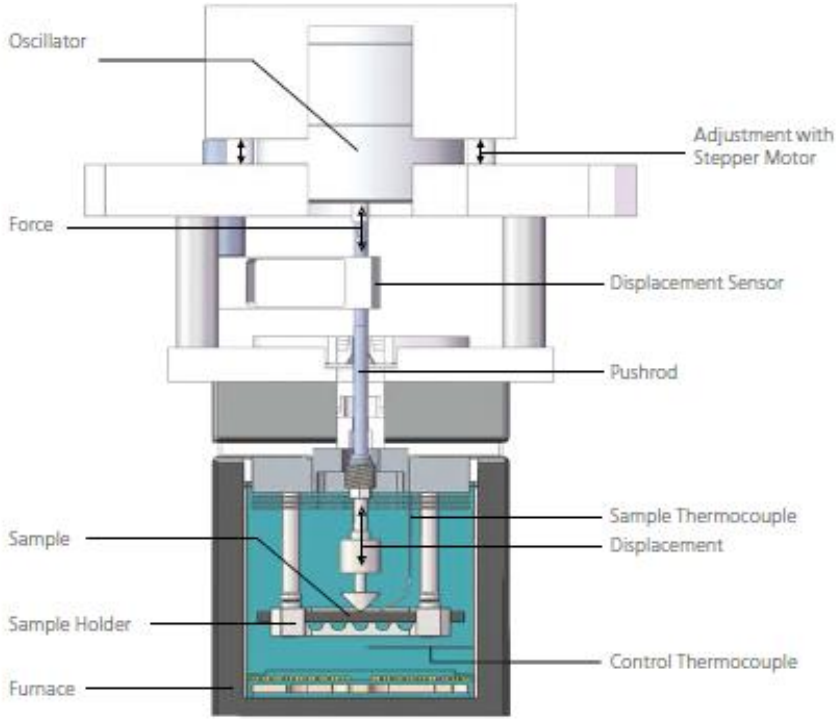

Figure 2.32 An example of a DMA, model 242 EArtemis (Menard, 2015)

Figure 2.33 shows hypothetical sinusoidal stress and strain curves obtained after testing a material sample in a DMA. The phase difference between the strain and stress curves is called phase angle (Dunson, 2017). The relationship between phase angle, storage modulus, and loss modulus is represented by Equation 2.12 as follows:

$$E''/E' = tan\delta \quad (2.12)$$

where,

E'' = Loss modulus

E' = Storage modulus

δ = Phase angle

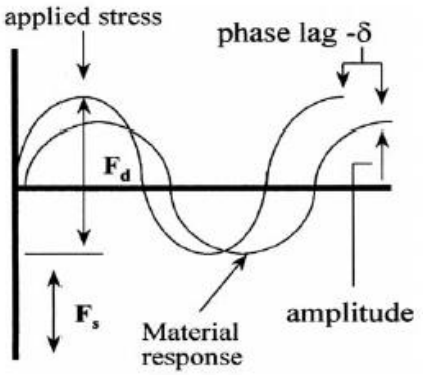

Figure 2.33 DMA sinusoidal stress and strain curves (Menard & Menard, 2015)

The transitions points of a material can be determined using a DMA because the modulus values change with temperature, as shown in Figure 2.34.

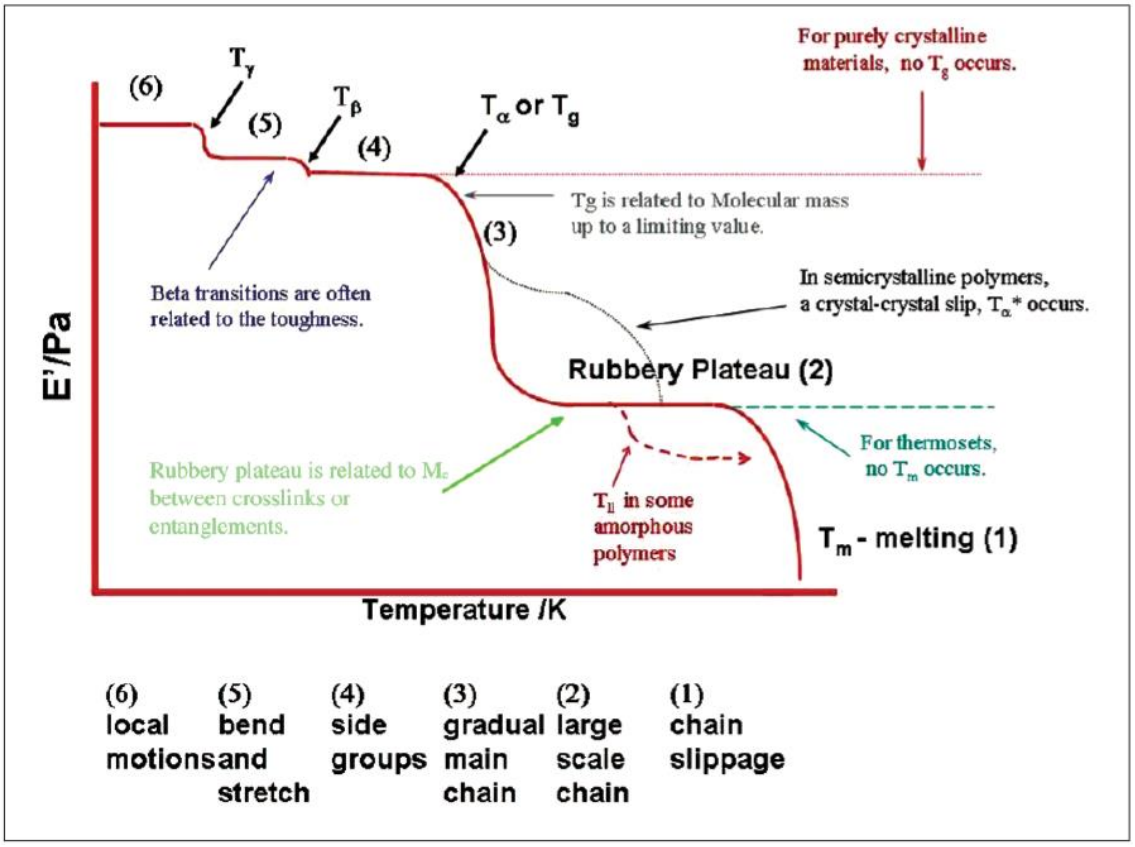

Figure 2.34 The transition points of a polymer from the DMA test (Elmer, 2012)

2.4.8.8 Other tests

1. Bulk density is the ratio of the mass of a polymeric material to the volume occupied by the material (Wudy & Drummer, 2016). This value can be obtained using a bulk density tester. Hausner ratio is a dimensionless number determined by dividing the tapped density of a material by its bulk density. The Hausner ratio determines the flowability of a material. The best flowability is obtained when the Hausner ratio is equal to one. In addition, the Hausner ratio is inversely proportional to the flowability of a material (Wudy & Drummer, 2016).
2. The viscosity number determines the viscosity of a polymeric material (Goodridge et al., 2012). Notably, the bonding of materials during the LS process is subject to melt viscosity. High melt viscosity leads to poor material bonding, which affects the integrity of the manufactured part (Goodridge et al., 2012).

3. The zero-shear tests can be performed on a rotational rheometer. The measurements are usually conducted between 0.005 s−1 and 0.01 s−1 shear rates (Dadbakhsh et al., 2017). In this measurement, powder tablets are commonly used to facilitate loading. These tablets are prepared using a plate press at a temperature and pressure of 80 and 100 bar, respectively (Dadbakhsh et al., 2017).
4. The molecular weight of the powders is determined using gel permeation chromatography (GPC), a type of size exclusion chromatography technique (SEC). The method involves separating the powder particles from the largest to the smallest (Rüsenberg et al., 2012). The molecular weight of the polymer is extracted based on retention time for penetration into a porous material. A 1260 GPC infinity model can be used. This equipment consists of an auto-sampler and a refractive index detector. 1,1,1,3,3,3-hexafluoro-2-propanol (HFIP) (99.5%) is used as the solvent. Potassium trifluoroacetate (0.1 mol/l) should be added to avoid aggregation of PA 12. Before the experiment, the samples must be filtered (Rüsenberg et al., 2012). The samples are dissolved in HFIP at 40, stirred for 24 hours, and then allowed to settle for 12 hours. The injection volume should be set as 20 µl and the flow rate as 0.700 ml/min. During the experiment, the columns should be kept at 30. The results shown in Figure 2.35 were conducted by Rüsenberg et al. (2012) on PA 12 and showed that the molecular weight of PA 12 increases with aging. This can be attributed to post-polymerization and post-chain networking, resulting in the formation of longer chains.

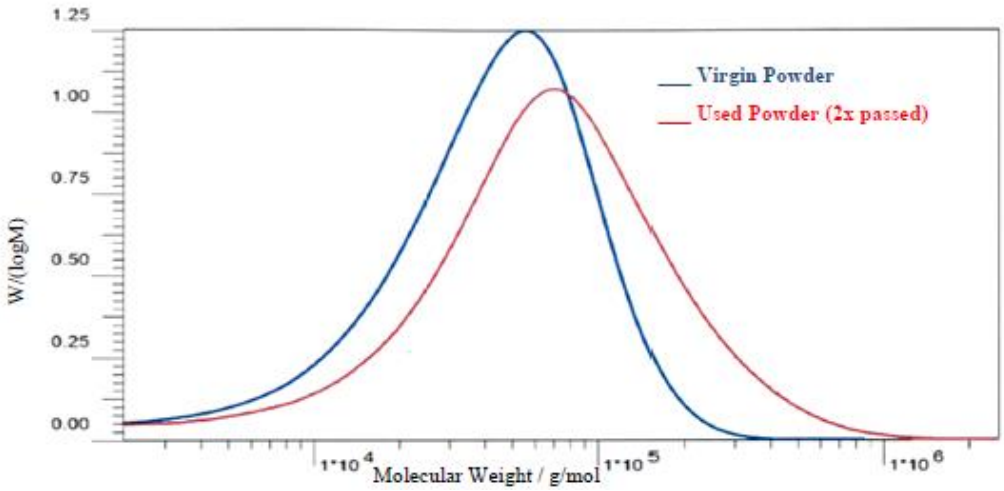

Figure 2.35 Molecular weight of fresh and aged PA 12 (Rüsenberg et al., 2012)

5. Shear punch testing is used to determine the shear strength and adhesion between the sintered layers of powder. The process involves pushing polymeric material through a die

using a pin or punch to exert shear stress on the material. The expression below is used to determine the shear stress.

$$\tau = \frac{F}{2\pi r_{avg} t} \quad (2.13)$$

where,

F = applied force

t = specimen thickness

r $_{avg}$ = average between the radius of the punch and the radius of the die

6. The apparent density can be determined by printing cubes of known dimensions and then measure the masses of the components (Wudy & Drummer, 2016). Density is then established using Equation 2.14, where ρ stands for density, m mass, and v volume. The apparent density can also be determined using micro–Computed Tomography (CT), where the grey values of the calibration disks are determined and the actual density calculated using the calibration function represented in Equation 2.15 (Du Plessis et al., 2013). The grey value is determined using CT and represents the pixels measured (luminance of pixels). The value is dependent on the material's density and atomic number (Du Plessis et al., 2013). Thus, it is the measure of a material's density. The CT technique is preferred because it is more accurate than the conventional approach.

$$\rho = \frac{m}{v} \quad (2.14)$$

Actual density (ρ_a) of a substance (polymer) is equal to:

$$\rho_a = 19.5 \text{ of the grey value} + 0.20 \quad (2.15)$$

2.5 Conclusion

The foregoing literature review provides pertinent information on polymers, especially polypropylene. Crucial information on AM, particularly on LS is also highlighted. It was concluded in the review that LS is a promising technology for processing polymers, but the uptake of the technology is limited because of scarce applicable materials. Therefore, the need for introduction of new materials, such as polypropylene. It was also evident from the review that aging of polymeric materials was a significant hindrance to the wider use of LS of polymers. Hence, the need to investigate recyclability and limits for new materials, such as polypropylene, using different techniques such as, MFI, DSC, and SEM.

CHAPTER 3 - RESEARCH METHODOLOGY

Some of the material presented in this chapter has been published in expanded form in peer-reviewed journals with the details:

1) Mwania, F. M, Maringa, M., & van der Walt, J. G. (2020). Powder Characterization for a New Selective Laser Sintering Polypropylene Material (Laser PP CP 60) after Single Print Cycle Degradation. *International Journal of Engineering Research and Technology, 13*(11), pp.3342-3358. http://www.irphouse.com/ijert20/ijertv13n11_33.pdf
2) Mwania, F. M., Maringa, M., & van der Walt, J. G. (2021). Preliminary Testing to Determine the Best Process Parameters for Polymer Laser Sintering of a New Polypropylene Polymeric Material. *Advances in Polymer Technology, 2021*(1), pp.1-13. https://doi.org/10.1155/2021/6674890

3.0 RESEARCH FLOW

This chapter presents details of the methodologies of the analysis conducted in the present work in accordance with the flow diagram shown in Figure 1. Sub-section 3.1 outlines the procedure for determining suitable processing parameters of Laser PP CP 60 powder, a grade of PP polymer from Diamond Plastics. Sub-section 3.2 provides the procedure for the characterization of Laser PP CP 60 powder. Lastly, sub-section 3.3 outlines the procedure for testing the recyclability of Laser PP CP 75, which is another grade of PP polymer from Diamond Plastics. The initial plan was to investigate the recyclability of Laser PP CP 60. However, due to the processing difficulties observed during the preliminary tests to established optimal process parameters, the focus was shifted to Laser PP CP 75, a modified version of Laser PP CP 60 from Diamond Plastics.

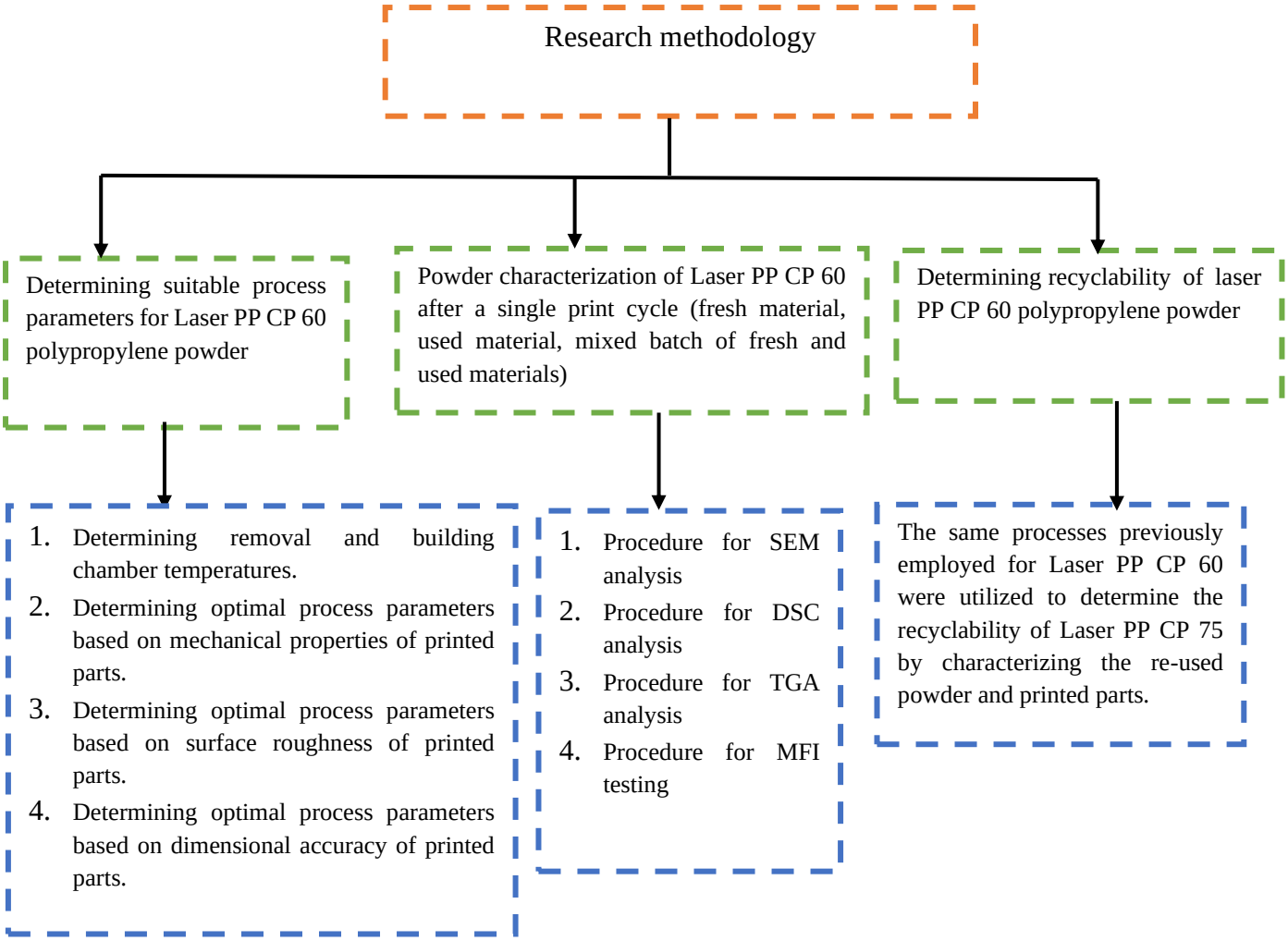

Figure 3.1. Research flow diagram

3.1 SUITABLE PROCESS PARAMETERS FOR LASER PP CP 60

Process parameters influence the mechanical properties, density, hardness, porosity, surface roughness, and dimensional accuracy of printed parts (Zhang & LeBlanc, 2018). Therefore, optimizing the process parameters is crucial in meeting part requirements. Moreover, most of these process parameters are related to each other. For example, a low powder bed temperature requires high laser power and vice versa (Marin, 2017). In addition, a combination of high powder bed temperature and laser power results in dense parts. However, it compromises the recyclability of the unsintered powder due to overbaking of the powder.

Conversely, low power and powder bed temperature result in components with better dimensional accuracy but with low density and leads to delamination of layers (Marin,

2017). Furthermore, low powder bed temperatures and removal chamber temperatures promote part curling, thus affecting the dimensional accuracy of the components and might, in extreme cases, halt the printing process as the recoater blade dislodges parts from the powder bed (Kleijnen et al., 2019). Low laser power requires low scanning speeds, while high laser power requires high scanning speeds to ensure the complete fusion of the powder particles (Marin, 2017). Improper bonding of powder particles encourages porosity, undermining the mechanical strength of printed articles (Marin, 2017). The objective of the present work was to determine the best process parameters for a new commercial PP powder for LS (Laser PP CP 60 from Diamond Plastics). The following process parameters were considered; removal chamber temperature, building chamber temperature, scanning speed fill, laser power fill, scanning speed contour, and laser power contour. The scanning speed fill is the speed of the laser beam as it scans the area of the part in each layer, whereas the scanning speed contour is the speed of the laser beam as it scans the edges of the part in each layer. The laser power fill is the power of the laser beam as it scans the area of the part in each layer, whereas the laser power contour is the power of the laser beam as it scans the edges of the part in each layer. The removal chamber temperature is set to ensure that printed parts cool at a regulated rate, while the building chamber temperature is set to ensure that the powder layer is preheated to a temperature just below the melting point of the material before sintering.

3.1.1 Determining the Best Removal and Building Chamber Temperatures

The best building and removal chamber temperatures were established before embarking on determining suitable process parameters for laser power fill, laser power contour, scanning speed fill, and scanning speed contour. This was carried out by observing the spreading of the powder on the build platform and inspecting the printed parts for the presence or absence of curling. Each build process involved first preheating the process chamber for 120 minutes. Then PP powder was deposited on the machine's building platform to a depth of six millimetres before printing a set of test coupons with the orientations shown in Figure 3.2.

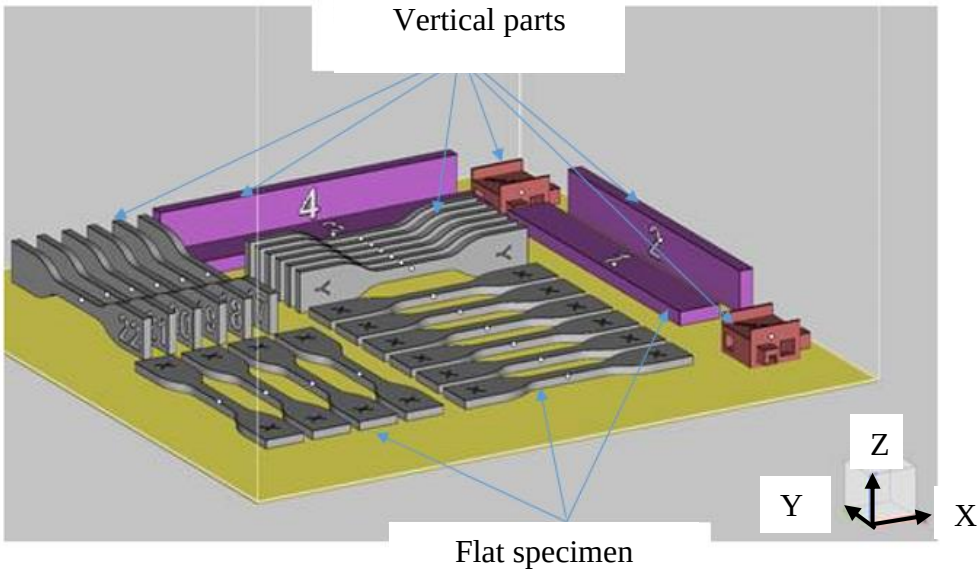

Figure 3.2 Test coupons to determine building and removal chamber temperatures

The parameters for different cycles in the series of builds are shown in Table 3.1.

Table 3.1 Determining the best removal and building chamber temperatures

Cycle	Temp. of the removal chamber (°C)	Temp. of the building chamber (°C)	Layer thickness (mm)	Hatch distance (mm)	Scanning speed fill (mm/s)	Laser power fill (W)	Scanning speed contour/edges (mm/s)	Laser power contour/edges (W)
1	100	120	0.15	0.25	4500	32.6	1500	19.8
2	115	125	0.15	0.25	4000	32.6	1500	19.8
3	120	130	0.15	0.25	4000	32.6	1500	19.8

4	120	125	0.15	0.25	4000	33.7	1500	15.3
5	120	125	0.15	0.25	3000	33.7	1000	15.3
6	125	125	0.15	0.25	4500	33.7	1500	15.3
7	124	125	0.15	0.25	4500	33.7	1500	15.3

3.1.2 Determining the Mechanical Properties of Built Parts

Once the most appropriate building chamber and removal chamber temperatures were established, different standard tensile specimens (ASTM D 638) were printed. These specimens were oriented in the building chamber, as presented in Figure 3.3.

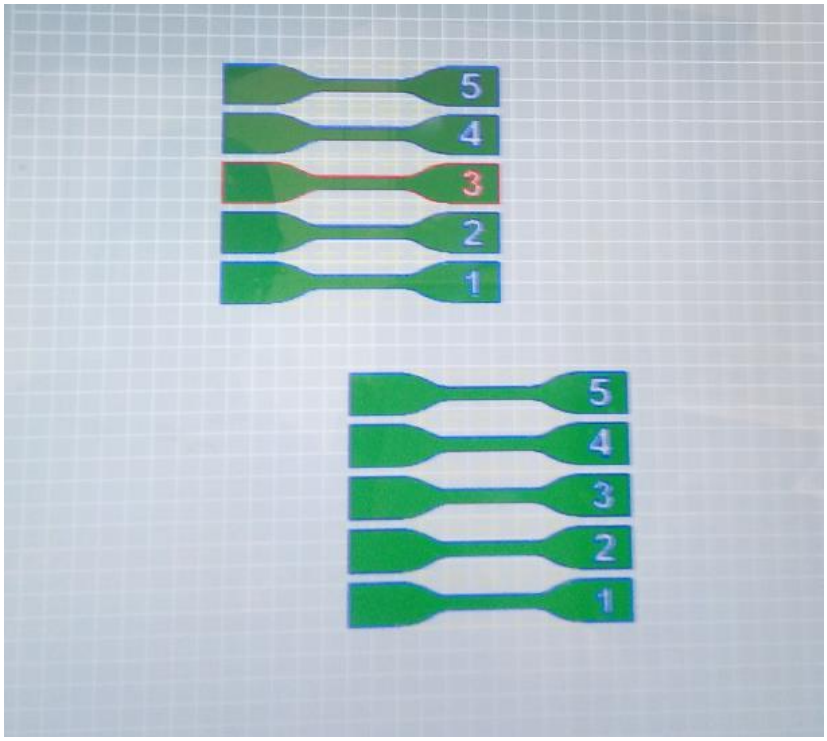

Figure 3.3 Orientation of the labelled test specimens (ASTM D 638)

The values of laser power fill, laser power contour, scanning speed fill, and scanning speed contour used to build each specimen are given in Table 3.2. The variations in the last four columns of the table were introduced from the operator's feel of the process, arising from years of use of the EOSINT P 380 machine with polymer powders.

Table 3.2 The process parameters used for different standard tensile specimens

Specimen	Temp. of the removal chamber (°C)	Temp. of the building chamber (°C)	Layer thickness (mm)	Hatch distance (mm)	Scanning speed fill (mm/s)	Laser power fill (W)	Scanning speed contour/ edges (mm/s)	Laser power contour/ edges (W)
1	125	125	0.15	0.25	2000	23.3	700	9.7
2	125	125	0.15	0.25	2500	25.5	700	13.0
3	125	125	0.15	0.25	2500	30.2	700	13.0
4	125	125	0.15	0.25	3500	31.5	1500	10.7
5	125	125	0.15	0.25	4500	34.7	1500	21.3

The printed specimens were subjected to tensile testing, surface roughness, and tests for dimensional accuracy at different process parameters to determine suitable process parameters for Laser CP PP 60. The built specimens were tested using an MTS Criterion ™, Model 43 universal testing machine. The speed of testing was 1.5 mm/min at room temperature.

3.1.3 Determining the Physical Property of Surface Roughness

The experiment began by calibrating the surface roughness measuring tester (SJ -210), as described in the user manual. The tester was then connected to the display, and the Surftest software launched. The ISO 4287: 1997 standards and a measuring distance of 2.5 mm were used during testing to measure the *Ra* value. The surface roughness of at least eight random areas on each specimen's top and bottom surfaces was recorded, and averages obtained. The *Ra* measurement represents the mean arithmetic deviation of the examined profile, *Rz* measurement the greatest height of the profile unevenness and *Rq* measurement the depth of the largest profile depression (Majchrowski & Morawski, 2015; Farkas & Drégelyi-Kiss, 2018). Small values of these three indicators of surface roughness denote smooth surfaces, and the values increase with increasing surface roughness of a component.

The *Ra* value was used to assess roughness because it provides a general representation of the overall surface roughness of a component.

3.1.4 Determining the Dimensional Accuracy of the Printed Parts

The dimensional accuracy of the printed parts was determined by measuring the dimensions of different sections of the specimen, as shown in Figure 3.4. An electronic Vernier calliper was used to measure the width of the narrow section (*W*), width overall (*WO*), and length overall (*LO*). The measurements obtained were compared to the dimensions of the standard parts as specified in ASTM D 638, presented in Table 3.3.

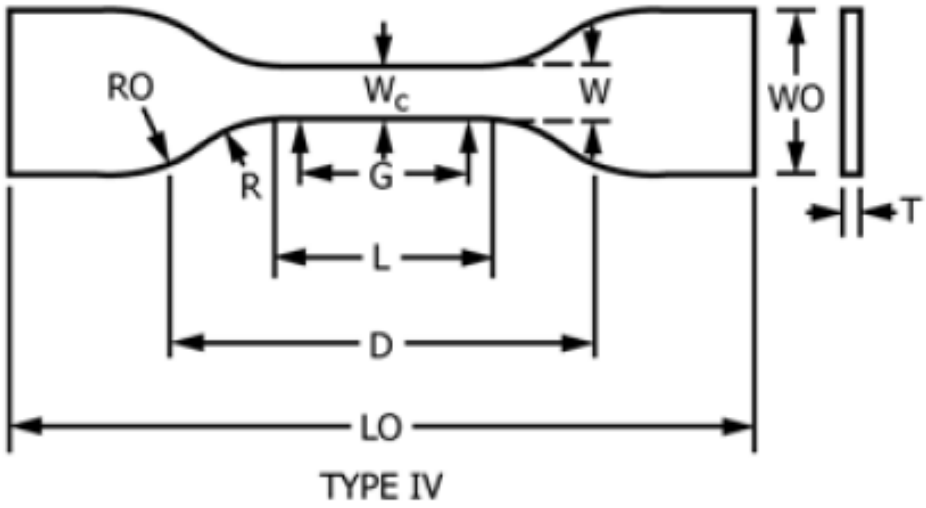

Figure 3.4 Standard tensile test specimen (ASTM D 638) (ASTM)

Table 3.3 Dimensions of the standard tensile test specimen (ASTM D 638)

Parameter	Dimension (mm)
T (thickness)	4
W (width of narrow section)	6
WO (width overall)	19
LO (length overall)	115
G (gauge length)	25
D (distance between grips)	65
R (radius of fillet)	14
RO (outer radius)	25

3.2 CHARACTERIZATION OF LASER PP CP 60 AFTER SINGLE PRINT

Experiments were conducted to characterize a new polymeric powder (PP CP 60) used in LS. Three different batches were tested in the study; virgin powder, used powder and a mixture (50% virgin: 50% used) powder. The three batches of powder were subjected to SEM, DSC, TGA and MFI testing. SEM was used to determine the morphology of particles. The distribution of powder particle sizes was established by analyzing the acquired SEM images using ImageJ software. DSC was used to determine the peak melting point, degree of crystallization, and the sintering window of the powder. TGA was used to determine temperatures of degradation of the powder. Lastly, MFI testing was used to determine the variation of flowability of the powder.

3.2.1 Scanning Electron Microscopy

SEM was conducted with a JEOL JSM-6610LV scanning electron microscope. The samples were first coated with about 6 nm of carbon to avoid supercharging, which affects the quality of the images. Using SEM software, the images were used to determine the morphology of the particles. The accelerating voltage was first set at 25 kV, which was later changed to 30 kV to obtain clearer images. Figure 3.5 shows the carbon coater machine, while Figure 3.6 shows the SEM equipment used in this study.

Figure 3.5 Carbon coater

Figure 3.6 JEOL JSM-6610LV scanning electron microscope

3.2.2 Differential Scanning Calorimetry Testing

DSC was conducted on single samples in a nitrogen atmosphere for three cycles using the Mettler Toledo DSC apparatus shown in Figure 3.7. Approximately six grams of powder was used for each of the three samples considered in the experiment. Furthermore, the heating and cooling cycles were performed between room temperature and 180 ℃ at a rate of 10 ℃/min. The heating and cooling phases were undertaken in a flow of 50 ml/min of nitrogen. The enthalpy of fusion for 100% PP material of about 209 J/g is used here as a reference (Wypych, 2012).

Figure 3.7 Mettler Toledo DSC (821e/700) equipment

3.2.3 Thermogravimetric Analysis

A Mettler Toledo (TGA/SDTA851) TGA apparatus, such as the one shown in Figure 3.8, was employed in this analysis. The powder materials were loaded into the machine using crucibles. Powder samples of about 9.04 g, 10.30 g, and 8.79 g were used for the virgin material, used material and used-virgin mixture, respectively. The samples were heated at 10 ℃/min from room temperature up to 550 ℃ in a nitrogen atmosphere.

Figure 3.8 Mettler Toledo (TGA/SDTA851) TGA apparatus

3.2.4 Melt Flow Index Testing

MFI testing was done using a tester from Ametex Ltd., shown in Figure 3.9, consisting of a 2.16 kg test load, charging rod, cleaning rod, tungsten carbide die with a capillary diameter of 2.095 mm and a piston. The testing process began by cleaning the barrel and die using the cleaning tool and a cotton cloth. After cleaning the barrel, about six grams of powder sample was loaded into it. The piston with a mounted test load was inserted into the barrel and the powder then preheated for about 6 minutes at 230 ℃ (as recommended by the manufacturer). The time taken by the piston to move between two marked points was then measured.

Figure 3.9. MFI Tester from Ametex Ltd.

3.3 DETERMINING THE RECYCLABILITY OF LASER PP CP 75

The methodology for testing the recyclability of PP involved printing a set of test coupons at pre-determined positions in the build volume of an EOSINT P 380 laser sintering AM machine (shown in Figure 3.10). The manufacturer's parameters were used for the Laser PP CP 75, except for the process and removal chamber temperatures, as illustrated in Table 3.4. The PP powder remaining in the machine and the cake powder surrounding the coupons was thoroughly mixed using a concrete mixer for 30 minutes, and a sample of the mixed powder was taken and kept for analysis. Table 3.5 summarizes the mass of the cake, overflow and supply powders for the re-use cycles. After the 1st cycle, only ten kilograms of powder was used (five kilograms for each supply bin). This explains the significant difference in mass between the 1st and 2nd cycles. The powder was then re-introduced into the machine and another set of test coupons produced. Five cycles of printing and four cycles of re-use of the powder were carried out, and the mass of cake, overflow and supply powders in each cycle recorded. The printing and cooling times for each cycle were about two hours, respectively. The building chamber was preheated for four hours for each cycle. Batches of powder sampled at each cycle were assessed using MFI testing, SEM, DSC and TGA analysis. The printed parts were subjected to physical inspection, tensile testing and measurements to assess their dimensional accuracy. The same processes for these tests described in sub-section 3.2 were employed here except for tensile testing, where ISO 572-2 standard was employed at an elongation rate of 1 mm/min.

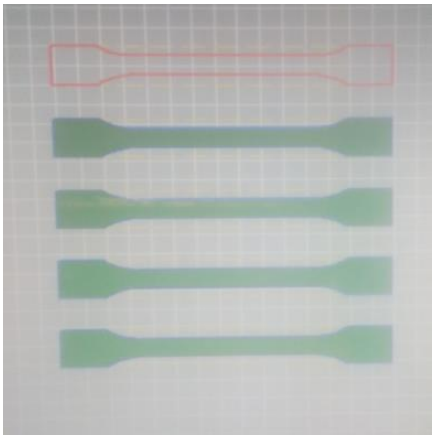

Figure 3.10 The set of test coupons at pre-determined positions

Table 3.4 Parameters for recyclability of Laser PP CP 75

Temp. of the removal chamber (°C)	Temp. of the building bed (°C)	Layer thickness (mm)	Hatch distance (mm)	Scanning speed fill (mm/s)	Laser power fill (W)	Scanning speed contour/edges	Laser power contour/edges (W)
125	128	0.15	0.25	4500	35.0	1500	20.0

Table 3.5 Mass of the cake, overflow and supply powders

Cycle number	Mass of cake powder (kgs)	Mass of supply bin powder (kgs)	Mass of overflow powder (kgs)
Cycle 1	4	13	1.5
Cycle 2	0.89	8.94	0.20
Cycle 3	0.92	7.91	0.57
Cycle 4	0.91	7.70	0.23

CHAPTER 4 - RESULTS AND ANALYSIS

Some of the material presented in this chapter has been published in expanded form in peer-reviewed journals with the details:

1. Mwania, F. M, Maringa, M., & van der Walt, J. G. (2020). Powder Characterization for a New Selective Laser Sintering Polypropylene Material (Laser PP CP 60) after Single Print Cycle Degradation. *International Journal of Engineering Research and Technology*, *13*(11), pp.3342-3358. http://www.irphouse.com/ijert20/ijertv13n11_33.pdf
2. Mwania, F. M., Maringa, M., & van der Walt, J. G. (2021). Preliminary Testing to Determine the Best Process Parameters for Polymer Laser Sintering of a New Polypropylene Polymeric Material. *Advances in Polymer Technology*, *2021*(1), pp.1-13. https://doi.org/10.1155/2021/6674890

4.0 SUMMARY

This chapter is divided into three sections as outlined in the flow diagram shown in Figure 4.1. Sub-section 4.1 discusses the test results to determine suitable process parameters for Laser PP CP 60 PP powder. Sub-section 4.2 analyses the properties of three batches of Laser PP CP 60 PP (virgin powder, used powder and a mixture (50% virgin: 50% used)) after a single print cycle. Sub-section 4.3 discusses the recyclability of Laser PP CP 75 PP. It is noted that recycling tests for Laser PP CP 60 PP were stopped after the 1st cycle as it exhibited processing difficulties that could not be addressed within the time available for this research project. Recycling tests were alternatively done for Laser PP CP 75 grade

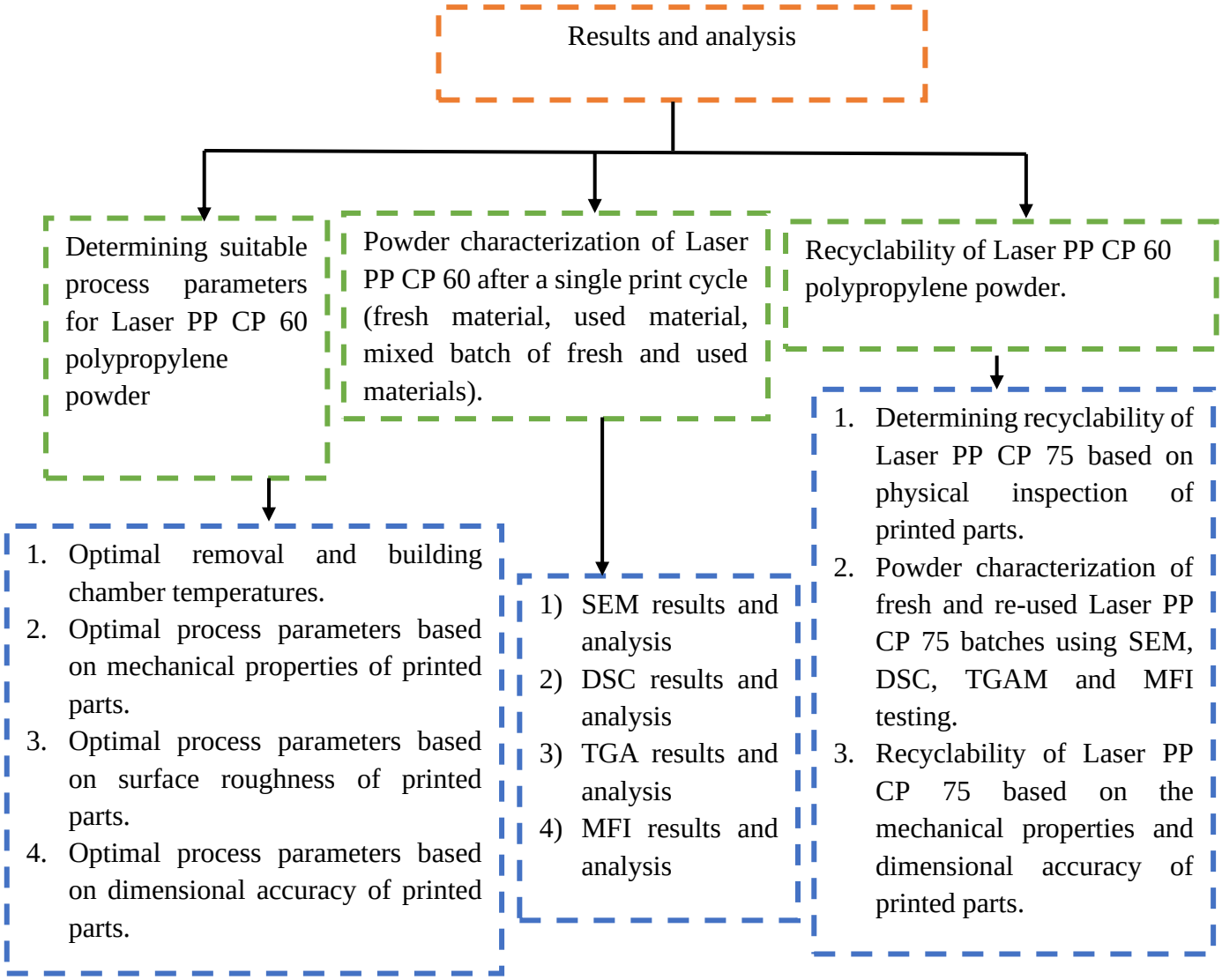

Figure 4.1. Flow diagram of results and analysis

4.1 SUITABLE PROCESS PARAMETERS FOR LASER PP CP 60

4.1.1 Determining the Best Building and Removal Chamber Temperatures

The process parameters and observations made in optimizing the build and removal chamber temperatures are presented in Table 4.1.

Table 4.1 Observations for removal and building chamber temperature test

Set of process parameters #	Temp. removal chamber (°C)	Temp. building phase (°C)	Layer thickness (mm)	Hatch distance (mm)	Scan speed fill (mm/s)	Laser power fill (W)	Scan speed contour/edges (mm/s)	Laser power contour/edges (W)	Observation
1	100	120	0.15	0.25	4500	32.6	1500	19.8	**
2	115	125	0.15	0.25	4000	32.6	1500	19.8	**
3	120	130	0.15	0.25	4000	32.6	1500	19.8	**
4	120	125	0.15	0.25	4000	33.7	1500	15.3	**
5	120	125	0.15	0.25	3000	33.7	1000	15.3	**
6	125	125	0.15	0.25	4500	33.7	1500	15.3	++
7	124	125	0.15	0.25	4500	33.7	1500	15.3	**

** Flat specimens were not grown to completion. ++ Flat specimens were grown to completion.

Seven different sets of process parameters were considered based on the operator's experience. It was observed that none of the specimens listed in Table 4.1 was printed to completion, except for the 6th set of process parameters, where the flat specimens were grown to completion. Figure 4.2 shows printed parts that were dislodged during printing.

Figure 4.2 Printed parts showing minimal curling and dislodged components

Figure 4.2 presents images of the build for the 1st set of process parameters. Similar behaviour was seen for all the other sets of process parameters except for the 6th set. The problem of dislodging of components was due to the curling observed on the edges of the printed parts. Curling is linked to low removal chamber temperatures, which facilitate rapid cooling of the built specimens and cause curling of the edges of the printed parts (Kleijnen et al., 2019). The dislodging of components resulted from the recoater blade picking up the curled components as it moved across the powder bed. It was decided that the removal and building chamber temperatures used for the 6th set of process parameters should be used to determine the best laser power and scanning speed for processing Laser PP CP 60. Furthermore, it was decided that since this was preliminary testing, further research would be conducted where only the removal and building chamber temperatures were varied separately, while all the other parameters were held constant. This is expected to confirm whether this set of process parameters was optimal for the temperatures of the build and removal chambers.

4.1.2 Mechanical Properties of Built Test Specimens

Table 4.2 presents the mechanical properties of five specimens printed using the different laser power and scanning speed process parameters given in Table 3.2.

Table 4.2 Some mechanical properties of built test specimens

Specimen	Elastic Modulus (MPa)	Manufacturer's value (MPa)	Percentage difference (%)	Percentage elongation (%)	Manufacturer's value (%)	Percentage difference (%)	Ultimate tensile strength (MPa)	Manufacturer's value (MPa)	Percentage difference (%)
1	582.8	1000	41.72	426.5	26	93.90	18.4	25	26.40

2	698.8	1000	30.12	470.1	26	94.46	20.0	25	20.00
3	635.5	1000	36.45	483.2	26	94.62	19.5	25	22.00
4	659.2	1000	34.08	462.7	26	94.38	18.0	25	28.00
5	668.4	1000	33.16	507.4	26	94.88	21.2	25	15.20
Average	648.9			470			19.4		
Standard deviation	38.8			26.5			1.1		
Coefficient of Variation	6.0			5.6			5.7		

In Table 4.2, the experimental values of mechanical properties are lower than the values from the manufacturer, with the highest percentage differences being for the stiffness. This raises a need for further investigation of the powder and testing of built specimens to establish the constitution and morphology of the powder and further vet the mechanical properties of the new LS material (Laser PP CP 60). It is notable that all the standard deviations obtained gave rise to values of Coefficient of Variation (CoV) much less than 10% for the elastic modulus, ultimate tensile strength, and elongation at break point of the five test specimens. This is an indication that the effect of the different process parameters on these mechanical properties of the printed parts is not statistically significant.

Figure 4.3 shows bar chart plots of the experimental values of stiffness for each of the five specimens tested, with errors bars clearly shown.

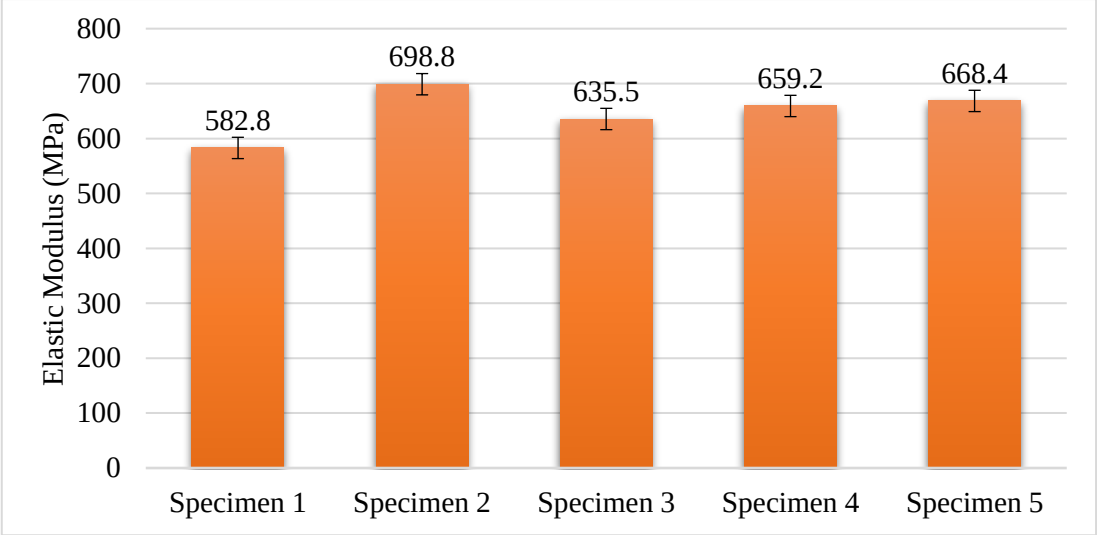

Figure 4.3 Comparison of the elastic modulus for the printed specimens

It is evident from Figure 4.3 that specimen 2 had the highest Young's modulus, followed by specimen 5, specimen 4 and then specimen 3. Specimen 1 had the lowest value of Young's modulus.

Figure 4.4 shows bar chart plots of the experimental values of percentage elongation for each of the five specimens tested, with errors bars clearly shown.

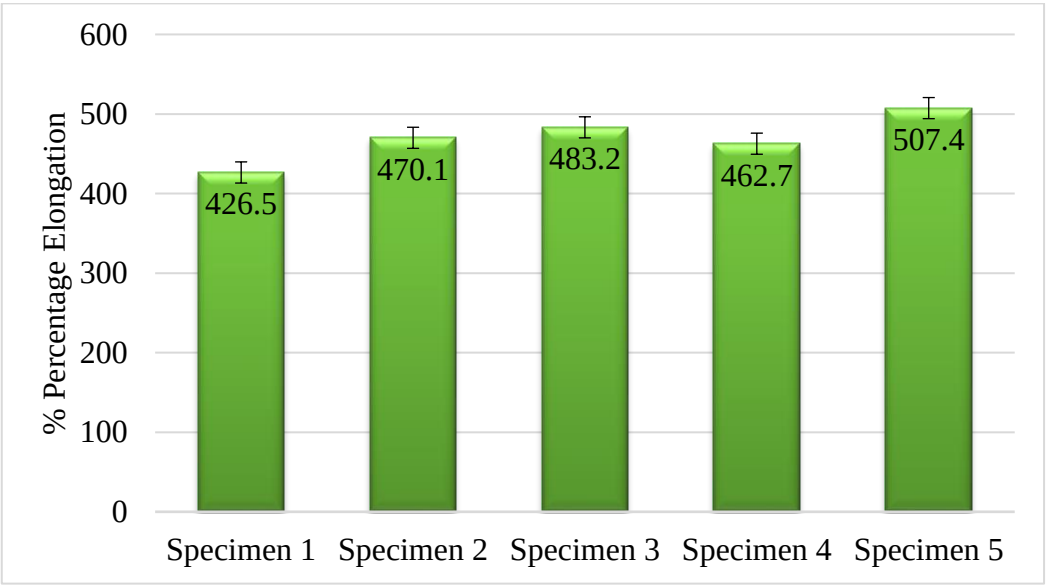

Figure 4.4 Comparison of the percentage elongation % for the printed specimens

The percentage elongation of the specimens in Figure 4.3 in descending order is; specimen 5, specimen 3, specimen 2, specimen 4 and specimen 1.

Figure 4.5 shows bar chart plots of the ultimate tensile strength experimental values for each of the five specimens tested, with errors bars clearly shown.

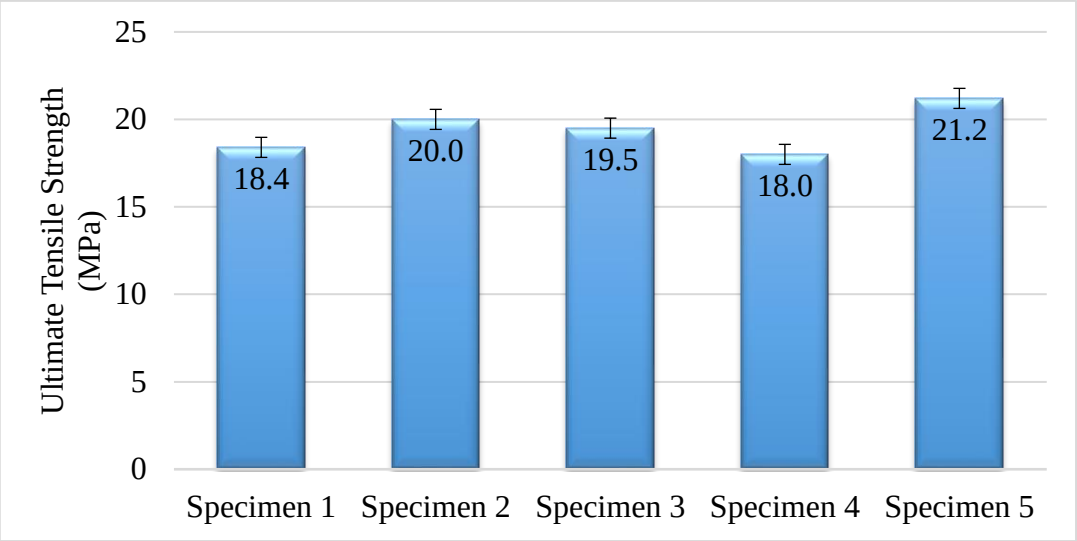

Figure 4.5 Comparison of the ultimate tensile strength for the printed specimens

The strength of the specimens in Figure 4.5 in descending order is; specimen 5, specimen 2, specimen 3, specimen 1 and specimen 4.

For applications requiring high Young's modulus, the process parameters for specimen 2 are recommended. Similarly, for applications necessitating high percentage elongation, the process parameters for specimen 5 are proposed. Lastly, for applications requiring high ultimate tensile strength, the process parameters for specimen 5 were the most suitable. In conclusion, in this preliminary testing, the best process parameters for Laser PP CP 60 are as summarized in Table 4.3, which also shows values recommended by the manufacturer. It is noted from Table 4.3 that these experimentally determined values are very similar to the process parameters provided by the manufacturer except for the removal chamber temperature. It was, however, decided that further research needed to be conducted where only one of the process parameters would be varied at a time while keeping all others constant.

Table 4.3 Experimental and supplier's process parameters for Laser PP CP 60

	Temp. of the removal chamber (℃)	Temp. of the building bed (℃)	Layer thickness (mm)	Hatch distance (mm)	Scanning speed fill (mm/s)	Laser power fill (W)	Scanning speed contour/edges (mm/s)	Laser power contour/edges (W)
Experimentally determined parameters	125	125	0.15	0.25	4500	34.7	1500	21.3
Manufacturer-specified parameters	115	120-125	0.15	0.25	4500	35.0	1500	20.0

It was observed from the experimental work carried out here that Laser PP CP 60 is characterized by relatively low ultimate tensile strength, with significantly high percentage elongation.

4.1.3 Surface Roughness of Built Test Specimens

Table 4.4 provides data on surface roughness for specimens 1, 2, 3, 4 and 5 for both the top and bottom surfaces. Average values and standard deviations are also presented in the table, and a comparison made using the bar charts shown in Figures 4.6 and 4.7.

Table 4.4 Surface roughness of built test specimens

Specimen number	Tested surface	Surface roughness parameter	Average	Standard deviation
Specimen 1	Top surface	*Ra* (µm)	20.206	4.302
	Bottom surface	*Ra* (µm)	19.476	2.043
Specimen 2	Top surface	*Ra* (µm)	21.009	5.589
	Bottom surface	*Ra* (µm)	15.038	1.450
Specimen 3	Top surface	*Ra* (µm)	20.198	4.014

	Bottom surface	*Ra* (µm)	20.075	2.382
Specimen 4	Top surface	*Ra* (µm)	19.616	3.277
	Bottom surface	*Ra* (µm)	14.957	2.190
Specimen 5	Top surface	*Ra* (µm)	20.743	4.049
	Bottom surface	*Ra* (µm)	16.652	3.359

Figures 4.6 and 4.7 show the bar chart plots of surface roughness based on the parameter *Ra* for the top and bottom surfaces of the five specimens tested here, respectively.

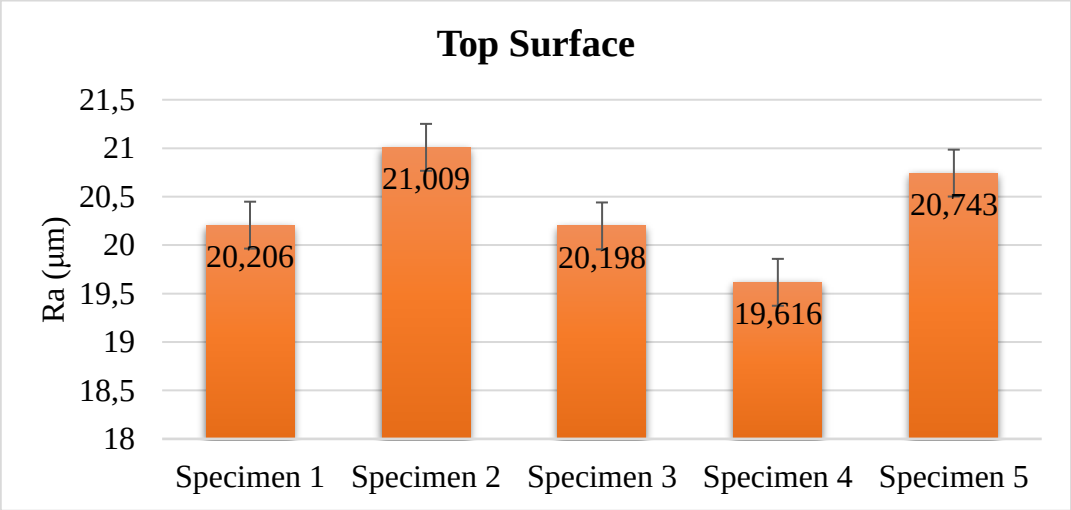

Figure 4.6 The mean arithmetic deviation (Ra) of the top surface of the specimens

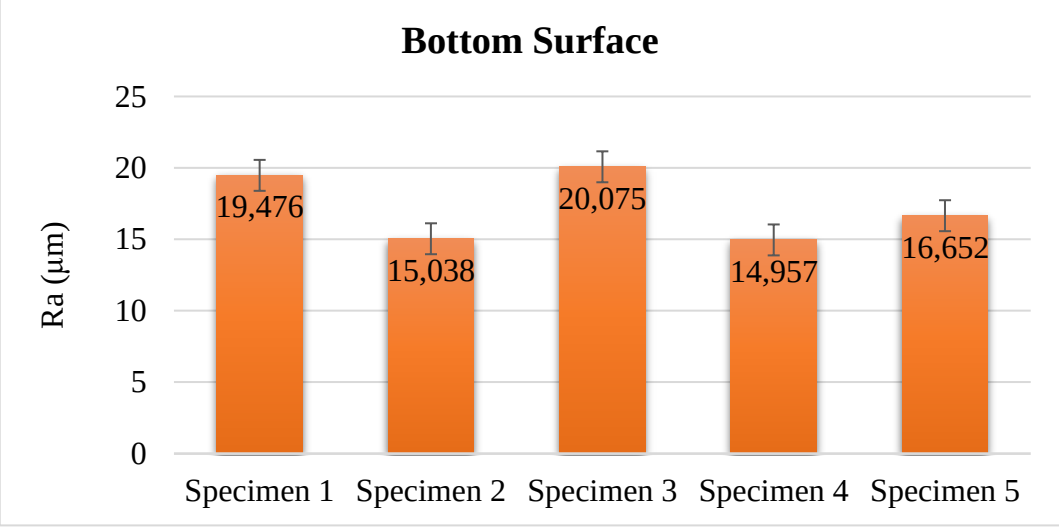

Figure 4.7 The mean arithmetic deviation (Ra) of the bottom surface

The results show that specimen 4 had the smoothest top surface, followed by specimen 3, then specimen 1. Specimen 5 came 4th, while specimen 2 had the roughest top surface. The results show that specimen 4 had the smoothest bottom surface, followed by specimen 2, then specimen 5. Specimen 1 came 4th, whereas specimen 3 had the roughest bottom surface. Considering PA 12 grade PA 220 from EOS as the reference material, as it is by far the most widely used polymer in LS, the surface roughness (*Ra*) of polymers should be approximately 15 µm (Guo et al., 2018). Specimen 2 gives the mean arithmetic deviation of the bottom surface (15.038 µm) closest to the selected reference value. The difference between this specimen and others implies the need for post-process grinding to improve the surface finish of components manufactured using Laser PP CP 60.

The process parameters used for specimen 4 gave the best top and bottom surface roughness since the sample yielded the lowest value of *Ra*. Therefore, for low surface roughness, Laser PP CP 60 should be printed using the process parameters set to produce specimen 4, as summarized in Table 4.5. However, further surface roughness testing should be done on three-dimensional parts where roughness is also measured on vertical surfaces across layers since surfaces at angles present the worst surface roughness because of the staircase effect across layers.

Table 4.5 Best process parameters for Laser PP CP 60 based on surface roughness

Source of parameters	Temp. of the removal chamber (°C)	Temp. of the building bed (°C)	Layer thickness (mm)	Hatch distance (mm)	Scanning speed fill (mm/s)	Laser power fill (W)	Scanning speed contour/edges (mm/s)	Laser power contour/edges (W)
Experimentally determined parameters	125	125	0.15	0.25	3500	31.5	1500	10.7

Manufacturer-specified parameters	115	120-125	0.15	0.25	4500	35	1500	20.0

4.1.4 Dimensional Accuracy of the Printed Parts

Dimensional accuracy was determined by measuring the length (*LO*), the width (*W*), and the overall width (*WO*) of specimens. The data obtained is presented in Tables 4.6, 4.7, and 4.8, respectively.

Table 4.6 Length (*LO*) of the test specimens

Specimen number	Ave LO1 (mm)	Ave LO2 (mm)	Ave LO3 (mm)	Total average (mm)	Standard deviation	Coefficient of Variation	Reference value (mm)	Percentage difference (%)
Specimen 1	112.03	111.96	112.16	112.05	0.08	0.07	115	3%
Specimen 2	112.59	112.66	112.46	112.57	0.08	0.07	115	2%
Specimen 3	113.10	113.26	112.49	112.95	0.33	0.29	115	2%
Specimen 4	112.29	112.29	112.47	112.35	0.08	0.07	115	2%
Specimen 5	112.42	111.63	112.33	112.13	0.35	0.31	115	2%

Table 4.7 Width (*W*) of the gauge length of the test specimens

Specimen number	Ave W1 (mm)	Ave W2 (mm)	Ave W3 (mm)	Total average (mm)	Standard deviation	Coefficient of Variation	Reference value (mm)	Percentage difference (%)
Specimen 1	5.26	5.35	5.36	5.32	0.04	0.75	6	11%
Specimen 2	5.63	5.70	5.69	5.67	0.03	0.53	6	5%
Specimen 3	5.79	5.73	5.98	5.83	0.11	1.89	6	3%
Specimen 4	5.67	5.36	5.61	5.54	0.13	2.35	6	8%
Specimen 5	5.40	5.42	5.59	5.47	0.09	1.65	6	9%

Table 4.8 Overall width (*WO*) of the test specimens

Specimen number	Ave WO1 (mm)	Ave WO3 (mm)	Ave WO3 (mm)	Ave WO3 (mm)	Total average (mm)	Reference value (mm)	Standard deviation	Coefficient of Variation	Percentage difference (%)
1	18.10	18.36	18.34	18.34	18.28	19	0.11	0.60	4%
2	18.65	18.89	18.45	18.45	18.65	19	0.18	0.97	2%

3	18.77	18.72	18.71	18.71	18.75	19	0.02	0.11	1%
4	18.34	18.22	18.12	18.12	18.33	19	0.09	0.49	3%
5	18.32	17.95	18.23	18.23	18.21	19	0.14	0.77	4%

That the measurements to test for dimensional accuracy presented in this section show values of coefficient of variation much lower than 10% for different parameters indicates the low significance of variation on the process parameters on the dimensions measured. There is also a slight variation between the experimental measurement and reference design values represented in the columns for percentage difference in Tables 4.6, 4.7, and 4.8. The slightly lower variations of the dimensions of printed parts are likely to have been due to shrinkage of the printed parts. Polymeric materials manufactured using LS tend to experience shrinkage, which affects their dimensional accuracy. Therefore, it is imperative to determine the magnitude of shrinkage of a particular material of interest. This value should be considered when sketching and slicing the CAD data. The value is referred to as the scaling factor. In this regard, a scaling value of about 1.8 was selected based on previous studies on Laser PP CP 75. Small discrepancies indicate that the scaling factor is acceptable for Laser CP 60 PP. However, curling was still observed on the printed parts. Considering the data presented in Tables 4.6, 4.7 and 4.8, the process parameters used for specimen 3, shown in Table 4.9, yielded the best results with the least overall percentage difference between the set and built dimensions.

Table 4.9 Process parameters for Laser PP CP 60 based on dimensional accuracy

Source of parameters	Temp. of the removal chamber (°C)	Temp. of the building bed (°C)	Layer thickness (mm)	Hatch distance (mm)	Scanning speed fill (mm/s)	Laser power fill (W)	Scanning speed contour/edges (mm/s)	Laser power contour/edges (W)
Experimentally determined parameters	125	125	0.15	0.25	2500	30.2	700	13.0
Manufacturer-specified parameters	115	120-125	0.15	0.25	4500	35.0	1500	20

4.1.5 Further Testing to Optimize the Process Parameters of Laser PP CP 60

After preliminary testing to determine suitable process parameters for Laser PP CP 60 powder, it was established that process and removal chamber temperatures are the most crucial factors to consider. The two parameters significantly influence the curling effect of polymers during the LS process, and in extreme cases, it terminates the printing process after the built parts block the recoater during the powder-spreading phase. Therefore, different process and removal chamber temperatures were tested, and the observations were recorded in Table 4.10.

Table 4.10 Process and removal chamber temperatures for Laser PP CP 60

Process and removal chamber temperatures	Comment/Observation
140 ℃ and 140 ℃	The powder melted. The process stopped.
130 ℃ and 130 ℃	The cake powder was completely baked. No recovery was made.
128 ℃ and 125 ℃	The cake powder was partially baked. Slight curling occurred, resulting in minimal damage to the edges. Parts were printed to completion with minimal damage to the edges.
126 ℃ and 124 ℃	The cake powder was partially baked. Significant curling occurred, resulting in notable damage to the edges. Parts were printed to completion, but the edges were significantly damaged by the recoater.
126 ℃ and 125 ℃	The cake powder was partially baked. Significant curling occurred, resulting in notable damage to the edges. Parts were printed to completion, but the edges were significantly damaged by the recoater.

The values of 128 ℃ and 125 ℃ were selected as the best process and removal chamber temperatures for Laser PP CP 60, respectively. These parameters result in partial baking of the cake powder, reducing the amount of powder recovered for re-use, and slight curling of the printed parts. Besides, higher values caused complete baking of the powder (zero recovery). Figure 4.8 shows partially baked cake powder at 126 ℃ and 124 ℃ process and removal chamber temperatures. Lower values result in significant curling that causes considerable damage to the edges of the printed parts and might lead to stoppage of the process after the recoater dislodges a component from the building chamber. Figure 4.9 illustrates the damaged edges of the printed parts at 126 ℃ and 124 ℃ process and removal chamber temperatures. Following the processing difficulties experienced where partial

baking of the powder and curling occurred, which resulted in damage to the edges of the printed parts, Laser PP CP 60 was discarded. The focus of testing recyclability of PP powder then turned to Laser PP CP 75. This PP powder grade was promising because it did not bake, and it showed minimal curling at the same parameters used for Laser PP CP 60. It is worth noting that the high curling effect of the material (Laser PP CP 60) was considerably reduced by pre-warming the machine for four- instead of two hours, probably due to the uniform distribution of heat across the building chamber.

Figure 4.8 Partially baked cake powder (Laser PP CP 60)

Figure 4.9 Damaged edges of the test specimen printed using Laser PP CP 60

4.2 CHARACTERIZING LASER PP CP 60 AFTER SINGLE PRINT

4.2.1 Powder Morphology from the Results of Scanning Electron Microscopy

Figures 4.10, 4.11, and 4.12 show the morphology of samples of virgin, used, and used-virgin Laser PP CP 60 powder, respectively, at different magnifications.

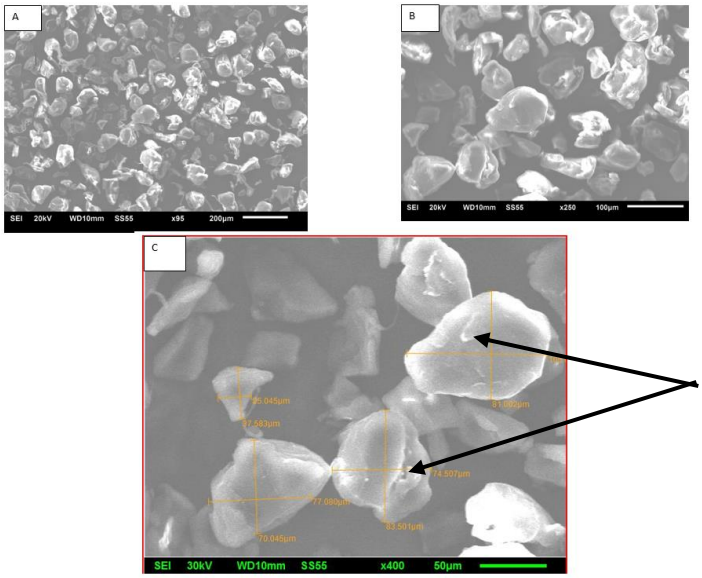

Figure 4.10 Powder morphology of virgin Laser PP CP 60

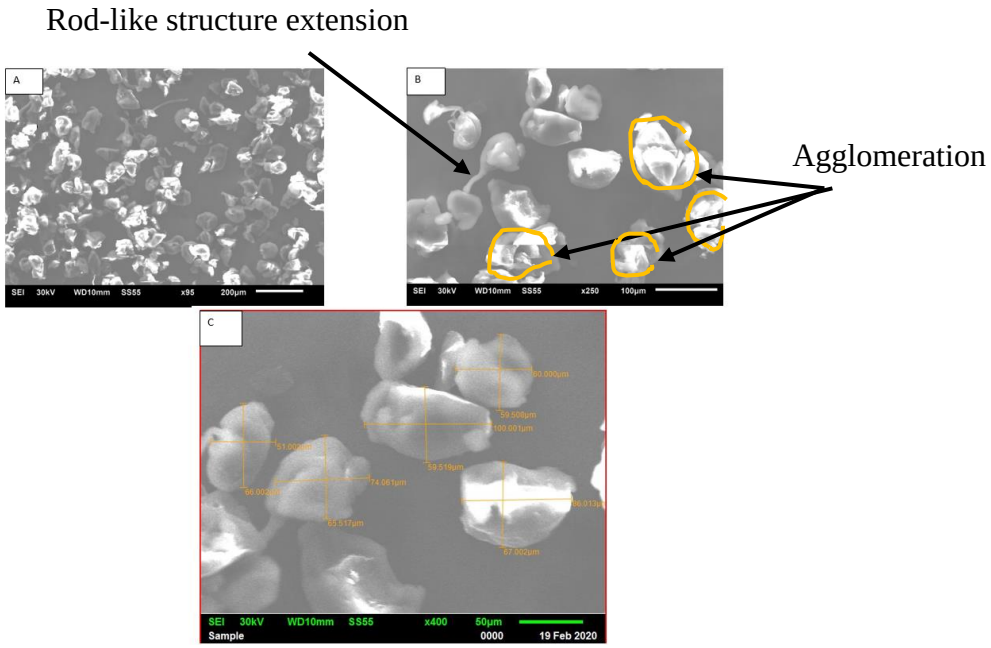

Figure 4.11 Powder morphology of used (1 cycle) Laser PP CP 60

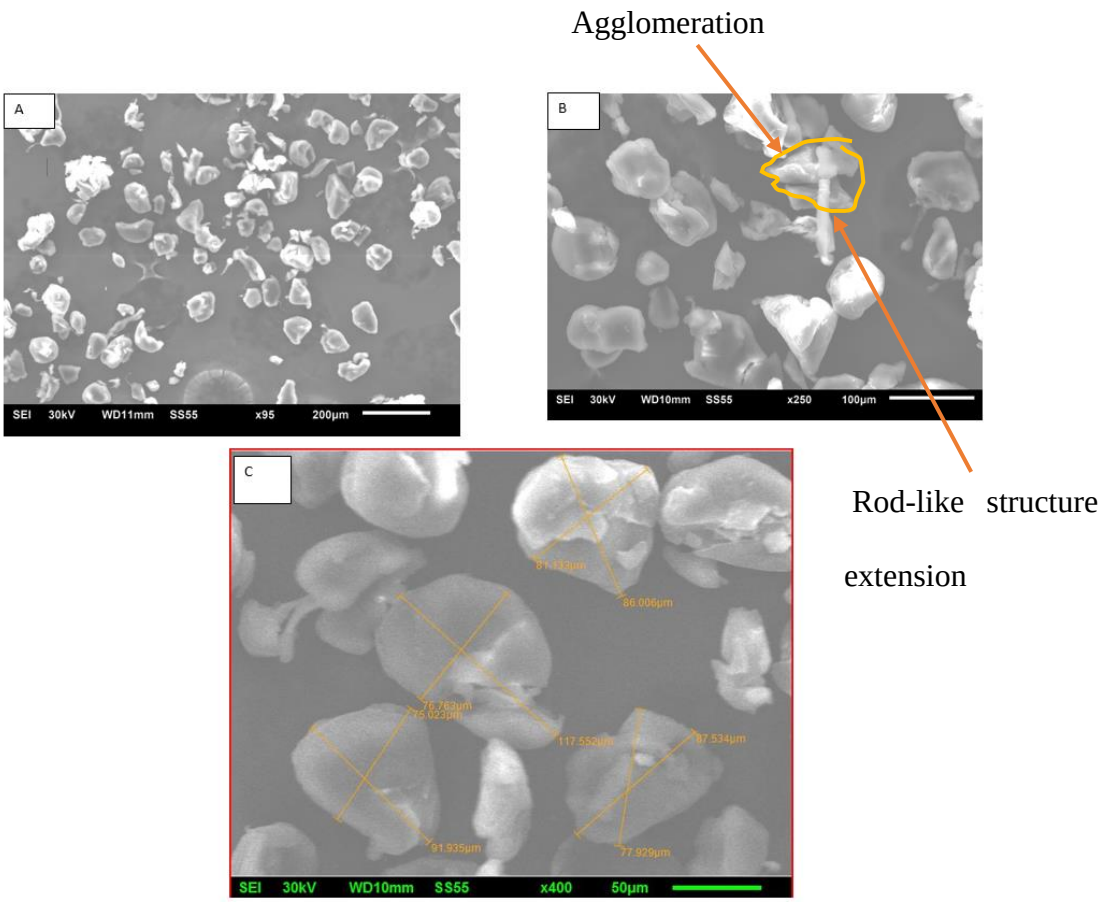

Figure 4.12 Powder morphology of used-virgin Laser PP CP 60

Figures 4.10, 4.11, and 4.12 illustrate that the powder particles of all three batches of Laser PP CP 60 are irregularly shaped. Polymer LS powders should be spherically shaped to ensure free-flowing behaviour (Sagar & Elangovan, 2017; Drummer et al., 2010). The fact that the three batches of powder all exhibited poor flowability during processing is probably due to their irregularly shaped particles.

Powders can be categorized as either free-flowing, random or ordered powders (Deveswaran et al., 2009; Poux et al., 1991). Over the years, ordered powders have also been termed interactive powders or adhesive powders (Poux et al., 1991). The random powders have also been referred to as non-interactive powders or cohesive powders (Poux et al., 1991). Figure 4.13 differentiates between ideally ordered and perfectly random mixtures.

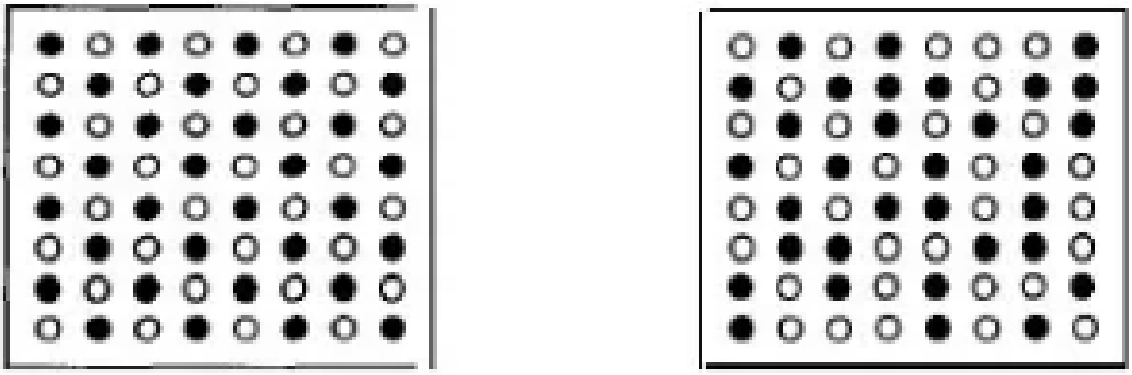

Figure 4.13 Ideally ordered and perfectly random mixtures (Poux et al., 1991)

Free-flowing powders move smoothly because of low inter-particulate forces. These powders have a problem of segregation after mixing. Therefore, they should be appropriately stored with minimal disturbance. As mentioned, LS powders should exhibit free-flowing behaviour, which encourages the spreading of the powders (Schmid & Wegener, 2016). As a result, the printed parts are free from porosity and, in turn, possess excellent mechanical properties. Besides, free-flowing polymeric powder reduces the chances of the recoater blade dislodging printed parts from the building bed. Non-free-flowing powders tend to clump together, leading to uneven deposition of powder on the powder bed, leading to non-uniform powder bed density, and in turn, compromises the mechanical strength of printed parts (Berretta et al., 2015). Cohesive (random) powders cling to each other due to significant inter-particle forces. Cohesive powders are also formed due to moisture and electrostatic charges (Deveswaran et al., 2009). They do not exhibit the free-flow phenomenon. Besides, cohesive powders have low segregation tendencies and are difficult to mix properly. Hence, cohesive powders are not suitable for use in LS. Ordered (adhesive) powders have uniformly distributed particles formed when small particles adhere to large particles (Deveswaran et al., 2009; Poux et al., 1991). Figure 4.14 shows an example of an ordered mixture. The concept of ordered powders is applied when developing polymer blends for LS to ensure suitable properties.

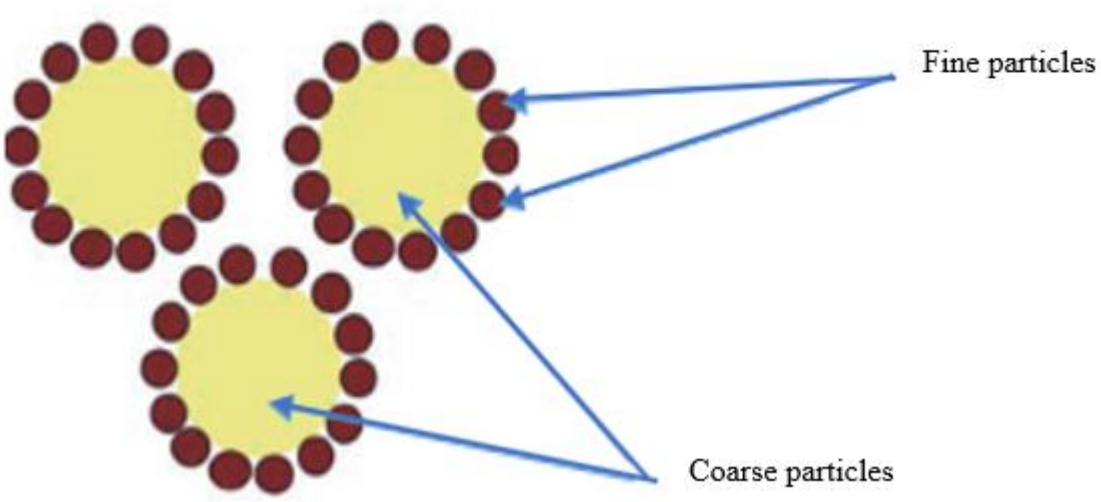

Figure 4.14 An example of an ordered mixture (Saharan et al., 2008)

The powder particles of the virgin material were not clumped, as evident in Figure 4.10a. However, for the used powder, agglomeration of powder particles was established. Figure 4.11b shows that mixing used powder with virgin material ameliorates agglomeration effects since there was a reduction in the number of agglomerated powder particles. By comparing Figures 4.11b and 4.112b, it is evident that the number of agglomerates for the same area reduces from four to one. It was also observed that the extension features altered the shapes of the particles into tadpole (rod-like) shapes, as shown in Figure 4.9b. The origin of the extensions is not clear, but they might be attributed to the shearing action of the process used to manufacture the powder. Mys et al. (2016) observed similar morphological inconsistencies when manufacturing syndiotactic polystyrene using a ball-and-rotor milling method.

The SEM images showed that the new Laser PP CP 60 exhibits relatively smooth surfaces. However, rough patches and flakes were also observed on the surface of the powder particles, as illustrated by Figure 4.10c, which might have also contributed to the poor flowability of the new Laser PP CP 60. The powder needs to be improved by altering its morphology to facilitate the flowability of the material. However, based on the information provided in Figure 4.10, the powder might be suitable for AM when appropriate parameters are selected.

The SEM micrographs did not identify any flow and antistatic agents, such as silica and glass beads, commonly used in polymeric materials to improve their flowability and reduce the effects of electrostatic charges. This, in addition to the irregularly shaped particles and incidences of particle agglomeration, explain the flowability and processing difficulties observed with the new Laser PP CP 60. Only flat tensile specimens could be printed because curling led to dislodging of parts from the building chamber, which prompted the stoppage of the LS process.

4.2.2 Distribution of Particle Sizes from the Results of Scanning Electron Microscopy

Table 4.11 and Figures 4.15, 4.16, and 4.17 illustrate the distribution of particle sizes of virgin, used, and used-virgin PP powder batches, respectively. The particle size distribution was determined using ImageJ software.

Table 4.11 Particle size distribution for the three batches of powders

Powder batch	Powder particle distribution	Mean powder particle size	Standard deviation of the particle size
Virgin powder	25.0–120 µm	63.7 µm	24.5 µm
Aged powder (one cycle)	19.0–105.0 µm	65.7 µm	23.7 µm
Mixed powder	26.2–115.5 µm	64.0 µm	21.1 µm

The particle size range for all the batches of powder was between 19 and 120 µm, as indicated in Table 4.12. This powder particle size distribution is slightly above the recommended range of between 20 and 80 µm (Schmid and Wegener, 2016) or 45 and 90 µm (Schmidt et al., 2019). However, it is still acceptable for LS processing because the average size of the virgin (63.7 µm), the used powder (65.7 µm), and used-virgin mixture (64.0 µm) were at least two times smaller than the build layer thickness of the EOSINT P 380 machine of between 100–150 µm. The build layer thickness should be at least twice the average size of powder particle to ensure that powder fusion happens in direct contact with the laser beam, rather than having particle-to-particle conduction, which results in partial coalescence and, subsequently, mechanically weak components (Berretta et al.,

2014). The mean particle size of the virgin powder increased from 63.7 µm to about 65.7 µm (3.14% increase) after one cycle of printing, which then reduced to 64.0 µm (a 2.59% increase) after mixing the two in equal volumes. This confirms the summation by Dadbakhsh et al. (2017) that the LS process does not significantly influence the particle size of polymeric powder particles.

The bar charts in the following three figures represent the actual particle size distribution, whereas the normal curve illustrates the expected particle size distribution. The actual particle size distribution is supposed to follow the normal curve. However, for all three batches, the actual particle size distribution was not well defined, which indicates the irregularity of the particle size distribution of Laser PP CP 60.

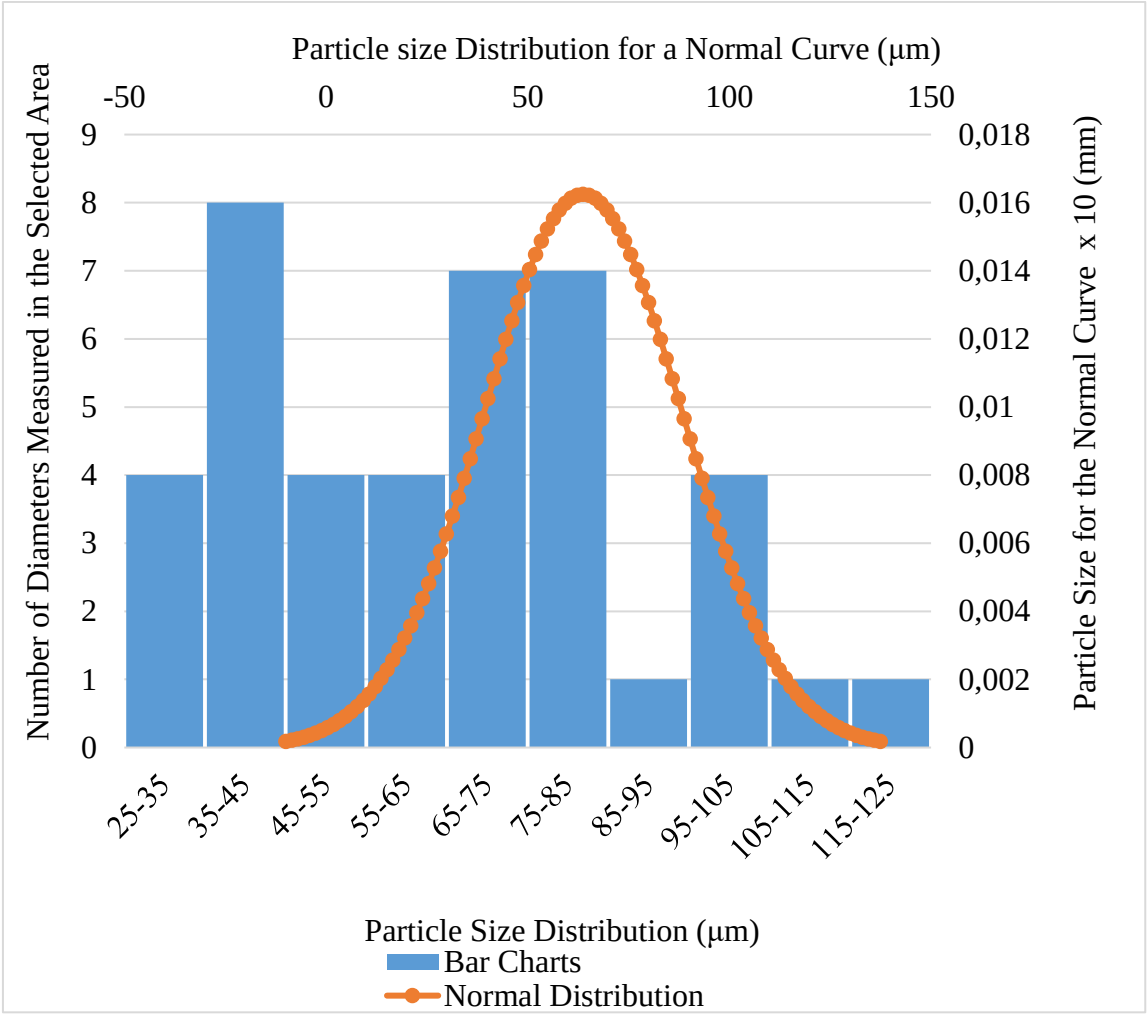

Figure 4.15 Distribution of particle sizes of the virgin Laser PP CP 60

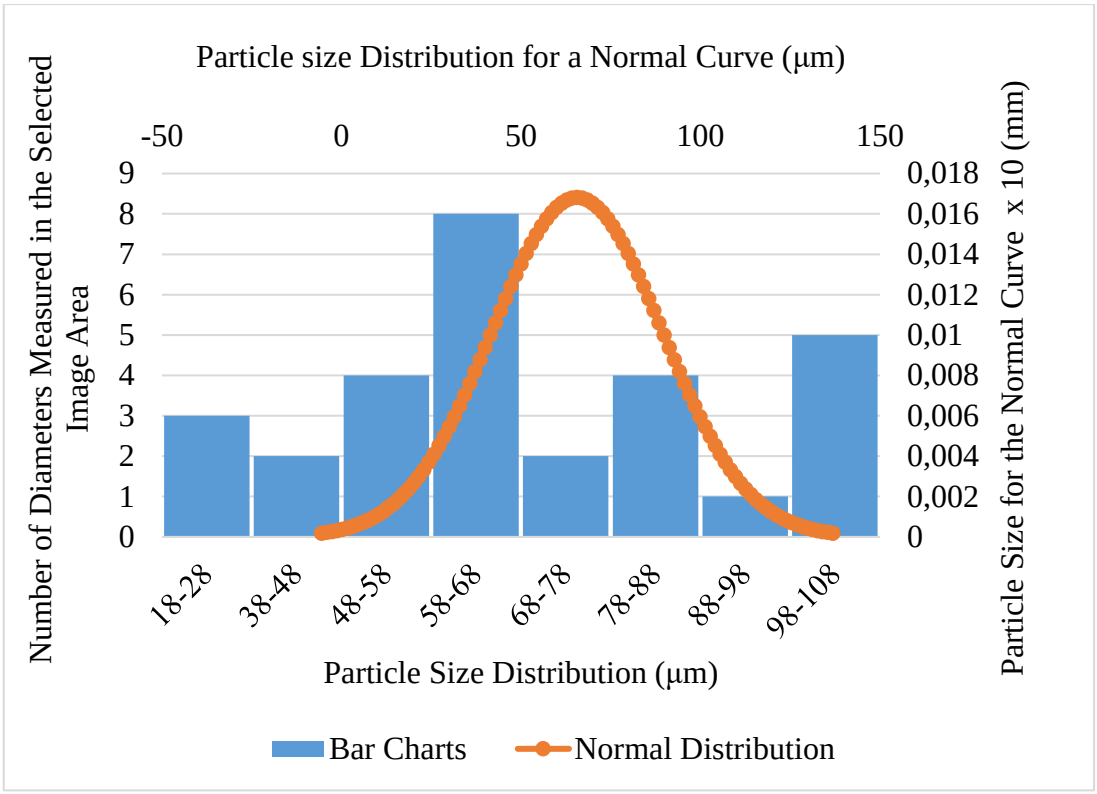

Figure 4.16 Distribution of particle sizes of the used (1 cycle) Laser PP CP 60

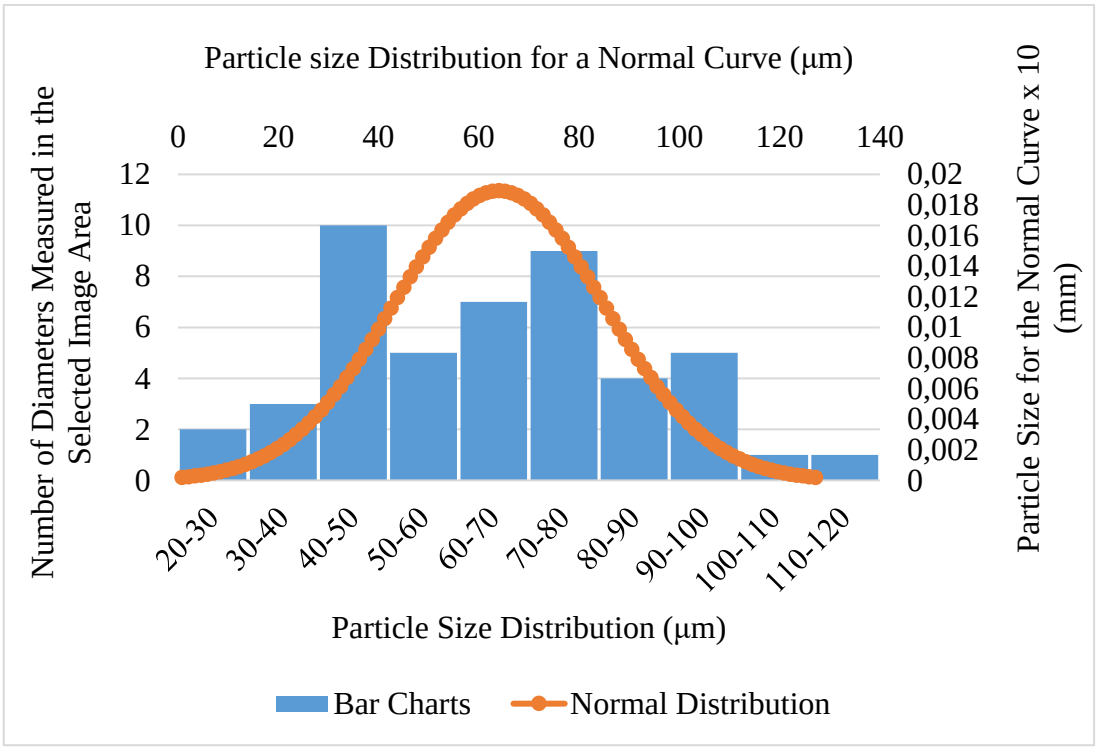

Figure 4.17 Distribution of particle sizes of the used-virgin Laser PP CP 60

These three figures show that the as-received virgin, used, and used/virgin mixed powders all exhibit irregular powder size distribution since most bar charts do not fall within the expected normal distribution curve. Schmid et al. (2017) suggested that materials with irregular power distribution exhibit medium flowability characteristics. The skewness values of the virgin, used, and used/virgin mixed powder particle size distribution were calculated as 0.445886, -0.15085, and 0.23085, respectively. The used powder showed the smallest variation in the distribution of particle sizes of all three batches, while the virgin powder was the highest.

4.2.3 Differential Scanning Calorimetry Testing

DSC was used to investigate the thermal properties of the three batches of PP powder in respect of peak melting point, peak crystallization point, onset of melting, onset of crystallization, melting shoulder interval, crystallization shoulder interval, sintering window, and degree of crystallinity. The results of this analysis are presented in Figures 4.18 to 4.20 and Table 4.12.

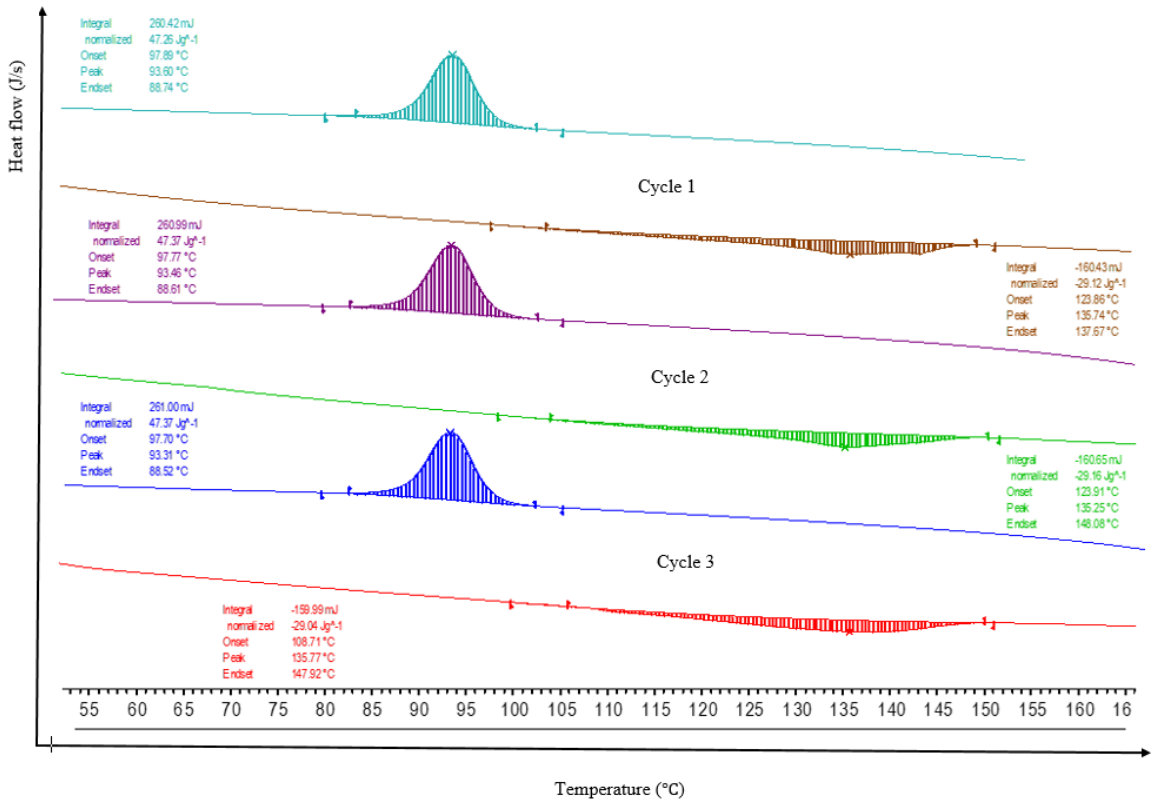

Figure 4.18 DSC thermogram of the virgin powder

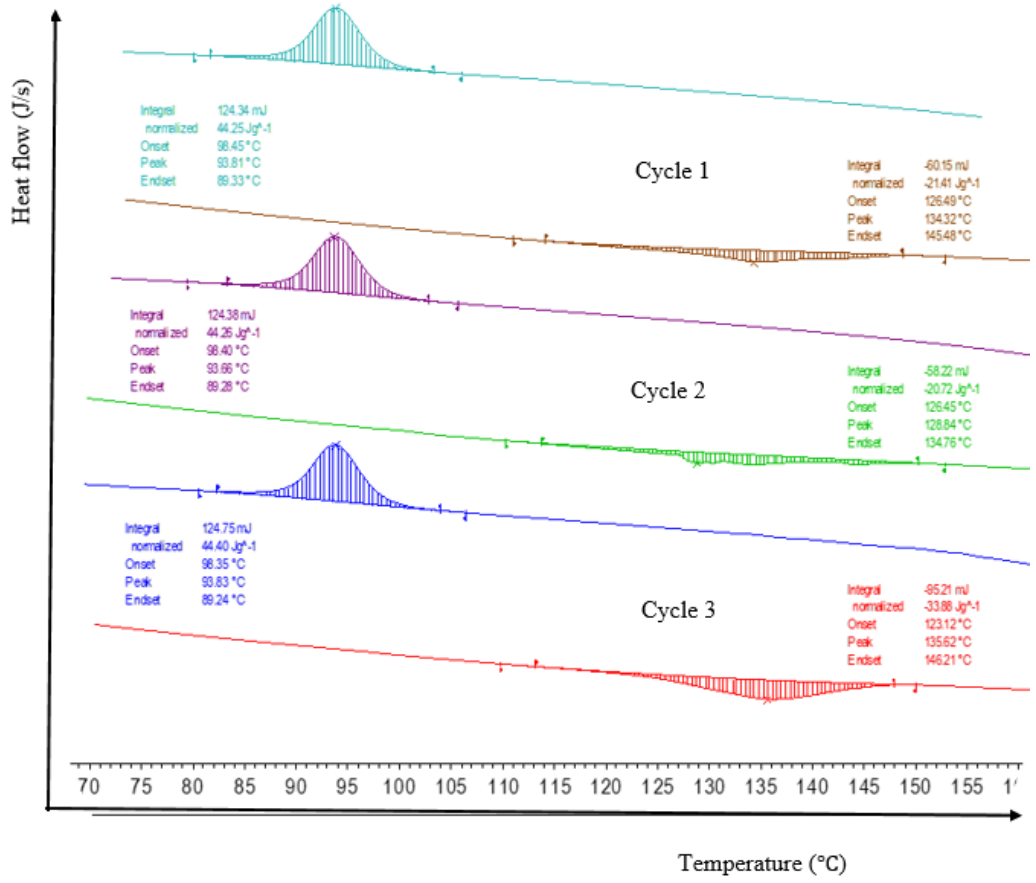

Figure 4.19 DSC thermogram of the used (1 cycle) powder

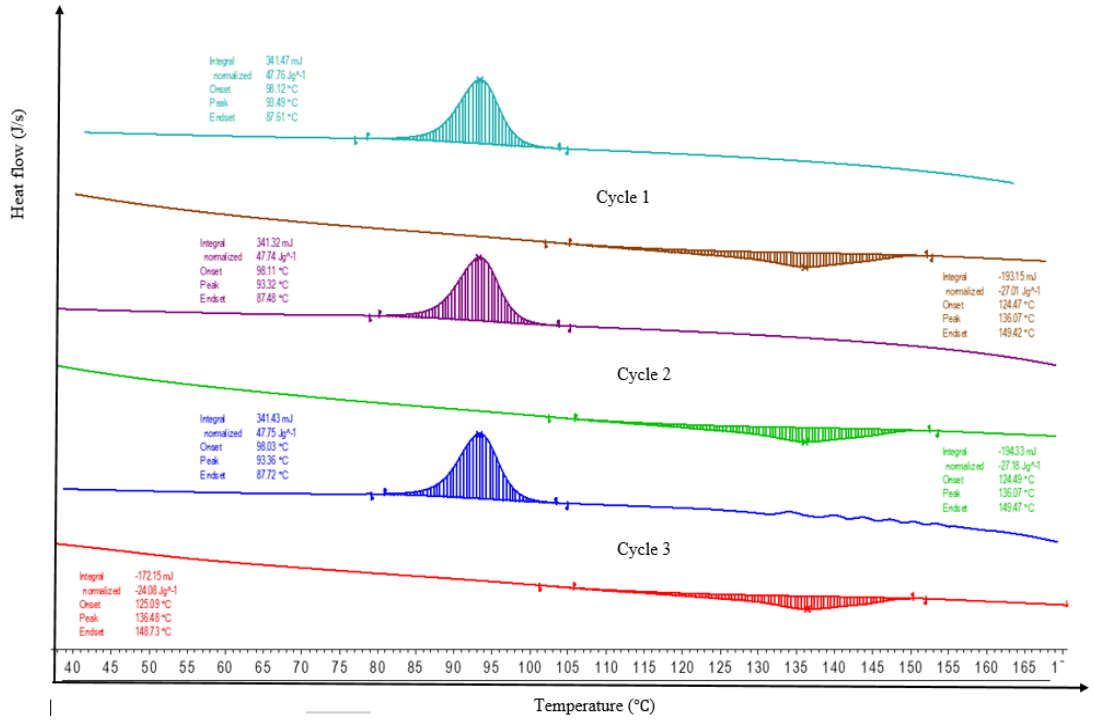

Figure 4.20 DSC thermogram of the used-virgin powder mixture

Table 4.12 DSC results of virgin, used, and used-virgin mixture Laser PP CP 60

Powder batch	Peak melting point (℃)	The onset of melting point (℃)	End-set of melting point (℃)	Melting shoulder interval (℃)	Peak crystallization point (℃)	Onset of crystallization point (℃)	End-set of melting point (℃)	Crystallization shoulder interval (℃)
Virgin material	135.59	118.83	144.56	25.73	93.46	97.79	87.60	10.19
Used (aged) material	132.93	125.35	142.13	16.78	93.76	98.40	89.28	9.12
Used-virgin mixture	136.21	124.80	149.21	24.41	93.39	98.09	87.60	10.49

The sintering window (*SW*) is given by the equation (Schmid et al., 2017)

$$SW = (T_m - T_c)_{\text{onset}} \quad (4.1)$$

where, the symbols T_m = onset melting point and T_c = onset crystallization. The degree of crystallization (DC) is given by Equation 4.2:

$$DC = (\Delta \text{Hm} / \Delta \text{H}^0{}_m) \times 100\% \quad (4.2)$$

where, the symbols ΔH_m = experimental melting enthalpy and, $\Delta H^0{}_m$ = theoretical melting enthalpy of the material. The theoretical melting enthalpy of 100% crystalline PP is equal to 209 J/g (Wypych, 2012).

Table 4.13 Sintering window values for the different batches of Laser PP CP 60

Powder batch	Onset of melting, T_m (℃)	Onset of crystallization, T_c (℃)	Sintering window, SW (℃)
Virgin powder	118.83	97.79	21.04
Used powder	125.35	98.40	26.95
Used-virgin powder mixture	124.80	98.09	26.71

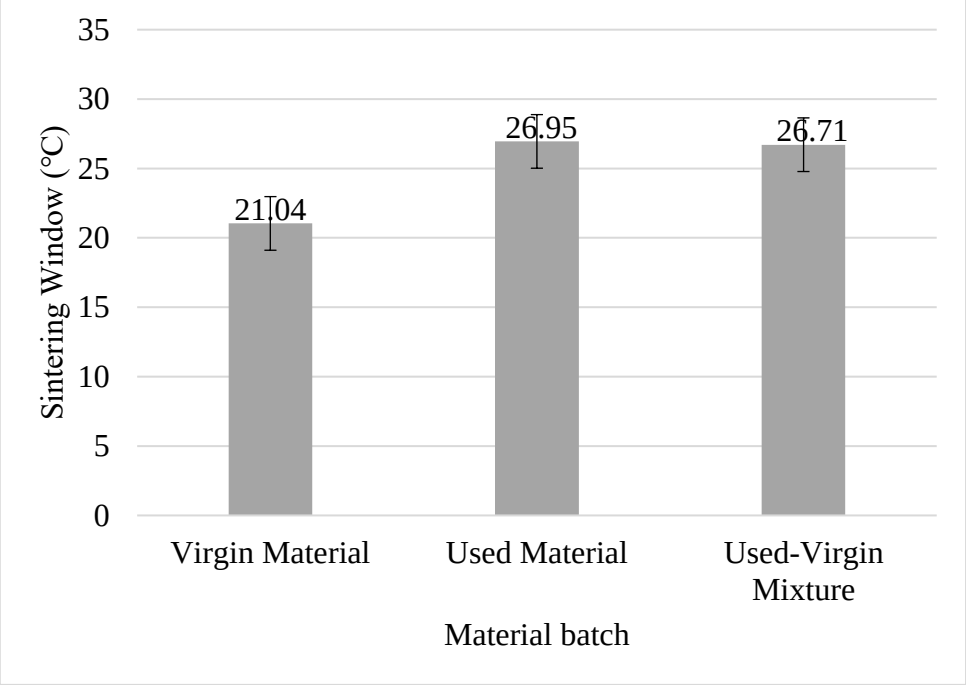

Figure 4.21 Sintering windows for virgin, used, and used-virgin powders

The sintering windows for the new Laser PP CP 60 increased from 21.04 ℃ (virgin material) to 26.95 ℃ (used material). The addition of 50% virgin material to 50% used material decreased the sintering window slightly from 26.95 ℃ to 26,71 ℃. The changes are associated with degradation and cross-linking of the materials, which shifts the thermal properties of polymers (Kuehnlein et al., 2010). The sintering window of the new Laser PP CP 60 is lower than the sintering window for PA 12, which ranges from 32 ℃ to 34 ℃ (Marin, 2017). It is, therefore, expected that difficulties would be experienced when

regulating the cooling rate of the printed parts using the new Laser PP CP 60 (Schmid et al., 2017). It also explains the problems of curling that were observed with the new material. However, the problem of curling can be resolved by determining the most suitable extraction chamber temperature for the new polymeric material. Schmid et al. (2017) suggest that homogeneous and stable thermal conditions reduce the curling and warpage issues associated with polymeric materials with narrow sintering windows.

Table 4.14 Degree of crystallization for the different batches of Laser PP CP 60

Powder batch	Experimental melting enthalpy of the material	Theoretical melting enthalpy of the material	Degree of crystallization of the material
Virgin material	29.10 J/g	209 J/g	13.92%
Used material	25.34 J/g	209 J/g	12.12%
Used-virgin mixture	26.09 J/g	209 J/g	12.48%

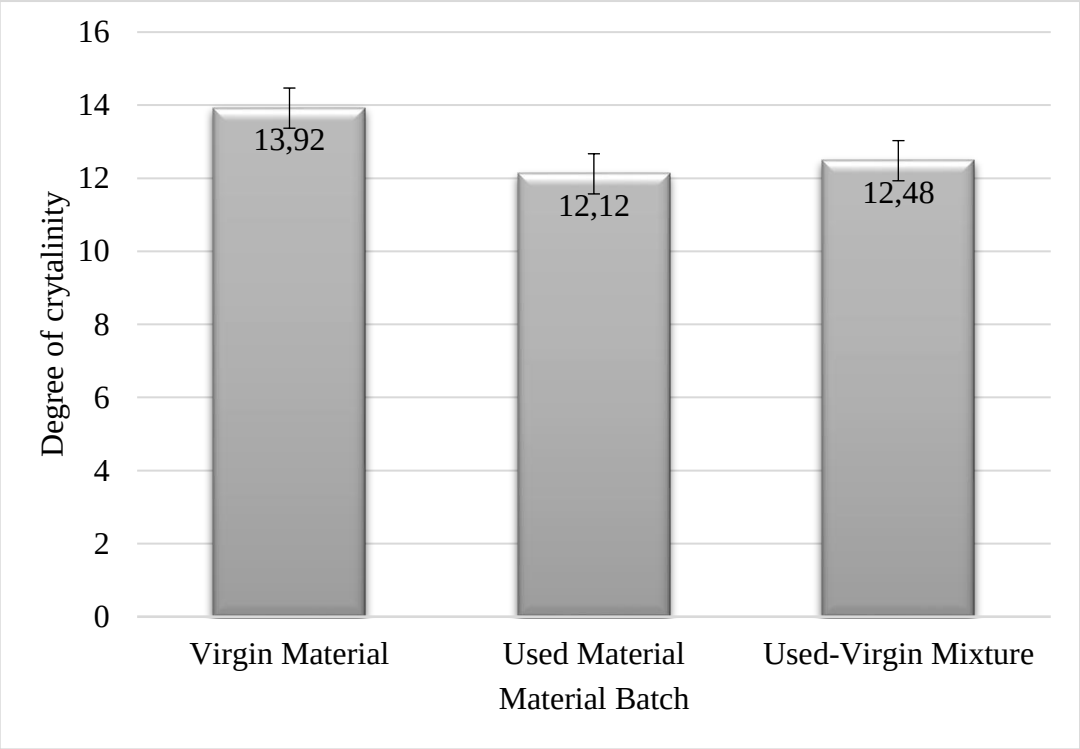

Figure 4.22. Degree of crystallinity of the virgin, used, and used-virgin powders

It was also observed that the degree of crystallinity of virgin material decreased slightly from 13.92% to 12.12% after printing a single cycle. This might have been due to the breakdown of the long carbon chains. The findings contradict research by Dadbakhsh et al. (2017), which suggests that powder crystallinity of PA 12 materials increases with aging. This raises speculation that PA 12 and PP powders degrade differently when subjected to high processing parameters. However, Chen et al. (2018) found that crystallinity of original PA 12 decreases from 46.94% to 44.22% when aged, which is consistent with the present work. The magnitude of crystallinity increased slightly to 12.48% with the addition of 50% virgin material, probably due to the restoration of long carbon chains.

4.2.4 Thermogravimetric Analysis

The TGA analysis was used to determine the degradation and break-up temperature (T_d) of the three PP powder batches (virgin material, used material, and used-virgin mixture). Figures 4.23, 4.24, and 4.25 illustrate the thermogravimetric thermogram of the three batches of Laser PP CP 60, while Table 4.15 and Figure 4.26 summarize the degradation temperature (℃) thread of the powders.

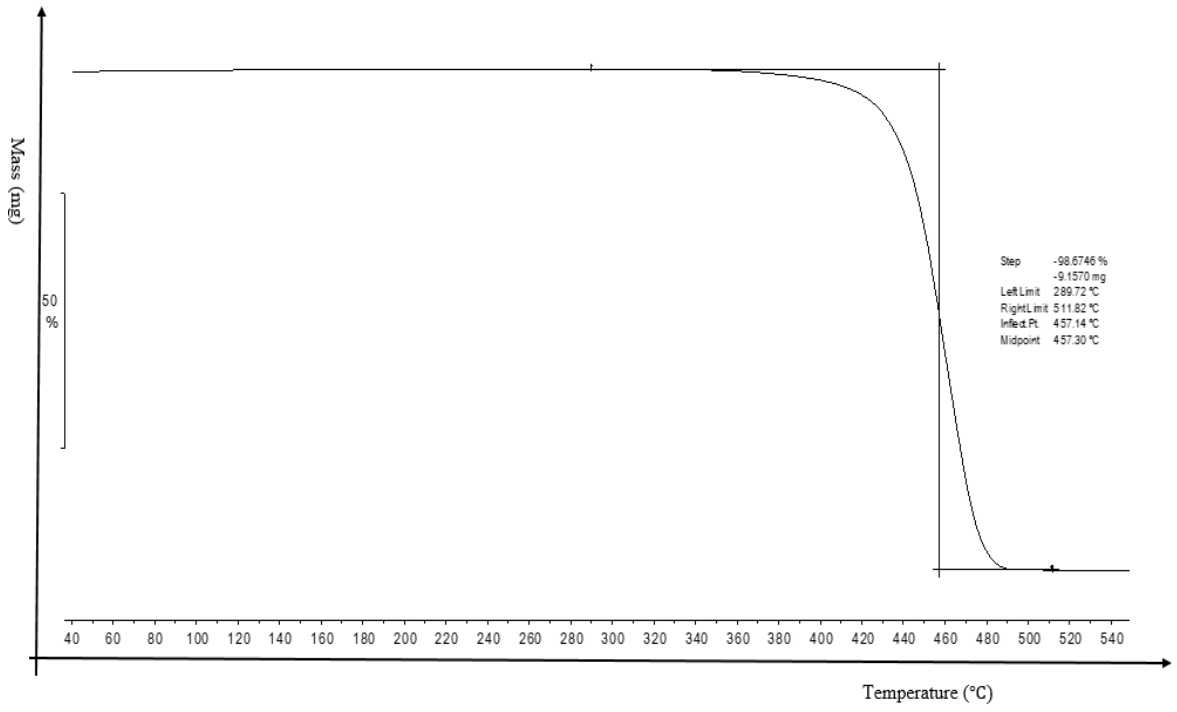

Figure 4.23 TGA thermogram of the virgin Laser PP CP 60

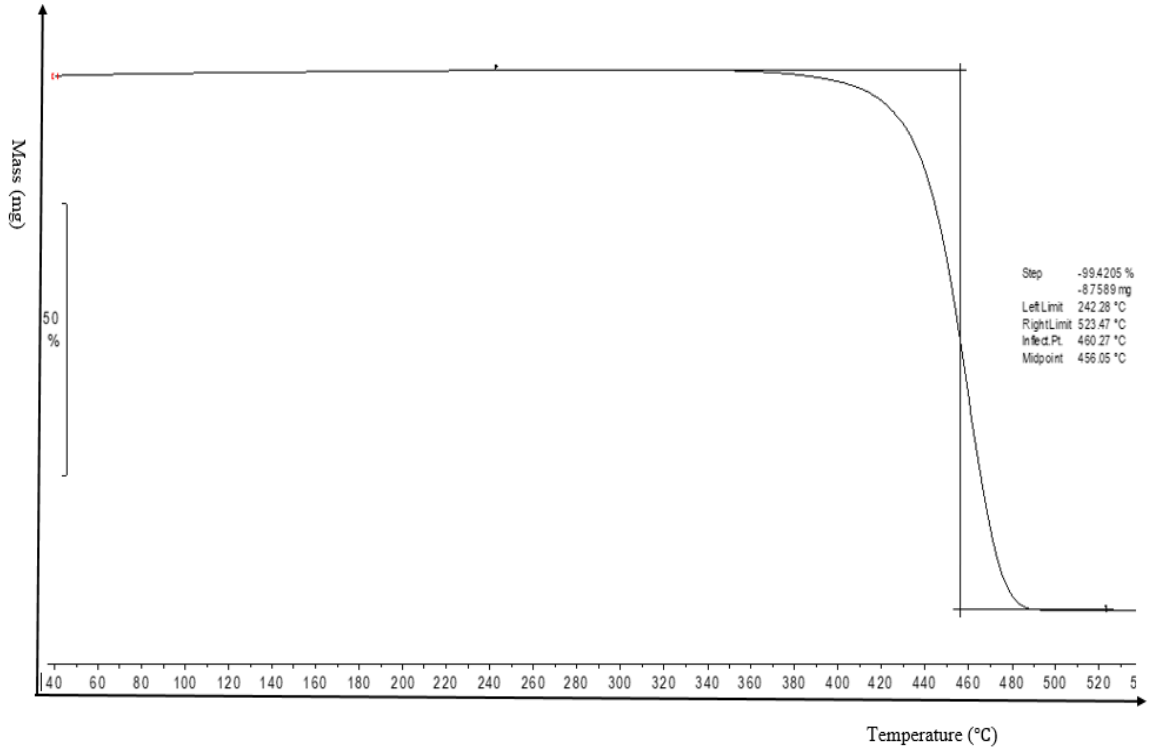

Figure 4.24 TGA thermogram of the used (1 cycle) Laser PP CP 60

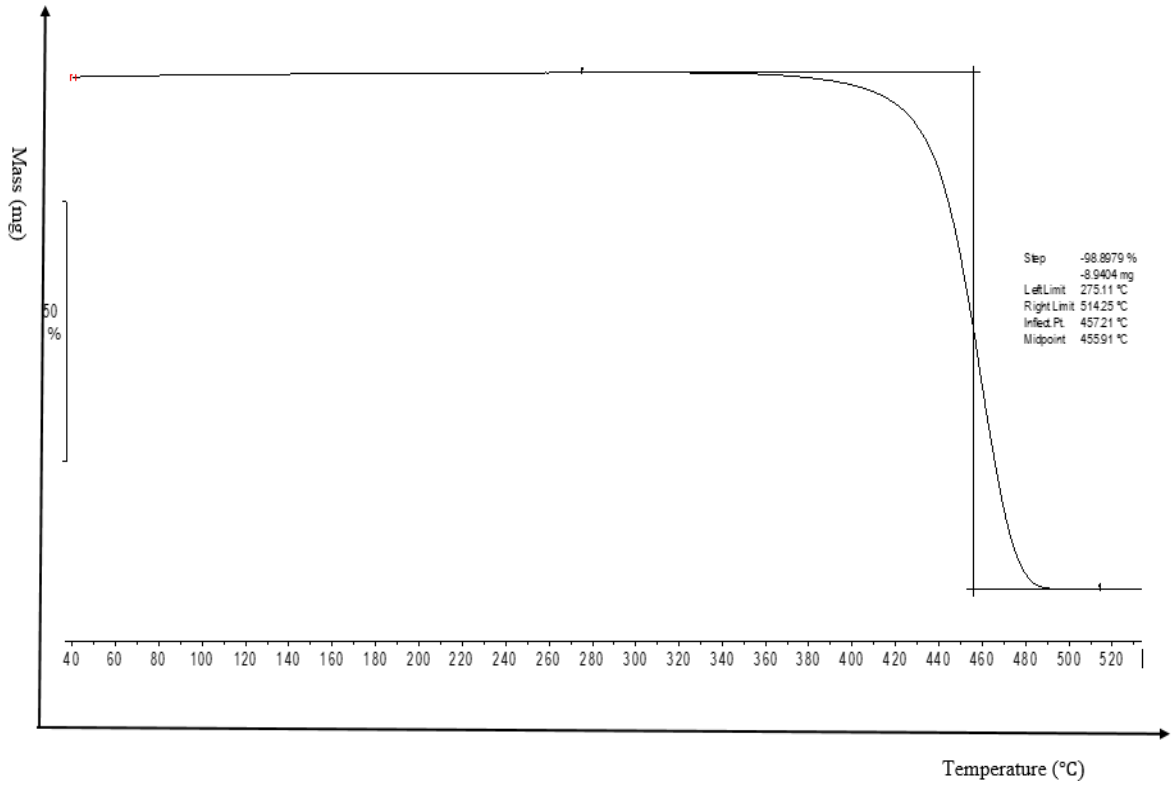

Figure 4.25 TGA thermogram of the used-virgin Laser PP CP 60 mixture

Table 4.15 Degradation temperature for the different batches of Laser PP CP 60

Powder batch	Degradation temperature (℃)
Virgin material	457.30
Used material	456.05
Used-fresh mixture powder	455.91

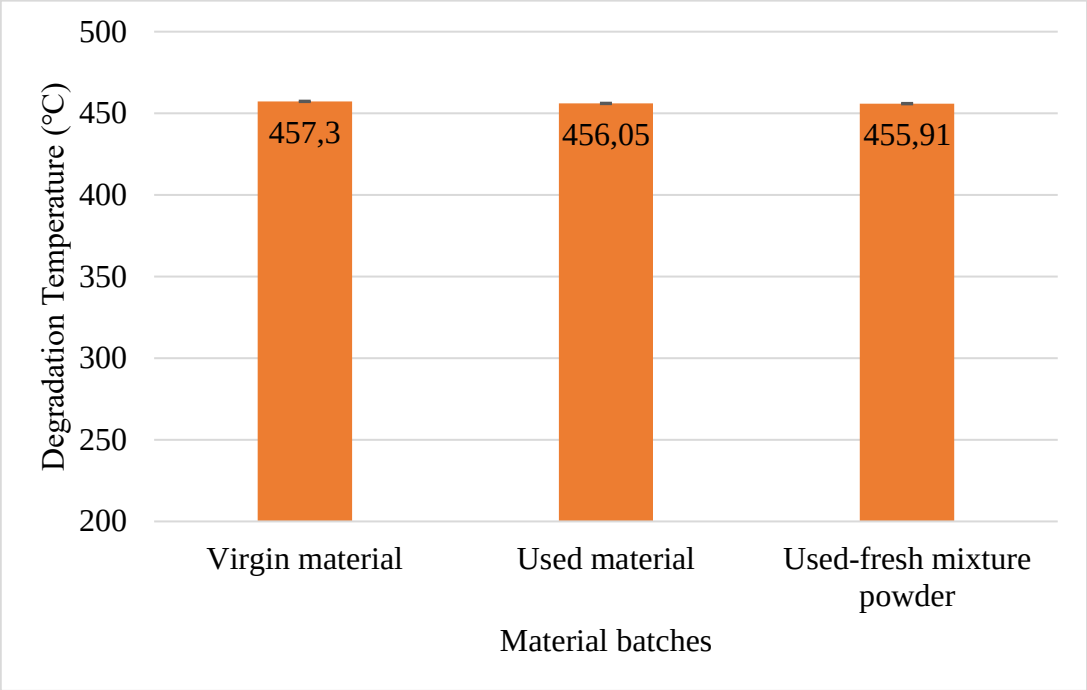

Figure 4.26 Degradation temperature of the virgin, used, and used-virgin powder

The degradation temperature (T_g) of virgin Laser PP CP 60 was reached at 457.30 ℃. The used and used-fresh batches had slightly lower degradation temperatures (T_g) of 456.06 ℃ and 455.91 ℃, respectively. The high temperatures of degradation and break-up of the three batches of Laser PP CP 60 illustrate that this polyolefin can be employed in LS since the process progresses at a temperature of about 125 ℃. Therefore, the material will not degrade and break up during processing.

4.2.5 Melt Flow Index Testing

Testing of the MFI of Laser PP CP 60 was used to determine the flowability and viscosity of the three batches of powder, with the results shown in Figure 4.27. Table 4.16 illustrates the average values from a total of six measurements for each of the batches.

Table 4.16 MFI for the virgin, used, and used-virgin mixture

Powder batch	MFI value g/10min
Virgin material	6.1
Used material	6.5
Used-virgin mixture	6.4

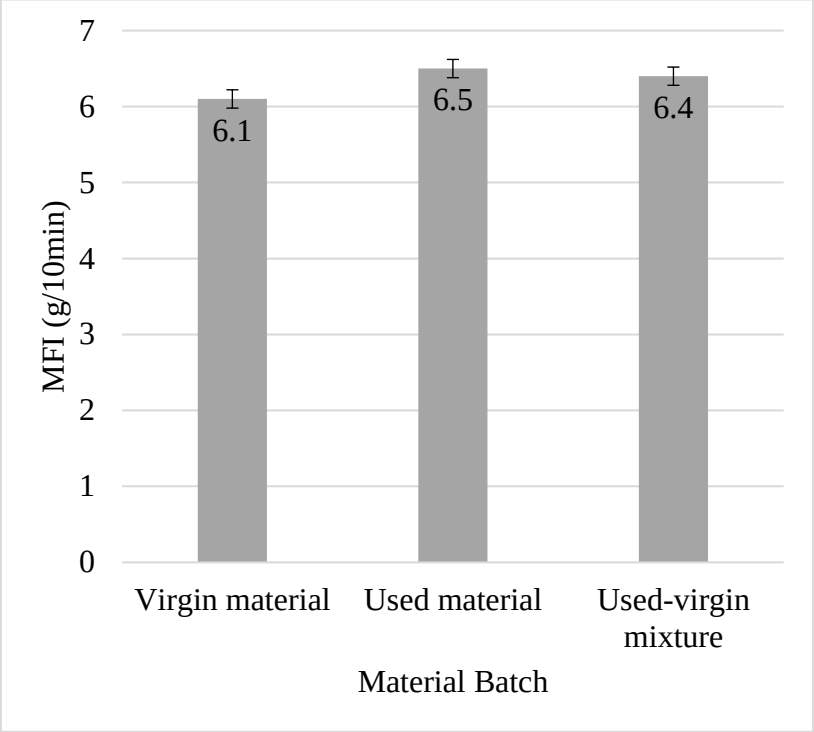

Figure 4.27 MFI of the virgin, used, and used-virgin mixture

The virgin Laser PP CP 60 material had a low MFI of 6.1 g/10 min, which increased slightly to 6.5 g/10 min after one recycle. The addition of 50% virgin material to the recycled powder slightly reduced the MFI of used powder to 6.4 g/10 min. The MFI value of a new PA 12 material from EOS is about 45–50 g/10 min, and it deteriorates from this range with repeated use. Once the value drops below 18 g/10 min, the powder is discarded (Dotchev & Yusoff, 2009). These values show that the melt of Laser PP CP 60 is highly viscous and will have low flowability and processing difficulties, as observed during these preliminary testing.

4.3 Recyclability of Laser PP CP 75 powder

The re-usability of the PP powder in this study was determined by characterizing and comparing the used powder with the fresh powder after each printing cycle. The printed specimens were examined for the presence of the "orange peel", which is common with PA 12. SEM, DSC, TGA, and MFI testing were used to characterize different powder batches (1st, 2nd, 3rd, 4th and 5th print cycles). Uniaxial tensile testing and dimensional analysis tests were employed to characterize the mechanical properties of the printed specimens. The relationship between printing cycles and re-use cycles is as follows:

0 – printing cycle using virgin material (1st print cycle) – zero re-use cycle.
1 – 2nd print cycle (1st re-use cycle).
2 – 3rd print cycle (2nd re-use cycle).
3 – 4th print cycle (3rd re-use cycle).
4 – 5th print cycle (4th re-use cycle).

4.3.1 Physical Inspection

Figures 4.28, 4.29, 4.30, and 4.31 show the parts printed for the 1st, 2nd, 3rd, and 4th re-use cycles, respectively. No "orange peel" was observed in the re-use cycles. The findings are in contrast to those of a study by Dotchev et al., 2009, which found that when PA 12 from EOS is recycled five times with or without small quantities of new material, the parts produced have a rough surface finish due to the formation of an "orange peel". Thus, it can be concluded that PP CP 75 powder is re-usable for the 1st five printing cycles without requiring the addition of virgin powder because it does not form an "orange peel" like PA 12, which has to be mixed with virgin material after every print cycle to prevent the formation of an "orange peel". The "orange peel" affects surface roughness, dimensional tolerance, and geometrical accuracy (Dotchev & Yusoff, 2009; Yamauchi et al., 2016; Kigure & Niino, 2017). Clearly, PP CP 75 has the upper hand over PA 12 regarding the "orange peel" phenomenon. The mixing ratio proposed by the manufacturers, EOS and 3D Systems, for PP CP 75 are 70:30 and 50:50 for aged to virgin powder, respectively (Dotchev & Yusoff, 2009).

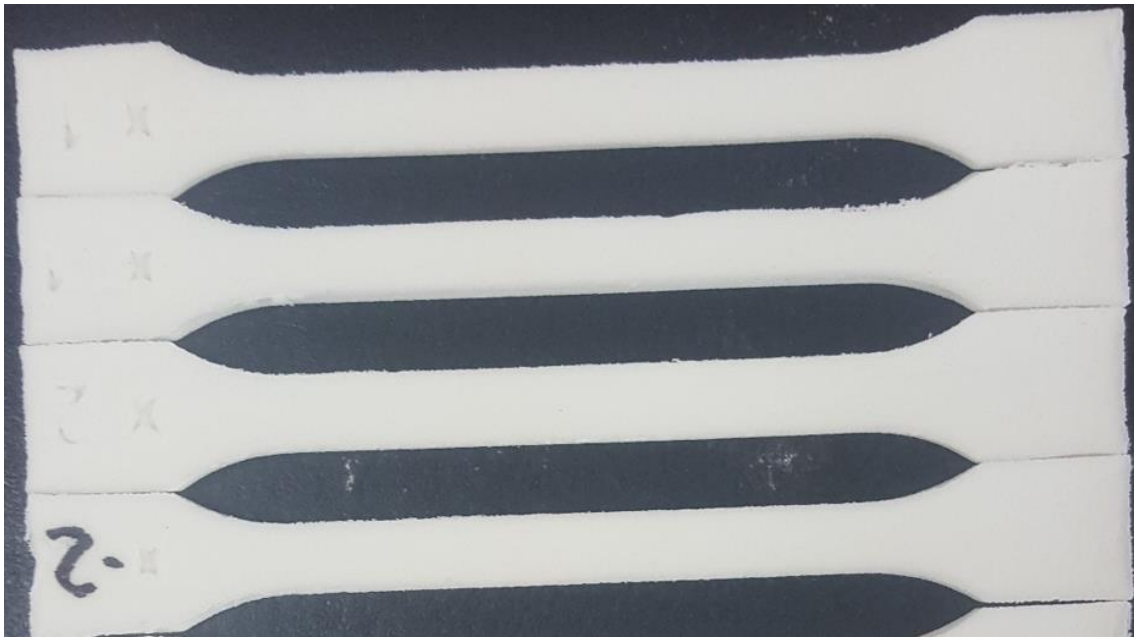

Figure 4.28 Test specimen printed with re-used Laser PP CP 75 (2nd cycle)

Figure 4.29 Test specimen printed with re-used Laser PP CP 75 (3rd cycle)

Figure 4.30 Test specimen printed with re-used Laser PP CP 75 (4th cycle)

Figure 4.31 Test specimen printed with re-used Laser PP CP 75 (5th cycle)

4.3.2 Characterization to Establish Recyclability of Laser PP CP 75

Powder characterization of Laser PP CP 75 was undertaken using MFI testing, DSC, TGA and SEM analysis to established what changes took place after each print cycle. The MFI experiments established the changes in powder flowability, while the DSC analysis determined the melting point of the powder and sintering window changes after each print cycle. The TGA analysis was conducted to investigate any changes in degradation

temperatures of the powder, and lastly, SEM testing determined the changes in the morphology of powder and particle size after each re-use cycle.

4.3.2.1 Melt flow testing of Laser PP CP 75 after 100% re-use

Table 4.17 summarizes the MFI values for the five batches of powder considered in the analysis. It also provides a comparison to PA 12.

Table 4.17 MFI values for the five batches of powder considered in the analysis

	Powder batch	**Value of MFI (g/10 min) for Laser CP PP 75**	**Percentage change in virgin material**	**Value of MFI (g/10 min) for PA 12 from a study by Gornet et al. (2002)**	**Percentage change in virgin material**
#	Manufacturer's stated value	4.50	-	-	-
1	Virgin material	4.78	0.00%	53	0.00%
2	Re-used powder after 1st cycle	4.69	1.88%	38	28.30%
3	Re-used powder after 2nd cycle	4.65	2.72%	32	39.62%
4	Re-used powder after 3rd cycle	4.60	3.77%	27	49.06%
5	Re-used powder after 4th cycle	4.58	4.1%	25	52.83%

Slight variations in the value of MFI were obtained with recycling, as illustrated in Figure 4.32. Differences of 0.09 (1.88% decrease in MFI), 0.13 (2.72% decrease in MFI), 0.18 (3.77% decrease in MFI), and 0.20 (4.1% decrease in MFI) were seen between the virgin material and the re-used batches after the 1st, 2nd, 3rd, and 4th re-use cycles, respectively.

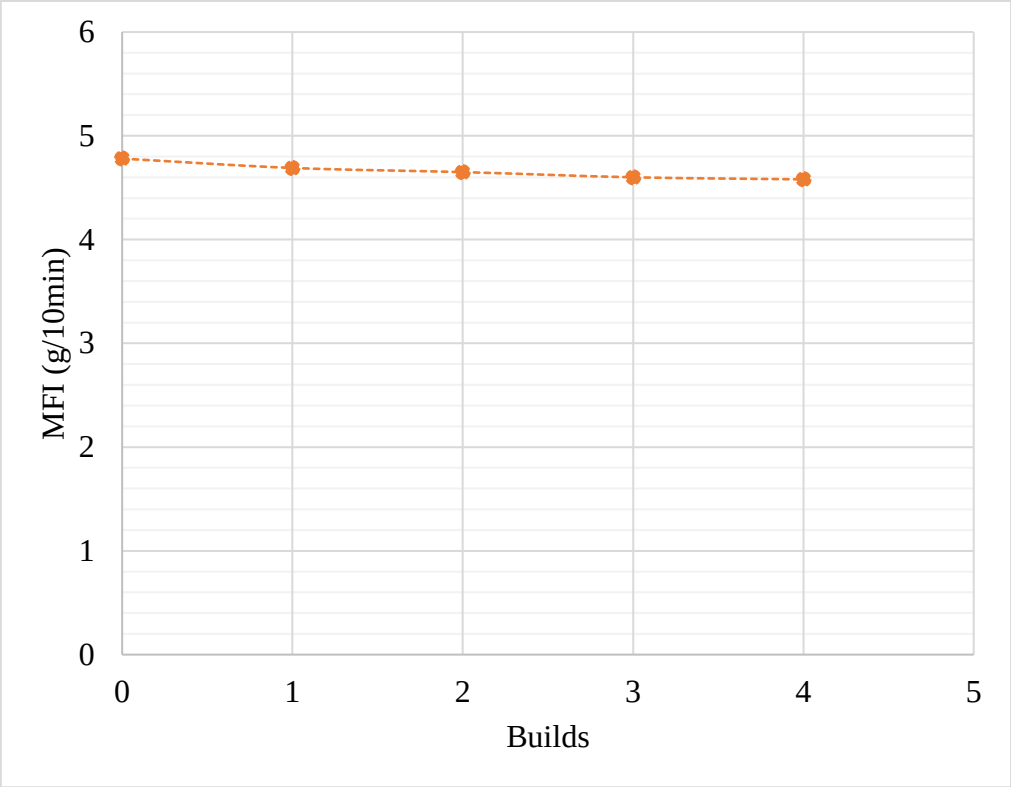

Figure 4.32 Trend of the MFI values for up to four re-use cycles

The findings here confirm the study by Wegner & Ünlü (2016), indicating that PP powder experiences a slight deterioration of rheological properties when used in the LS process. The authors found that the MFI of PP decreases by only 3% when the powder is re-used for a single cycle. This decreasing trend (Figure 4.32) indicates that the powder might experience complete degradation at some point. Changes giving rise to this trend are attributed to changes in the molecular weight of the materials, which also affects the degree of crystallinity of the powder. Dadbakhsh et al. (2017) determined that the crystallinity of PA 12 increases with aging to a maximum point, after which it starts to decrease. Gornet et al. (2002) investigated the effects of repeated re-use of PA 12 from 3D Systems. The authors measured the flow characteristics using an extrusion plastometer, where it was established that MFR decreased with each build cycle, as indicated by Figure 4.33.

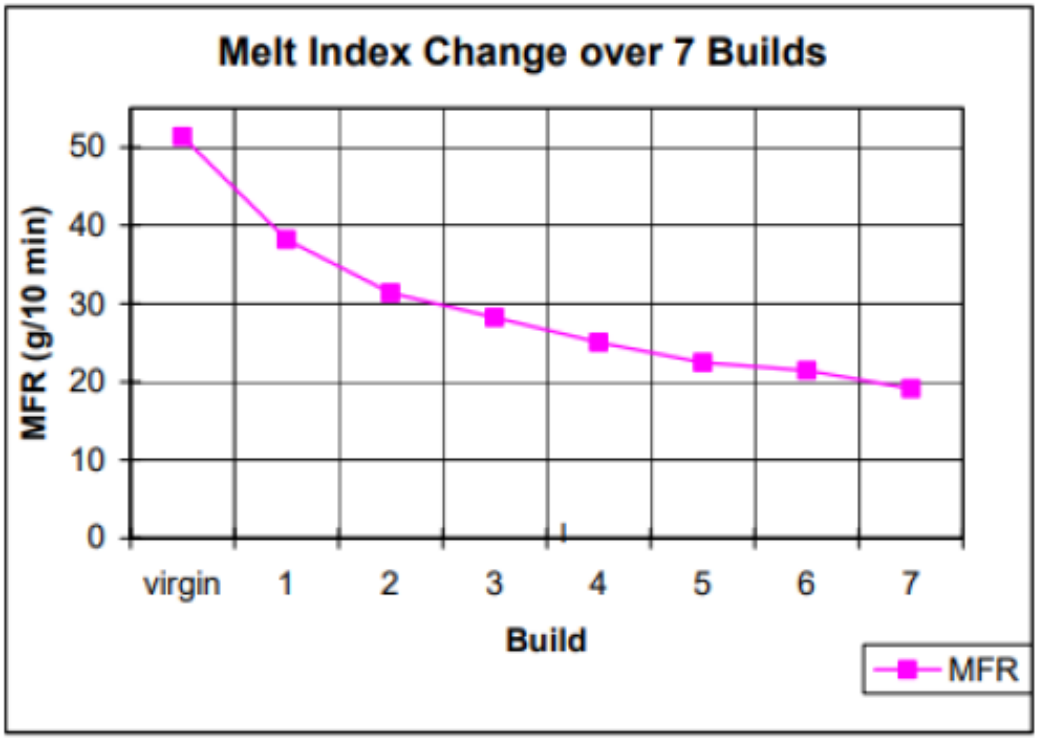

Figure 4.33 MFR of PA 12 with re-use cycles (Gornet et al., 2002)

Kuehnlein et al. (2014) also found that the viscosity of PA 12 increases with processing time. The MFR of the powder used by the authors reduced significantly, from 28 cm^3/10 min to 7 cm^3/10 min after 4 hours of storage in an oven at 170 ℃. Aldahsh (2013) established that the viscosity of a cement/PA 12 composite increased with processing time and temperature. It is evident from the preceding reviews that the characteristics of PA 12 change significantly with re-use cycles. The changes are much more significant than those of PP, as illustrated in Table 4.17. Hence, the PP has superior characteristics compared to PA 12 in terms of deterioration of rheological properties.

4.3.2.2 Results of DSC for Laser PP CP 75 after 100% re-use

The DSC results were used to establish the melting point and sintering window of the five batches of powder, each from a different number of recycles. Tables 4.18 and 4.19 show the melting points and sintering windows of the five batches. The equations used in calculating the sintering window and crystallinity are presented in sub-section 4.23.

Table 4.18 Changes in melting point of Laser PP CP 75 after four re-use cycles

Powder batch	**Peak melting point** (℃)
Fresh material	134.48
1st re-use cycle	135.11
2nd re-use cycle	135.66
3rd re-use cycle	135.75
4th re-use cycle	136.10

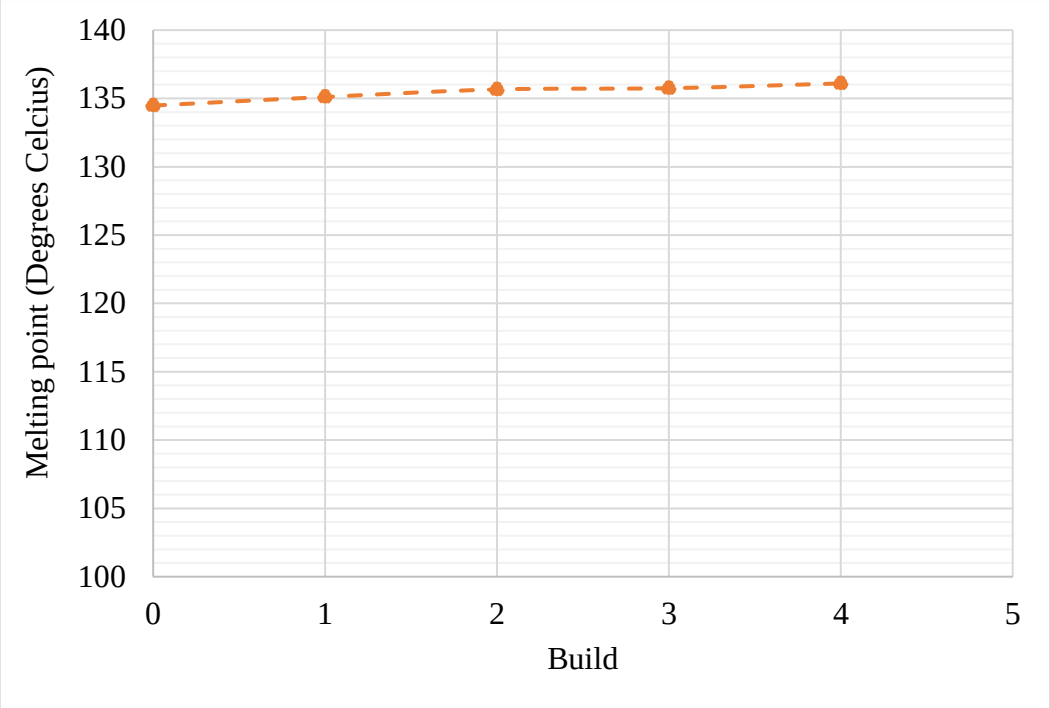

Figure 4.34 Melting points of Laser PP CP 75 for a number of re-use cycles

In Figure 4.34, the melting points of Laser PP CP 75 are seen to increase with each re-use cycle, starting from a value of 134.48 ℃ after the 1st re-use cycle to 136.16 ℃ after the 4th re-use cycle. This behaviour of the material is similar to that of PA 12. Gornet et al. (2002) used DSC to investigate the influence of re-using PA 12 on the melting point of the material. The authors found that the melting point increases with the number of build cycles, as illustrated in Figure 4.35. This trend of the melting point indicates that increasingly higher laser energy is required to fuse the material with each re-use cycle,

which would contribute to further deterioration of the material. It was noted in the literature review in Chapter 2 that suitable polymers should have a narrow melting point region to prevent the use of high laser energy when fusing the particles of powder. This is to avoid more significant degradation of the powder supporting the components being printed and limiting the recyclability of the powder (Goodridge et al., 2012; Marin, 2017). However, as observed here, the melting point of Laser PP CP 75 increases with the number of re-use cycles, which necessitates higher laser beam energy, encouraging further deterioration of the material.

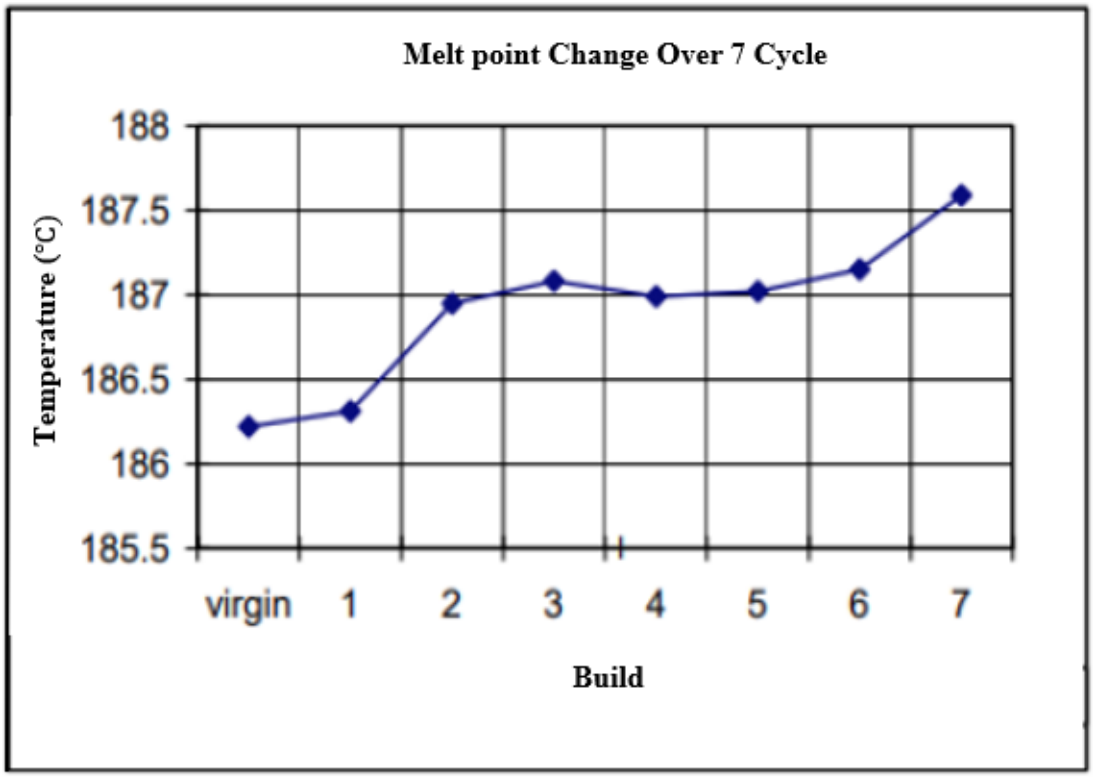

Figure 4.35 Melting points of PA 12 for 7-re-use cycles (Gornet et al., 2002)

The DSC results further illustrate that the sintering window of Laser PP CP 75 increases with each re-use cycle (Figure 4.36). This phenomenon is attributed to the degradation and cross-linking of the long carbon chains (Kuehnlein et al., 2010). A similar phenomenon was also observed by Dadbakhsh et al. (2017), who investigated the effects of re-use cycles on the sintering window of PA 12. The difference between the two materials might be ascribed to the differences in changes of the long carbon chains when subjected to high

temperatures. Figure 4.37 shows that the gap between melting and crystallization points is wider for aged powder than for virgin PA 12.

Table 4.19 Calculated sintering window of Laser PP CP 75 after four re-use cycles

Powder batch	**Sintering window, *SW* (℃)**
Fresh material	18.14
1st re-use cycle	18.21
2nd re-use cycle	20.14
3rd re-use cycle	21.12
4th re-use cycle	22.12

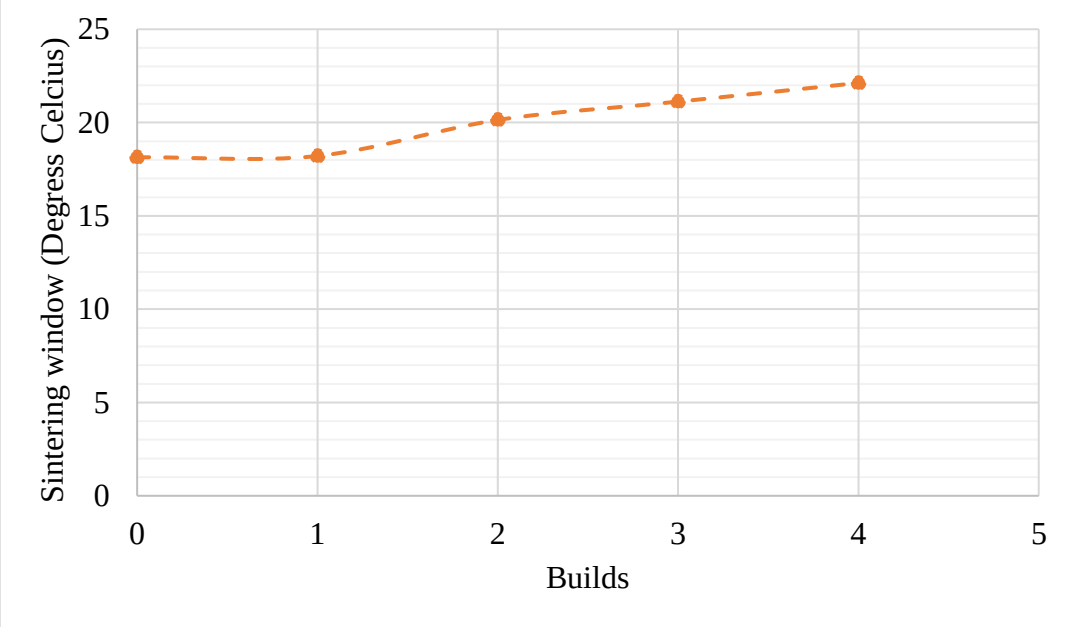

Figure 4.36 Sintering window of Laser PP CP 75 versus re-use cycles

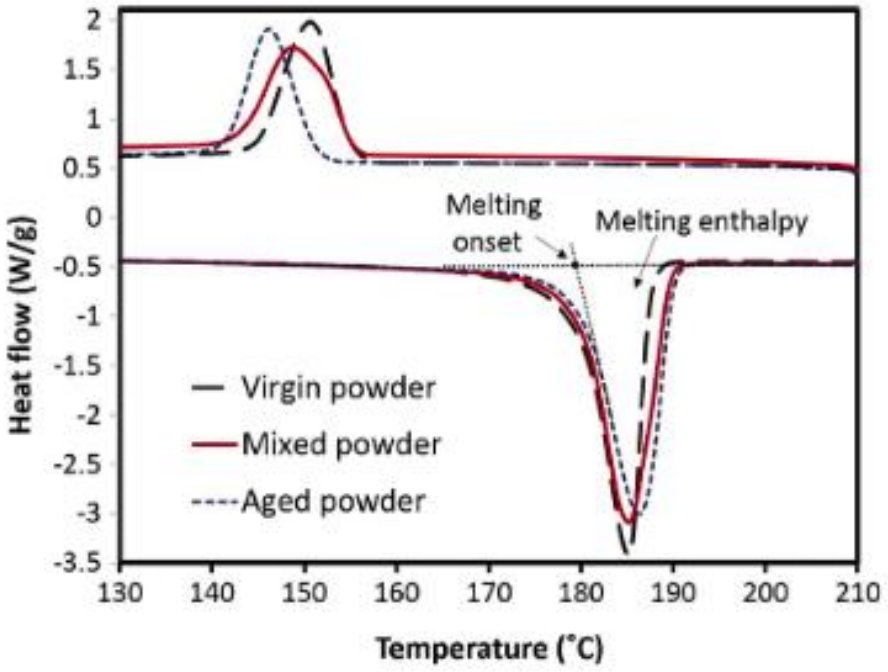

Figure 4.37 DSC thermogram for virgin, aged and mixed PA 12 powder

The sintering window of the new Laser PP CP 75, ranging from 18.14 ℃–22.12 ℃ (Table 4.19), is lower than the sintering window for PA 12, which ranges from 32 ℃–34 ℃ (Marin, 2017). It is, therefore, expected that difficulties would be experienced when regulating the cooling rate of the printed parts using the new Laser PP CP 75. It also explains the problems of curling observed in the present work while printing with the material. The issue of curling can be resolved by establishing the most suitable extraction and building chamber temperatures. Schmid et al. (2017) stated that homogeneous and stable thermal conditions minimize the curling and warpage phenomena. Their findings further indicated that the shrinkage and curling rates might reduce with the re-use cycles because of a wide and sufficient sintering window, preventing crystallization of the polymers during processing (Goodridge et al., 2012; Marin, 2017). Rapid crystallization of printed components is a significant hurdle in LS because it encourages curling and affects the surface finish and dimensional accuracy of the parts (Schmid et al., 2015). The sintering window affects the cooling rate of printed parts, and materials with large sintering windows are known to exhibit even cooling rates. Hence, a larger sintering window decreases the curling and shrinkages rates of printed parts.

4.3.2.3 Results of TGA for Laser PP CP 75 after 100% re-use

The results of TGA analysis were used to establish the degradation and breakdown temperatures of the five batches of powder, each after several re-use cycles. The results of the tests are summarized in Table 4.20.

Table 4.20 TGA results for Laser PP CP 75 after 100% re-use

Powder batch	Degradation temperature (℃)
Fresh material	455.53
1st re-use cycle	455.75
2nd re-use cycle	455.75
3rd re-use cycle	456.04
4th re-use cycle	457.53

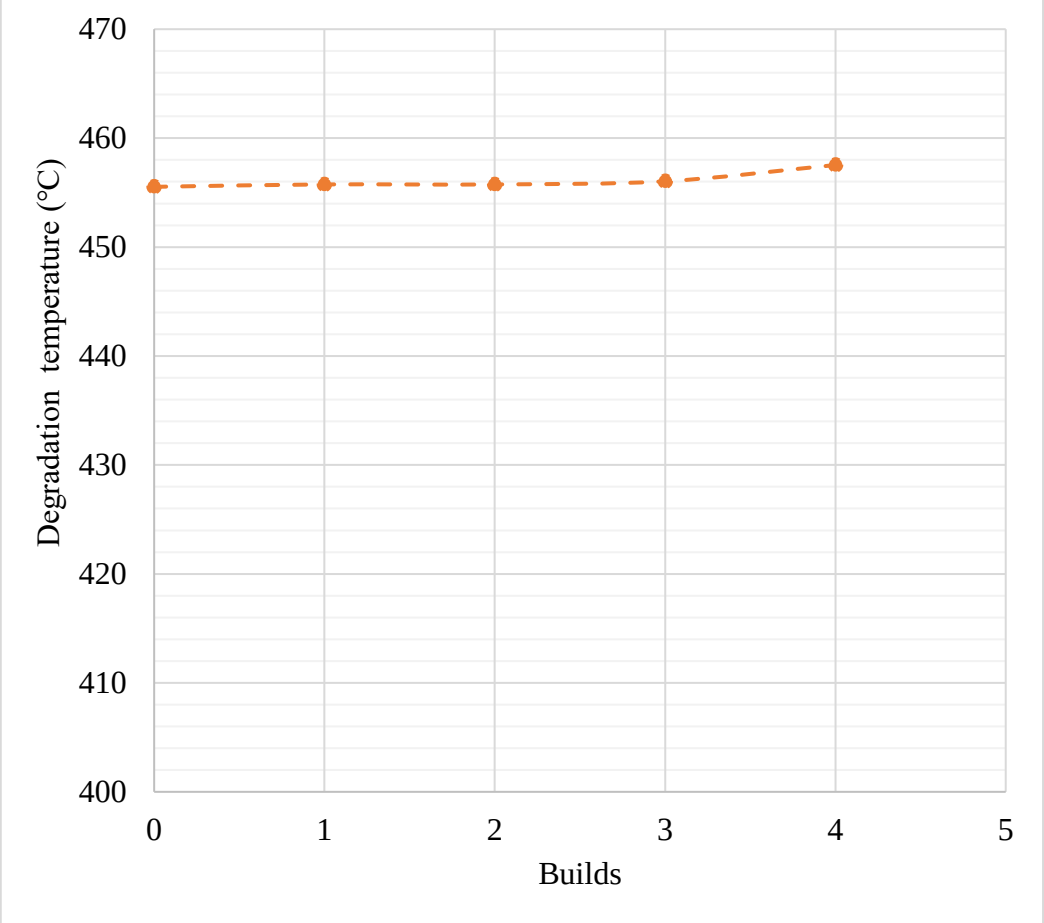

Figure 4.38 Degradation temperature of Laser PP CP 75 versus re-use cycles

The breakdown temperature of Laser PP CP 75 increased slightly with the re-use cycles from 455.53 ℃ (virgin material) to 457.53 ℃ after the 4th re-use cycle (Figure 4.38), probably due to increased crystallinity of the material from cross-linking of the long carbon chains. Building and removal chamber temperatures of 125 ℃ and 128 ℃ were used when printing the material. These temperatures are significantly lower than the registered breakdown temperatures. Hence, the material is not expected to break down during printing, making it suitable for LS processing. Marin (2017) stated that polymers should have high degradation temperatures because LS occurs at high temperatures.

4.3.2.4 Results of SEM for Laser PP CP 75 after 100% re-use

An SEM analysis was undertaken to determine changes in the morphological and powder particle distribution of the PP powder after each re-use cycle.

Table 4.21 illustrates the distribution of particle sizes of Laser PP CP 75 for fresh material and after different re-use cycles. The particle size distribution was determined using ImageJ software.

Table 4.21 Particle size distribution

Powder batch	Powder particle size distribution (µm)	Mean powder particle size (µm)	Standard deviation of the particle size (µm)
Fresh material	64.54–248.49	150.23	39.30
1st re-use cycle	55.45–250.76	143.87	31.97
2nd re-use cycle	74.73–266.59	148.18	39.40
3rd re-use cycle	59.54–273.94	158.66	43.43
4th re-use cycle	69.44–274.65	156.32	36.45

The powder particle distribution for Laser PP CP 75 is far above the recommended range, which should be between 20 µm and 80 µm according to Schmid and Wegener (2016), and 45 and 90 µm based on a study by Schmidt et al. (2019). It was noted in the literature review that extremely large particles affect the spreading of powder using a recoater roller or blade. Large particles also discourage fusion, which introduces porosity and, in turn, reduces the mechanical integrity of printed parts (Schmid & Wegener, 2016). The mean particle size varied for the five batches of powder, and the difference between the value for fresh powder and powder after the 4th print cycle was 6.09 µm, which is a small 4.05% change. This finding confirms a study by Dadbakhsh et al. (2017) that concludes that particle size of polymeric powder particles is not significantly influenced by re-use cycles. The data in Table 4.21 shows that the build layer thickness for processing Laser PP CP 75 should be around 300 µm because, according to Berretta et al. (2014), the build layer thickness for processing should be at least twice the average size of the powder particles to ensure that powder fusion happens on direct contact with the laser beam rather than having particle-to-particle conduction. Particle-to-particle conduction results in the partial coalescence of the particles that then leads to the production of mechanically weak components.

The effect of recycling on the morphology and agglomeration of PP CP 75 was investigated using SEM, and the micrographs are shown in Figure 4.35. The micrographs show that Laser PP CP 75 is a composite of two materials. One of the materials has irregularly shaped particles, and the other material has perfectly spherical particles, both of different sizes. Based on the results obtained from scanning of Laser PP CP 60 presented in sub-section 4.3.2, the irregularly shaped particles are Laser PP CP 75 polymer particles consisting of pure PP. The perfectly shaped particles are glass beads (according to the manufacturer) that were added to improve the difficulties of flowability experienced with Laser PP CP 60. The preliminary work on Laser PP CP 60 showed the presence of agglomeration after the 1st print cycle (Figure 4.11). However, Laser PP CP 75 exhibited a different behaviour and did not show signs of agglomeration for the 1st, 2nd, and 3rd re-use cycles, and only showing it after the 4th re-use cycle, as illustrated in Figure 4.39.

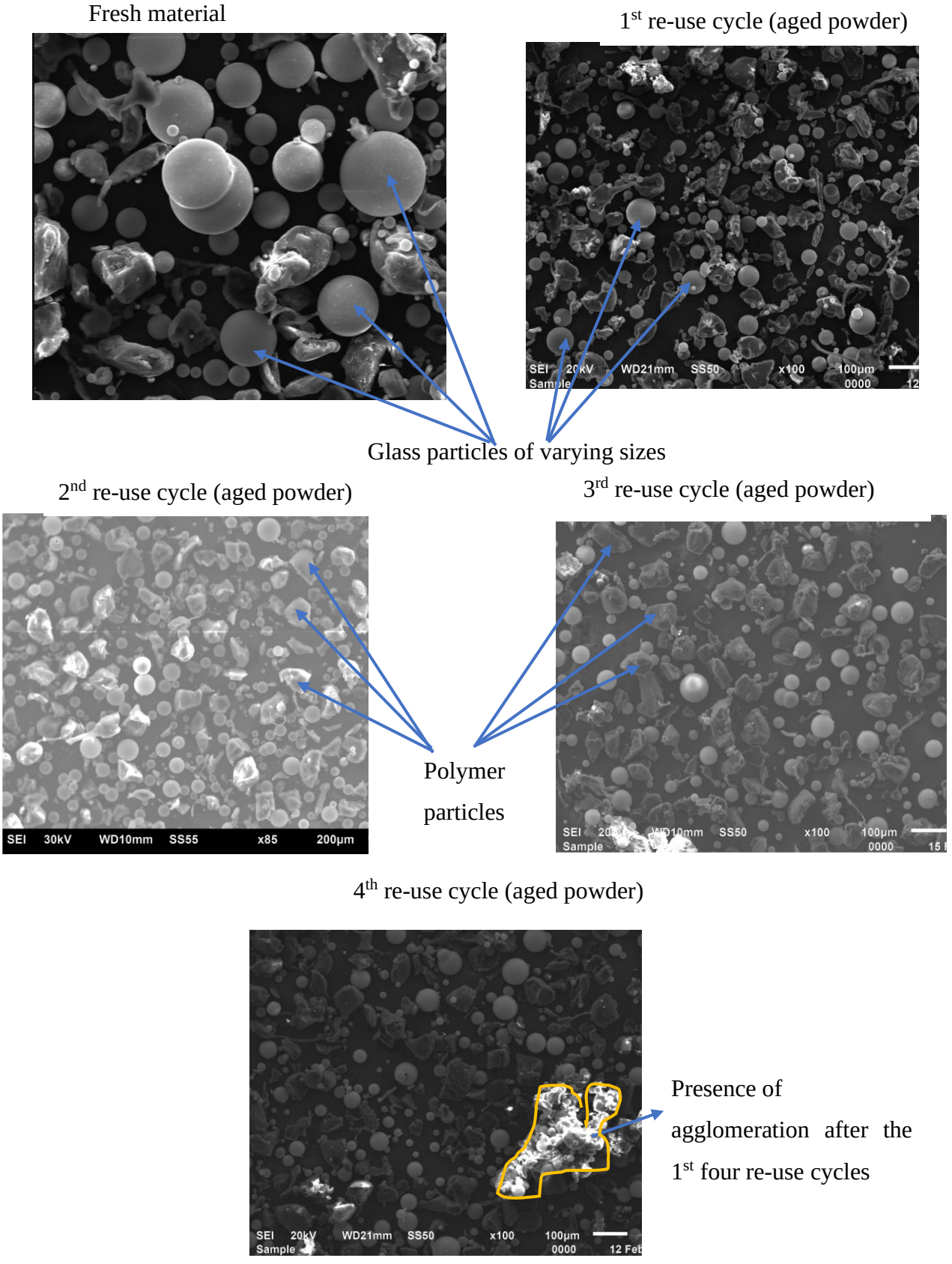

Figure 4.39. Powder morphology for Laser PP CP 75

4.3.3 Part Characterization to Establish Recyclability of Laser PP CP 75

After each re-use cycle, the printed parts were also subjected to tensile testing and analysis for dimensional accuracy to investigate changes in the mechanical and physical properties of the components printed using Laser PP CP 75 material.

4.3.3.1 Uniaxial tensile test for Laser PP CP 75 after 100% re-use

The average values of tensile strength, Young's modulus, and percentage elongation at break for the five samples tested after each re-use cycle are summarized in Tables 4.22, 4.23, and 4,24, respectively. The trends of these mechanical properties are illustrated in Figures 4.40, 4.41, and 4.42.

Table 4.22 Ultimate tensile strength of printed parts after 100% re-use

#	Powder batch	Ultimate tensile strength (MPa)
1	Virgin powder (1st print cycle)	6.7
2	Re-used powder (2nd print cycle)	7.1
3	Re-used powder (3rd print cycle)	7.4
4	Re-used powder (4th print cycle)	6.7
5	Re-used powder (5th print cycle)	6.6

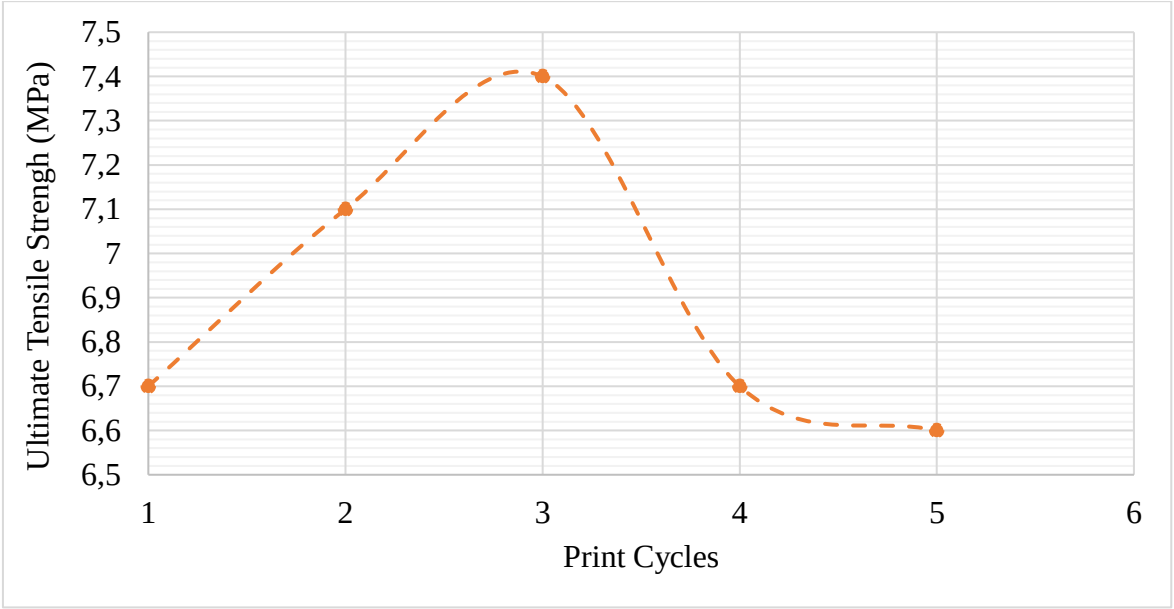

Figure 4.40 Ultimate tensile strengths of parts printed using Laser PP CP 75

In Figure 4.40, the tensile strength of the printed parts is seen to have increased slightly, from 6.7 MPa to 7.4 MPa, with the re-use of powder up to the 2nd re-use cycle. After the 2nd re-use cycle, the value tensile strength of the printed parts decreased to below that of the parts printed from fresh powder.

Table 4.23 Young's modulus of printed parts after 100% re-use

#	Powder batch	Young's modulus (MPa)
1	Virgin powder (1st print cycle)	1141.273
2	Re-used powder (2nd print cycle)	929.623
3	Re-used powder (3rd print cycle)	807.638
4	Re-used powder (4th print cycle)	934.513
5	Re-used powder (5th print cycle)	1080.075

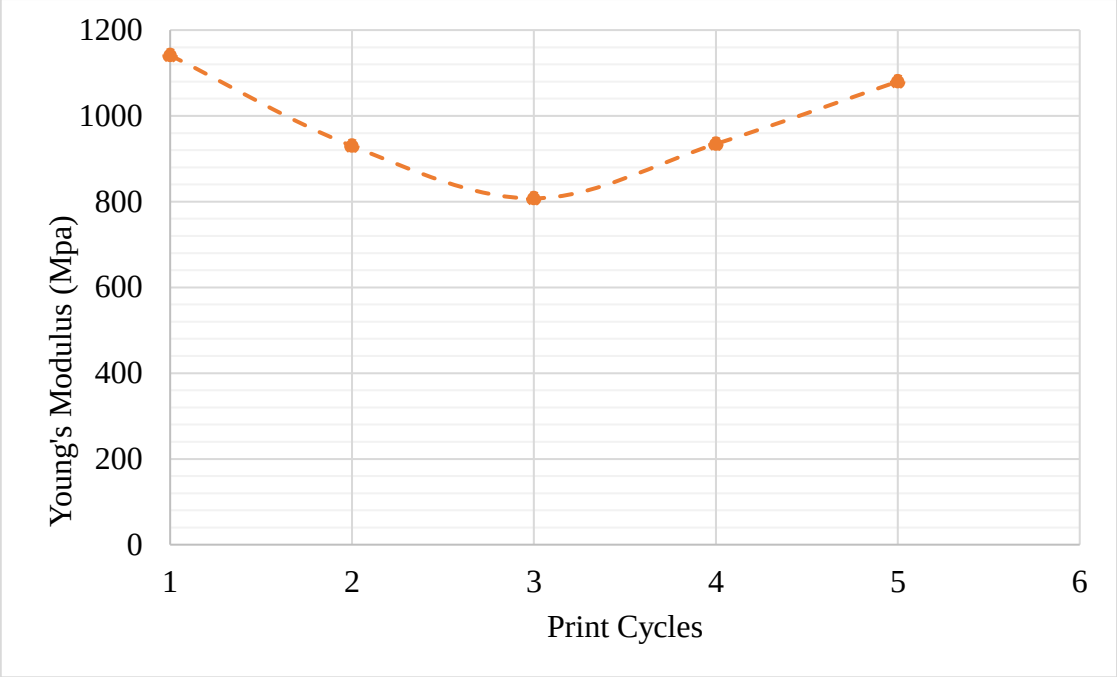

Figure 4.41 Young's modulus of parts printed using Laser PP CP 75

The Young's modulus of the printed parts decreased continuously with re-use of the powder up to the 2nd re-use cycle from an initial value of 1141.273 MPa for the 1st print cycle to 807.638 MPa after the 3rd print cycle. After this, the Young's modulus starts to increase with each re-use cycle.

Table 4.24 Percentage of elongation at break of printed parts after 100% re-use

#	Powder batch	Percentage of elongation at break (%)
1	Virgin powder (1st cycle)	61.91
2	Re-used powder (2nd cycle)	55.56
3	Re-used powder (3rd cycle)	29.73
4	Re-used powder (4th cycle)	45.40
5	Re-used powder (5th cycle)	46.46

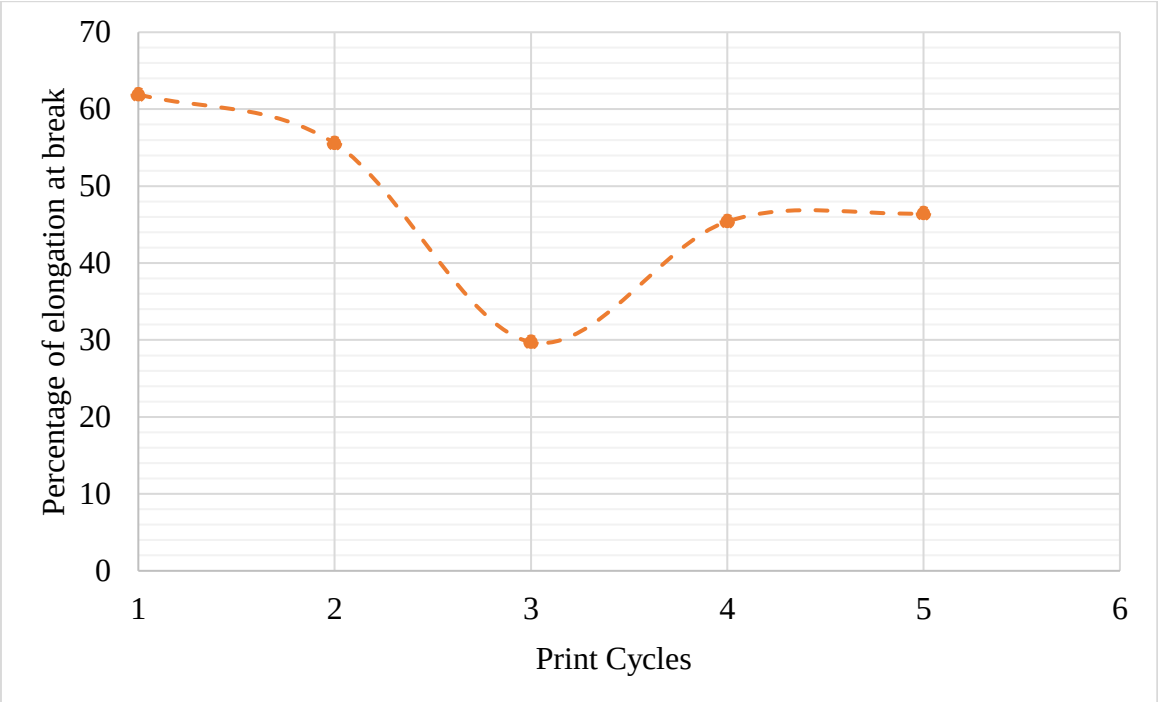

Figure 4.42 Percentage elongation at break of Laser PP CP 75 printed parts

The percentage elongation of the printed parts decreased continuously with the re-use of powder up to the 2nd re-use cycle, starting with 61.91% for parts printed with virgin powder to 29.73% after the 3rd print cycle. After the 2nd re-use cycle, the percentage elongation increases for the next re-use cycle and then levels out beyond this.

The trends seen in the curves of the variation of the strength, stiffness and percentage elongation of printed parts might be due to changes in the crystallinity of the material, which is ascribed to the entanglement and in-ordered chain folding of the long carbon

chains during the LS process, which gives rise to a rise and drop in crystallinity, respectively, (Dadbakhsh et al., 2017). An increase in crystallinity raises the ultimate tensile strength of printed parts at the expense of the percentage of elongation to break, which decreases (Goodridge et al., 2012). It can be seen from the preceding figures that Laser PP CP 75 attained the highest ultimate tensile strengths for the 2nd re-use cycle.

Another study by Wegner & Ünlü (2016) found that the mechanical properties of parts produced using PP decreased with the number of re-use cycles (Figure 4.43). The magnitude of the reduction of mechanical factors was found to be significantly influenced by the energy density of the laser beam used. This emphasizes the need for suitable process parameters to be used when printing polymeric materials.

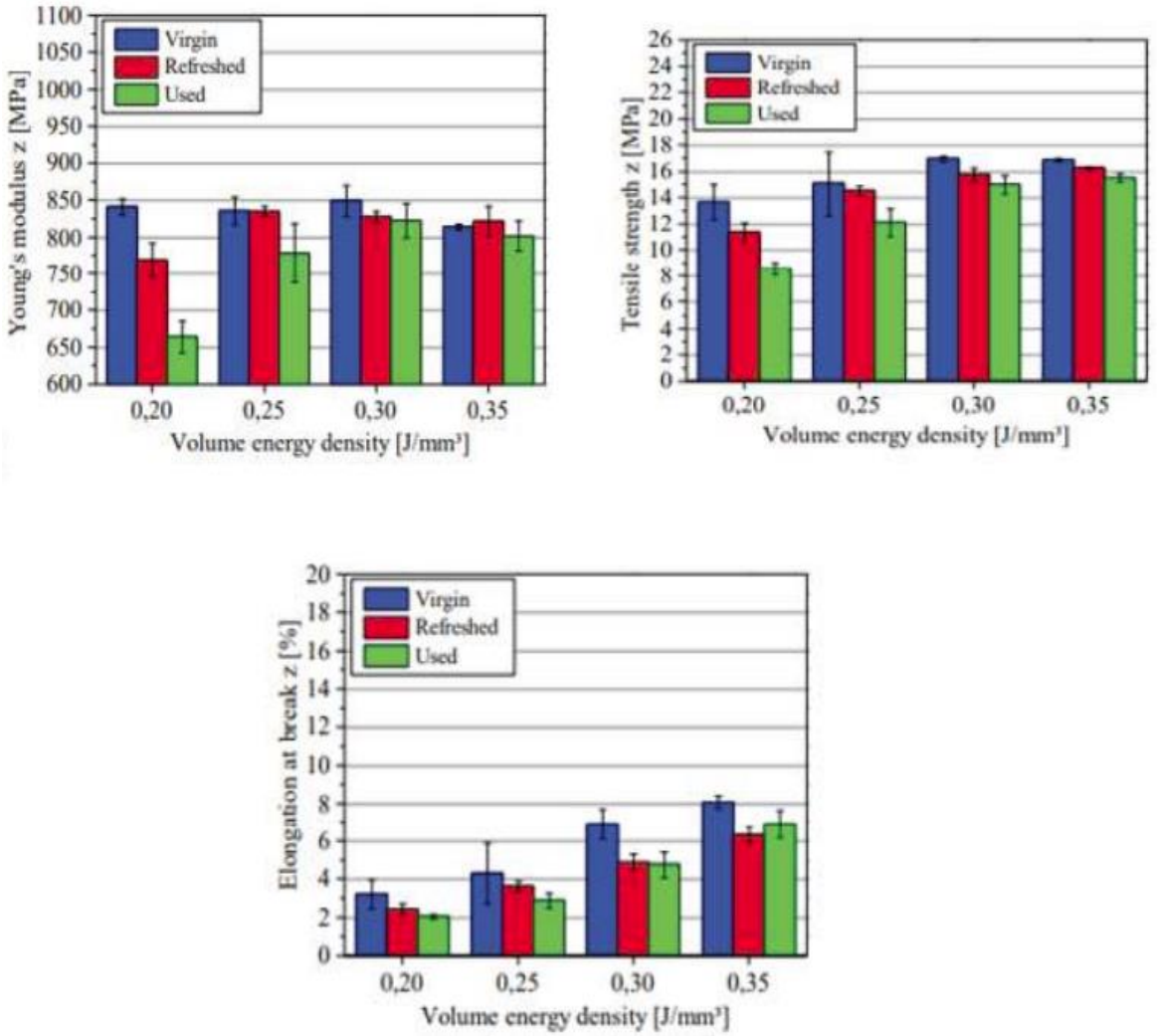

Figure 4.43 Effects of re-use cycles on the mechanical properties of PP

4.3.3.2 Dimensional accuracy of parts printed using Laser PP CP 75

The dimensional accuracy of the printed parts was expressed using error *S1*, as recorded in Table 4.25. In this study, ten measurements were taken for five samples, and the average value determined. The dimensions measured include the total length, width, and thickness of the specimen. The dimensional error *S1* was calculated using Equation 4.3 by Singh et al. (2012).

$$S_1 = \frac{A_1 - A_0}{A_0} * 100\% \quad (4.3)$$

where,

A_0 = Design size of the CAD diagram

A_0 = Actual size measured using a Vernier calliper

Table 4.25. Dimensional errors of LS printed parts

Measurement	Specimen 1 (S1%)	Specimen 2 (S1%)	Specimen 3 (S1%)	Specimen 4 (S1%)	Specimen 5 (S1%)
Thickness	5.0	7.5	2.5	5.0	10.0
Length	0.55	0.34	0.0	0.62	0.68
Width	3.5	6.5	1.5	3.0	1.5
Average (S1%)	3.02	4.78	1.33	2.87	4.06

Specimen 1 - Parts produced using virgin material (1st cycle)

Specimen 2 - Parts produced using re-used powder (2nd cycle)

Specimen 3 - Parts produced using re-used powder (3rd cycle)

Specimen 4 - Parts produced using re-used powder (4th cycle)

Specimen 5 - Parts produced using re-used powder (5th cycle)

Table 4.25 indicates that dimensions of the printed parts differed from those of the CAD diagram, with maximum errors of up to 10%, 0.68%, and 6.5% for the thickness, length, and width occurring for the 5th print cycle parts, respectively. The errors are thought to have been caused by the expansion of parts due to the effect of heating in the LS process (Singh et al., 2012). The trend for the average dimensional error is presented in Figure 4.44 and was used as a representative figure for ease of analysis. The average dimensional error increased for the 1st re-use cycle from 3.02% to 4.78%. It then dropped to 1.33% for the 3rd

print cycle. After this, the average dimensional error increased to 2.87% and 4.06% for the 4th and 5th print cycles, respectively. It can be concluded that the lowest average dimensional error of 1.33% was achieved from parts printed during the 3rd print cycle. Overall, the dimensional variation of the printed parts indicates that Laser PP CP 75 material might not be suitable for commercial purposes due to the high dimensional tolerance required of commercial parts. Besides, significant curling was experienced, which affected the edges of the printed parts (see Figures 4.28–4.31).

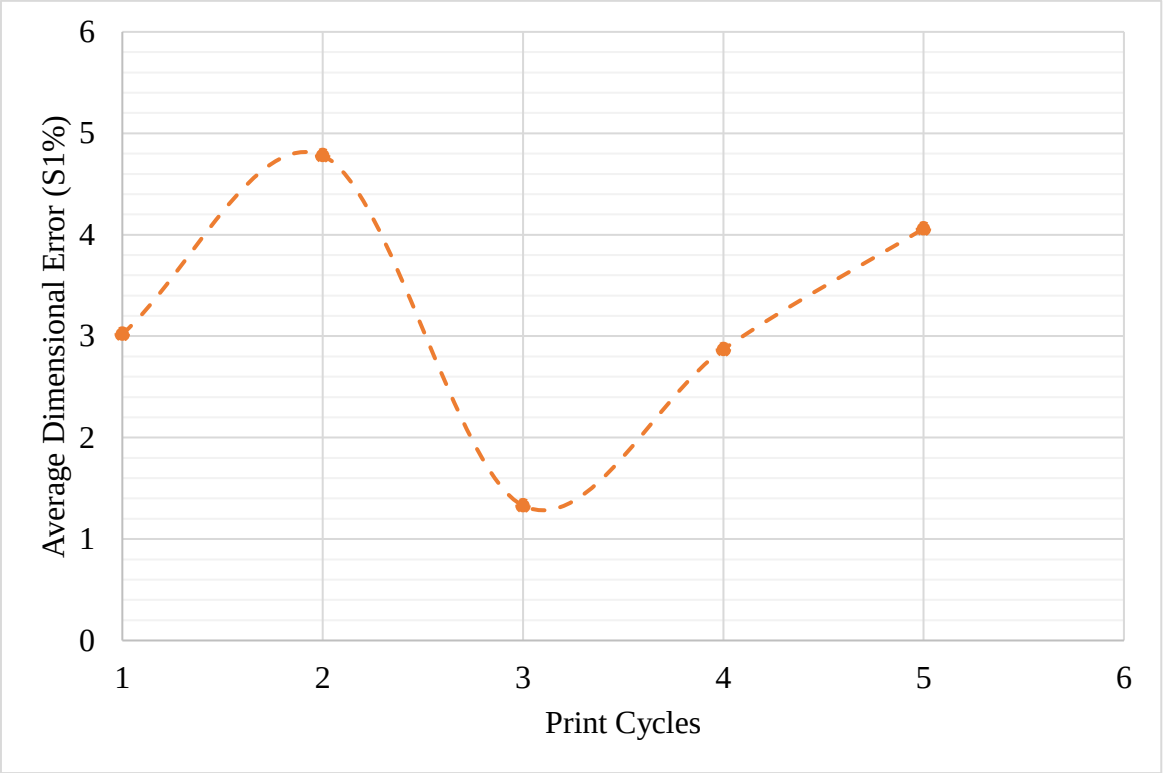

Figure 4.44 Average dimensional error for parts printed using Laser PP CP 75

CHAPTER 5 – CONCLUSION AND RECOMMENDATIONS

5.0 CONCLUSIONS

- Preliminary testing to determine the optimal processing parameters for Laser PP CP 60 showed that:
    1) The most suitable temperature for both the building and removal chambers for Laser CP PP 60 was obtained as 125 ℃. However, after further testing, the appropriate parameters were 125 ℃ and 128 ℃ for the removal and process chamber temperatures, respectively. Partial baking of the cake powder was observed for different combinations of temperatures tested, which is deleterious and undesirable as it affects the recyclability of the material. Therefore, the focus turned to Laser PP CP 75.
    2) The process parameters that yielded the highest ultimate tensile strength (tensile test) for Laser CP PP 60 were 125 ℃, 125 ℃, 0.15 mm, 250 µm, 4500 mm/s, 34.7 W, 1500 mm/s, and 21.3 W for the removal chamber temperature, building chamber temperature layer thickness, hatch distance, scanning speed fill, laser power fill, scanning speed contour, and laser power contour, respectively.
    3) The following process parameters were considered the most suitable, based on the smoothest surface roughness: 125 ℃, 125 ℃, 0.15 mm, 250 µm, 3500 mm/s, 31.5 W, 1500 mm/s, and 10.7 W, for the same respective parameters.
    4) The most suitable process parameters for dimensional accuracy were 125 ℃, 125 ℃, 0.15 mm, 250 µm, 2500 mm/s, 30.2 W, 700 mm/s, and 13.0 W.
    5) Only flat tensile specimens could be printed with Laser PP CP 60, even with the best process parameters determined here. Problems with curling affected the spreading of the powder, as the recoater blade kept dislodging parts on the print table, causing the process to terminate. This is another reason why the focus was turned to Laser PP CP 75.
- Laser PP CP 60 characterization for a single print cycle showed that:
    1) All three batches of Laser PP CP 60 powder (virgin, aged, virgin-aged mixture) showed poor (not 100% spherical) but allowable morphology and particle size distribution. It was also concluded that the used Laser PP CP 60 showed the presence of agglomeration, which can be ameliorated by adding virgin powder and proper mixing.

2) The sintering windows for all three batches of Laser PP CP 60 were lower than that for PA 12 (32 ℃–34 ℃), which might have contributed to high shrinkage rates observed due to difficulties regulating the cooling rate of the printed parts that led to the parts curling.
3) The degree of crystallinity of virgin Laser PP CP 60 decreased from 13.92% to 12.12% after a single printing cycle and then increased to 12.48% after the addition of 50% virgin powder.
4) The high degradation and break-up temperatures of the three batches of Laser PP CP 60 powder (457.30 ℃, 456.05 ℃, and 455.91 ℃ for the virgin powder, used powder, and a 50% virgin: 50% used mixture, respectively) determined from TGA analysis, makes the material suitable for LS processing.
5) The low values of MFI of the three batches of Laser PP CP 60 powder (6.1, 6.5, and 6.4 g/10min for the virgin powder, used powder, and a 50% virgin: 50% used mixture, respectively) implies a high viscosity of the powder, and therefore, poor flowability of the material, and may explain the difficulties experienced processing the powder.

- From the experiments to investigate the recyclability of Laser PP CP 75, it was concluded that:
    1) The manufacturer's recommended process parameters were suitable except for the process and removal chamber temperatures. Preliminary optimization indicated that the most suitable temperatures with minimal curling were 128 ℃ and 125 ℃ for the process and removal chambers, respectively. These two process parameters are the most crucial to consider when optimizing LS processing of polymers because they determine curling, a common problem with polymers.
    2) Initially, high curling of built parts was experienced with Laser PP CP 75, impeding the printing process. However, pre-warming the EOSINT P 380 machine for four hours instead of two hours helped ameliorate the curling phenomenon to levels that allowed printing to continue.
    3) Laser PP CP 75 can be re-used 100% for five print cycles without mixing with virgin material because it does not form an "orange peel", as is the case with PA 12 (used in this dissertation as reference material).

4) The MFI value of the powder exhibited small changes, with a 4.1% decrease after the 4th re-use cycle, indicating that the viscosity of the material does not degrade significantly by re-use and therefore promotes recyclability of the powder.
5) The melting point increased from 134.48 ℃ to 136.16 ℃ after the 1st four re-use cycles, which indicates that higher laser energy might be required to fuse the powder with increasing re-use. This is undesirable as higher beam energy densities promote further deterioration of the polymeric material.
6) The DSC test results established that the sintering window of Laser PP CP 75 increased with each re-use cycle. The sintering window increased from 18.14 ℃ for the virgin material to 21.12 ℃ after the 4th re-use cycle. This implies that the shrinkage and curling rate will reduce with the number of re-use cycles because a wide and sufficient sintering window prevents the crystallization of the polymers during processing.
7) The breakdown temperature of Laser PP CP 75 increased slightly with the number of re-use cycles, from 455.53 ℃ (virgin material) to 457.53 ℃ after the 4th re-use cycle, based on the TGA test. Thus, the material does not break down at these temperatures, making it suitable for LS processing and recycling.
8) The SEM analysis revealed that the difference between the mean particle size for the fresh and the powder after the 4th re-use cycle was 6.09 µm, a small 4.05% change. Hence, it can be stated that the average size of Laser PP CP 75 powder particles is not significantly influenced by cycling, making the powder good for this purpose. The powder was found to have irregularly shaped particles, which impedes spreading, but the material did not exhibit signs of agglomeration for the 1st, 2nd, and 3rd cycles. However, this became evident in the 4th re-use cycle.
9) Tensile testing revealed that the parts built from this powder attained the highest ultimate tensile strength after the 3rd print cycle (2nd recycle cycle) (7.4 MPa), after which the values of strength decreased with each recycling.
10) Overall, it can be concluded that PP has superior recyclability properties than PA 12, which has to be mixed with virgin material after every print cycle. Besides, MFI value changes of 4.1% after four re-use cycles are notable compared to those of PA 12, where changes of up to 52.83% have been

recorded. Clearly, the rheological properties of Laser PP CP 75 are not significantly affected by recycling. Moreover, the mean particle size only changes by 4.05%, which cannot hamper the re-use of the material due to difficulties of spreading the powder across the build chamber. Lastly, the changes in thermal properties (sintering window and breakdown temperatures) encourage the recycling of the powder.

11) However, Laser PP CP 75 might not be commercially applicable because of the observed significant errors of dimensional accuracy. The parts printed with virgin Laser PP CP 75 had an average dimensional error of 3.02% for the virgin powder and 4.06% after the 4^{th} re-use cycle, which changes, though small, are significant errors where high dimensional tolerance is required.

5.1 RECOMMENDATIONS

- Attempts should be made to build components with complex geometries to determine the geometrical accuracy and capability of printing intricate components using Laser PP CP 60 and Laser PP CP 75.
- The SEM images revealed that the Laser PP CP 60 did not have flow agents. Therefore, the best flow/antistatic agents and their proportion for addition to this powder should be determined without compromising the mechanical and physical properties of the printed parts.
- Further experiments should be undertaken to determine the exact cut-off re-use cycles for Laser PP CP 75 powder.

References

[1] *4D printing : Is this the Fourth Industrial Revolution?* (n.d.). Retrieved from https://www.iberdrola.com/innovation/what-is-print-4d. (Accessed on 13/10/2021).

[2] Aklonis, J. J. 1981. *Mechanical properties of polymers*. ACS: Washington, D.C.

[3] Aldahsh, S. 2013. Dependence of SLS parameters on thermal properties of composite material of cement with polyamide 12. *Journal of Applied Mechanical Engineering*, Vol.2, No.5, pp.1-7.

[4] Aly, A. A. 2015. Heat treatment of polymers: a review. *Int. J. Materials Chemistry and Physics*, Vol.1, No.2, pp.132-140.

[5] Amado, A., Schmid, M., Levy, G., & Wegener, K. 2011. Advances in SLS powder characterization. *Group*, Vol.7, No.10, pp.12-27.

[6] American Society for Testing and Materials. 2014. D638 − 14. *Standard test method for tensile properties of plastics*, 17. Retrieved from https://doi.org/10.1520/D0638. (Accessed on 08/03/2021).

[7] Arroyo, A. 2016. Additive manufacturing. *Industrial Revolution*, Vol.4, No.1, pp.1-5.

[8] ASM. 2004. Introduction to Tensile Testing. *Tensile Testing*, pp.1-13. Retrieved from https://www.asminternational.org/documents/10192/1849770/05106G_Sample_BuyNow.pdf/b4838889-d1dc-4bf5-a8bd-d6771fa36bf8. (Accessed on 08/03/2021).

[9] Aydin, M. 2015. Additive manufacturing: Is it a new era for furniture production? *Journal of Mechanics Engineering and Automation*, Vol.5, No.1, pp.338-347.

[10] Bassam, I. K. 2014. Introduction of polymers. *Medical and Biological Polymers*, Vol.2, No.1, pp.1-7.

[11] Bauman, I., Ćurić, D., & Boban, M. 2008. Mixing of solids in different mixing devices. *Sadhana*, Vol.33, No.6, pp.721-731.

[12] Berretta, S., Evans, K. E., & Ghita, O. 2015. Processability of PEEK, a new polymer for high temperature laser sintering HT-LS. *European Polymer Journal*, Vol.68, No.1, pp.243-266.

[13] Berretta, S., Ghita, O., & Evans, K. E. 2014. Morphology of polymeric powders in Laser Sintering (LS): from polyamide to new PEEK powders. *European Polymer Journal*, Vol.59, No.1, pp.218-229.

[14] Berretta, S., Wang, Y., Davies, R., & Ghita, O. R. 2016. Polymer viscosity, particle coalescence and mechanical performance in high-temperature laser sintering. *Journal of Materials Science*, Vol.51, No.10, pp.4778-4794.

[15] Beyler, C. L., & Hirschler, M. M. 2002. Thermal decomposition of polymers. *SFPE Handbook of Fire Protection Engineering*, Vol.2, No.1, pp.1-22.

[16] Bodycomb, J. 2012. *Laser diffraction theory when a light beam strikes a particle*. Retrieved from https://www.horiba.com/fileadmin/uploads/Scientific/Documents/PSA/Webinar_Slides/TE017.pdf. (Accessed on 08/03/2021).

[17] Bourell, D. L, Beaman, J. J., Leu, M. C., & Rosen, D. W. 2009. A brief history of additive manufacturing and the 2009 roadmap for additive manufacturing: looking back and looking ahead. *US-TURKEY Workshop on Rapid Technologies*, Vol.2009. No.1, pp.1-8.

[18] Bourell, D. L., Watt, T. J., Leigh, D. K., & Fulcher, B. 2014. Performance limitations in polymer laser sintering. *Physics Procedia*, Vol.56, No.2014, pp.147-156.

[19] Callister, W. D., & Rethwisch, D. G. 2007. *Materials Science and Engineering: an introduction.* John Wiley & Sons, New York.

[20] *Chapter 8 Metrology of Surface Finish Surface Metrology Concepts. (n.d.).* Retrieved from http://site.iugaza.edu.ps/aabuzarifa/files/METRO20152_CH81.pdf. (Accessed on 08/03/2021).

[21] Chen, P., Wu, H., Zhu, W., Yang, L., Li, Z., Yan, C., & Shi, Y. 2018. Investigation into the processability, recyclability and crystalline structure of selective laser sintered polyamide 6 in comparison with polyamide 12. *Polymer Testing*, Vol.69, No.1, pp.366-374.

[22] Craft, G. M. 2018. *Characterization of nylon-12 in a novel additive manufacturing technology, and the rheological and spectroscopic analysis of peg-starch matrix interactions*. Dissertation from the University of South Florida.

[23] Dadbakhsh, S., Verbelen, L., Verkinderen, O., Strobbe, D., Van Puyvelde, P., & Kruth, J. P. 2017. Effect of PA12 powder reuse on coalescence behaviour and microstructure of SLS parts. *European Polymer Journal*, Vol.92, No.2, pp.250-262.

[24] Davis, T. E., Tobias, R. L., & Peterli, E. B. 1962. Thermal degradation of polypropylene. *Journal of Polymer Science*, Vol.56, No.164, pp.485-499.

[25] Deveswaran, R., Bharath, S., Basavaraj, B. V., Abraham, S., Furtado, S., & Madhavan, V. 2009. Concepts and techniques of the pharmaceutical powder mixing process: A current update. *Research Journal of Pharmacy and Technology*, Vol.2, No.2, pp.245-249.

[26] Dilberoglu, U.M., Gharehpapagh, B., Yaman, U. and Dolen, M. 2017. The role of additive manufacturing in the era of industry 4.0. *Procedia Manufacturing*, Vol.11, No.1: 545-554.

[27] Dimitris, S., & Achilias, L. A. 2014. Recent advances in the chemical recycling of polymers (PP, PS, LDPE, HDPE, PVC, PC, Nylon, PMMA). *Mater Recycle Trends Perspect*, Vol.3, No.2, pp.1-64.

[28] Dotchev, K., & Yusoff, W. 2009. Recycling of polyamide 12 based powders in the laser sintering process. *Rapid Prototyping Journal*, Vol.15, No.3, pp.192-203.

[29] Dowling, N. 1993. *Hardness test. Mechanical behaviour of materials*. Pearson: Boston.

[30] Drummer, D., Greiner, S., Zhao, M., & Wudy, K. 2019. A novel approach for understanding laser sintering of polymers. *Additive Manufacturing*, Vol.27, No.1, pp.379-388.

[31] Drummer, D., Rietzel, D., & Kühnlein, F. 2010. Development of a characterization approach for the sintering behavior of new thermoplastics for selective laser sintering. *Physics Procedia*, Vol.5, No.1, pp.533-542.

[32] Du Plessis, A., Meincken, M., & Seifert, T. 2013. Quantitative determination of density and mass of polymeric materials using microfocus computed tomography. *Journal of Nondestructive Evaluation*, Vol.2, No.4, pp.413-41.

[33] Duddleston, L. J. 2015. *Polyamide (Nylon) 12 powder degradation during the selective laser sintering process*. Master's Thesis, University of Wisconsin.

[34] Dunson, D. 2017. Characterization of polymers using dynamic mechanical analysis (DMA). *Eurofins Material Science.* Vol.1, No.1, pp.1-8.

[35] Ebewele, R. O. 2000. *Polymer science and technology*. CRC Press: Florida.

[36] ECHA. *Guidance for monomers and polymers.* Wiley Publishers: London, 2012.

[37] Elmer, P. 2012. *DMA Perkin Elmer*, pp.1-38. Retrieved from https://www.perkinelmer.com/CMSResources/Images/44 74546GDE_IntroductionToDMA.pdf. (Accessed on 08/03/2021).

[38] Farkas, G., & Drégelyi-Kiss, Á. 2018. Measurement uncertainty of surface roughness measurement. *IOP Conference Series: Materials Science and Engineering*, Vol.448, No.1, pp.012020- 012033.

[39] Ferraris, C. F., 2001. Concrete mixing methods and concrete mixers: state of the art. *Journal of Research of the National Institute of Standards and Technology*, Vol.106, No.2, pp.391-399.

[40] Fiedler, L., Garcia Correa, L. O., Radusch, H. J., Wutzler, A., & Gerken, J. 2007. Evaluation of polypropylene powder grades in consideration of the laser sintering processibility. *In: Zeitschrift Kunststofftechnik, Bd*, Vol.3, No.1, pp.1-14.

[41] Flores Ituarte, I., Wiikinkoski, O., & Jansson, A. 2018. Additive manufacturing of polypropylene: a screening design of experiment using laser-based powder bed fusion. *Polymers*, Vol.10, No.12, pp.1293-1306.

[42] Ford, S. L. 2014. Additive manufacturing technology: potential implications for U.S. manufacturing competitiveness. *Journal of International Commerce & Economics*, Vol.6, No.1, pp.24- 40.

[43] Garrison, T. F., Murawski, A., & Quirino, R. L. 2016. Bio-based polymers with potential for biodegradability, *Polymer Science*, Vol.8, No.7, pp.1-262.

[44] Gong, X., Anderson, T., & Chou, K. 2012. Review on powder-based electron beam additive manufacturing technology. *2012 International Symposium on Flexible Automation*, Vol.1, No.1, pp.507-515.

[45] Goodridge, R. D., Tuck, C. J., & Hague, R. J. M. 2012. Laser sintering of polyamides and other polymers. *Progress in Materials Science*, Vol.57, No.2, pp.229-267.

[46] Gornet, T. J., Davis, K. R., Starr, T. L., & Mulloy, K. M. 2002. Characterization of selective laser sintering materials to determine process stability. *Paper presented at the Solid Freeform Fabrication Symposium, Austin*, Vol.1, No.1, pp.546-553.

[47] Gotro, J., & Prime, R. B. 2002. Thermosets. *Encyclopedia of Polymer Science and Technology*, Vol.1, No.1, pp.1-75.

[48] Grigore, M. 2017. Methods of recycling, properties and applications of recycled thermoplastic polymers. *Recycling*, Vol.2, No.4, pp.1-24.

[49] Guo, J., Bai, J., Liu, K., & Wei, J. 2018. Surface quality improvement of selective laser sintered polyamide 12 by precision grinding and magnetic field-assisted finishing. *Materials & Design*, Vol.138, No.3, pp.39-45.

[50] Hesse, N., Dechet, M. A., Bonilla, J. S. G., Lübbert, C., Roth, S., Bück, A., & Peukert, W. 2019. Analysis of tribo-charging during powder spreading in selective laser sintering: assessment of polyamide 12 powder ageing effects on charging behavior. *Polymers*, Vol.11, No.4, pp.609-681.

[51] Hiorns, R. C., Boucher, R. J., Duhlev, R., Hellwich, K. H., Hodge, P., Jenkins, A. D., Jones, R. G., Kahovec, J., Moad, G., Ober, C. K., & Smith, D. W. 2013. A brief guide to polymer nomenclature. *Polymer Degradation and Stability*, Vol.98, No.1, pp.1-2.

[52] Hogg, R., 2009. Mixing and segregation in powders: evaluation, mechanisms, and processes. *KONA Powder and Particle Journal*, Vol. 27, No.1, pp.3-17.

[53] Ignatyev, I. A., Thielemans, W., & Vander Beke, B. 2014. Recycling of polymers: a review. *ChemSusChem*, Vol.7, No.6, pp.1579-1593.

[54] International Association of Plastics Distribution. (n.d.). *International Association of Plastics Distribution–Typical properties of polypropylene*. 152. Retrieved from http://www.sdplastics.com/pdf/pp.pdf. (Accessed on 30/05/2021).

[55] International Organisation for Standard (ISO). 2010. Standard test method for melt flow rates of thermoplastics by extrusion plastometer. *ASTM International*, pp.1-16. https://doi.org/10.1520/D1238-13. (Accessed on 08/03/2021).

[56] ISO/ASTM 52900:2015. Additive manufacturing - general principles – terminology. Retrieved from https://www.iso.org/obp/ui/#iso:std:iso-astm:52900:ed-1:v1:en. (Accessed on 19/09/2021).

[57] Jagtap, T. U., & Mandave, H. A. 2015. Machining of plastics: a review. *International Journal of Engineering Research and General Science*, Vol.3, No.2, pp.577-581.

[58] Josupeit, S., Lohn, J., Hermann, E., Gessler, M., Tenbrink, S., & Schmid, H. J. 2015. Material properties of laser sintered polyamide 12 as function of build cycles using low refresh rates. *Solid Freeform Fabrication Symposium*, Vol.1, No.1, pp.540-548.

[59] Karger-Kocsis, J. 2012. *Polypropylene structure, blends and composites*. Springer Science & Business Media: Berlin.

[60] Kasser, I. 2007. Chemistry Part II (NCERT XII), pp.425-438. Retrieved from https://www.selfstudys.com/books/ncert-new-book/english/12th/Chemistry-Part-II/8455. (Accessed on 08/03/2021).

[61] Katz, H. S., & Mileski, J. V. eds. 1987. *Handbook of fillers for plastics*. Springer Science & Business Media: Berlin.

[62] Kigure, T., & Niino, T. 2017. Improvement of recycle rate in laser sintering by low temperature process. *Solid Freeform Fabrication Symposium*, Vol.28, No.2017, pp. 550-557.

[63] Kleijnen, R.G., Schmid, M., & Wegener, K. 2019. Production and processing of a spherical polybutylene terephthalate powder for laser sintering. *Applied Sciences*, Vol.9, No.7, pp.1308-1329.

[64] Klein, R. 2011. Material properties of plastics. *Laser Welding of Plastics: Materials, Processes and Industrial Applications*, Vol.1, No.2, pp.3-69.

[65] Klose, R. 2017. Additive Manufacturing: 4. Industrial revolution. focus additive manufacturing. *New Materials*, Vol.9, No.1, pp.1-5.

[66] Kratochvíl, P., & Suter, U. W. 1990. Macromolecular division commission on macromolecular nomenclature: Definitions of terms relating to individual macromolecules,

their assemblies, and dilute polymer solutions. *Polymer Science USSR*, Vol.32, No.8, pp.1683-1704.

[67] Kuehnlein, F., Drummer, D., Rietzel, D., & Seefried, A. 2010. Degradation behavior and material properties of PA 12 plastic powders processed by powder based additive manufacturing technologies. *Annals of DAAAM for 2010 & Proceedings of the 21st International DAAAM Symposium*, Vol.21, No.1, pp.1-2.

[68] Kumar, A., & Gupta, R. K. 2003. *Fundamentals of polymer engineering revised and expanded*. CRC Press: Florida.

[69] Lambert, P. 2014. SLS method & FDM process for 3D printing with plastic. *Sculpteo*. Retrieved from https://www.sculpteo.com/blog/2014/05/13/right-plastic-production-method/. (Accessed on 08/03/2021).

[70] Lamberti, G., Peters, G. W. M., & Titomanlio, G. 2007. Crystallinity and linear rheological properties of polymers. *International Polymer Processing*, Vol.22, No.3, pp.303-310.

[71] Landel, R. F., & Lawrence E. N. 1993. *Mechanical properties of polymers and composites*. CRC Press: Boca Raton.

[72] Langhauser, F., Kerth, J., Kersting, M., Kölle, P., Lilge, D. & Müller, P. 1994. Propylene polymerization with metallocene catalysts in industrial processes. *Macromolecular Materials and Engineering*, Vol.223, No.1, pp.155-164.

[73] Lexow, M. M., & Drummer, D. 2016. New materials for SLS: The use of antistatic and flow agents. *Journal of Powder Technology*, Vol.2016, No.4101089, pp.1-9.

[74] Ligon, S. C., Liska, R., Stampfl, J., Gurr, M., & Mülhaupt, R. 2017. Polymers for 3D printing and customized additive manufacturing. *Chemical Reviews*, Vol.117, No.15, pp.10212-10290.

[75] Liverani, E., Lutey, A. H., Fortunato, A., & Ascari, A. 2017. Characterization of lattice structures for additive manufacturing of lightweight mechanical components. *International Manufacturing Science and Engineering Conference*, Vol.50732, No.1, pp.1-18.

[76] Maconachie, T., Leary, M., Lozanovski, B., Zhang, X., Qian, M., Faruque, O., & Brandt, M. 2019. SLM lattice structures: Properties, performance, applications and challenges. *Materials & Design*, Vol.183, No.1, pp.108137-108155.

[77] Maddah, H. A. 2016. Polypropylene as a promising plastic: A review. *American Journal of Polymer Science*, Vol.6, No.1, pp.1-11.

[78] Majchrowski, R., & Morawski, K. 2015. Surface roughness measurements method based on non-contact optoNCDT sensor. *Paper presented at the XXI IMEKO World Congress Measurement in Research and Industry*, Vol.21, No.1, pp.1-7.

[79] Marin, T.M. *Selective laser sintering of polyolefins.* Master's thesis, Tampere University of Technology, 2017, pp.1-205.

[80] Mark, J. E. *Physical properties of polymers handbook*. ed. 2007, Vol.1076. Springer: New York.

[81] *Materials for Automobiles Lec 17 Plastics Adhesives Material Costs*. (n.d.).

[82] Matos, F., Godina, R., Jacinto, C., Carvalho, H., Ribeiro, I. and Peças, P. 2019. Additive Manufacturing: Exploring the Social Changes and Impacts. *Sustainability*, Vol.11, No.14: 2-18.

[83] Maynard, E. P. 2007. Mixing and blending. Retrieved from https://www.powderbulksolids.com/article/mixing-blending-1. (Accessed on 08/03/2021).

[84] Menard, K. P., & Menard, N. R. 2015. Dynamic mechanical analysis in the analysis of polymers and rubbers. *Encyclopedia of Polymer Science and Technology*. https://doi.org/10.1002/0471440264.pst102.pub2. (Accessed on 08/03/2021).

[85] Mikhaiel, G. 2013. Innovative mixing technology. *Pharmaceutical Engineering*, Vol.2, No.2, pp.86-88.

[86] Mitaľ, G., Dobránsky, J., Ružbarský, J., & Olejárová, Š. 2019. Application of laser profilometry to evaluation of the surface of the workpiece machined by abrasive waterjet technology. *Applied Sciences*, Vol.9, No.10, pp.2134-2148.

[87] Mohamed, O. A., Masood, S. H., & Bhowmik, J. L. 2015. Optimization of fused deposition modeling process parameters: a review of current research and future prospects. *Advances in Manufacturing*, Vol.3, No.1, pp.42-53.

[88] Müller, R. 2005. Biodegradability of polymers: regulations and methods for testing. *Biopolymers online*, Vol.2, No.5, pp.1-20.

[89] Murr, L. E., Gaytan, S. M., Ramirez, D. A., Martinez, E., Hernandez, J., Amato, K. N., & Wicker, R. B. 2012. Metal fabrication by additive manufacturing using laser and electron beam melting technologies. *Journal of Materials Science & Technology*, Vol.28, No.1, pp.1-14.

[90] Mys, N., Verberckmoes, A., & Cardon, L. 2016. Processing of syndiotactic polystyrene to microspheres for part manufacturing through selective laser sintering. *Polymers*, Vol.8, No.11, pp.383-399.

[91] Mys, N., Verberckmoes, A., & Cardon, L. 2018. Expanding the material palette for Selective Laser Sintering: two production techniques for spherical powders. *Paper*

presented at the 8th Bi-annual International Conference on Polymers and Moulds Innovations (PMI 2018). University of Minho. Institute of Polymers and Composites.

[92] Obianyo, I. 2019. Laboratory manual for hardness test. Retrieved from https://www.researchgate.net/publication/331481791_Laboratory_Manual_for_Hardness_Test. (Accessed on 08/03/2021).

[93] Ogawa, H. 2009. Review on development of polypropylene manufacturing process. *Sumitomo Kagaku*, Vol.2009, No.2, pp.1-11.

[94] Ojeda, T. 2013. Polymers and the environment. *Polymer Science. InTech*, Vol.2, No.6, pp.1-5.

[95] Pham, D. T., Dotchev, K. D., & Yusoff, W. A. Y. 2008. Deterioration of polyamide powder properties in the laser sintering process. *Proceedings of the Institution of Mechanical Engineers, Part C: Journal of Mechanical Engineering Science*, Vol.222, No.11, pp.2163-2176.

[96] Polymerization, R. (n.d.). Polymerization chain transfer, pp.354–383.

[97] Poux, M., Fayolle, P., Bertrand, J., Bridoux, D., & Bousquet, J., 1991. Powder mixing: some practical rules applied to agitated systems. *Powder Technology*, Vol.68, No.3, pp.213-234.

[98] Prime, R. B. 2009. An Introduction to thermosets. John Wiley & Sons: London.

[99] Rüsenberg, S., Weiffen, R., Knoop, F., Schmid, H. J., Gessler, M., & Pfisterer, H. 2012. Controlling the quality of laser sintered parts along the process chain. *Proceedings of the 23rd International Solid Freeform Fabrication Symposium (SFF 2012), The University of Texas at Austin*, Vol.23, No.1, pp.1024-1044.

[100] Sagar, M. B., & Elangovan, K. 2017. Consolidation & factors influencing sintering process in polymer powder based additive manufacturing. *Materials Science & Engineering*, Vol.225, No.1, pp.012075-012084.

[101] Saharan, V. A., Kukkar, V., Kataria, M., Kharb, V., & Choudhury, P., 2008. Ordered mixing: mechanism, process, and applications in pharmaceutical formulations. *Asian Journal Pharmaceutical of Sciences*, Vol.3, No.6, pp.240-59.

[102] Sanchez, S. L. 2015. *Study of polymers recycling for 3D printing –PLA characterization*. Vol.77, No.7, pp.223-265.

[103] Schick, C. 2009. Differential scanning calorimetry (DSC) of semi-crystalline polymers. *Analytical and bioanalytical chemistry*, Vol.395, No.6, pp.1589-1611.

[104] Schmid, M, Amado, A., & Wegener, K. 2014. Materials perspective of polymers for additive manufacturing with selective laser sintering. *Journal of Materials Research*, Vol.29, No.17, pp.1824-1832.

[105] Schmid, M., & Wegener, K. 2016. Additive manufacturing: polymers applicable for laser sintering (LS). *Procedia Engineering*, Vol.149, No.1, pp.457-464.

[106] Schmid, M., & Wegener, K. 2016. Thermal and molecular properties of polymer powders for Selective Laser Sintering (SLS). *AIP Conference Proceedings*, Vol.1779, No.1, pp.1-7.

[107] Schmid, M., Amado, A., & Wegener, K. 2015. Polymer powders for selective laser sintering (SLS). *AIP Conference Proceedings*, Vol.1664, No.1, pp.160009-160024.

[108] Schmid, M., Kleijnen, R., Vetterli, M., & Wegener, K. 2017. Influence of the origin of polyamide 12 powder on the laser sintering process and laser sintered parts. *Applied Sciences*, Vol.7, No.5, pp.462-479.

[109] Schmidt, J., Dechet, M. A., Bonilla, J. G., Hesse, N., Bück, A., & Peukert, W. 2019. Characterization of polymer powders for selective laser sintering. *Proceedings of the 30th Annual International Solid Freeform Fabrication Symposium*, Vol.1, No.1, pp.1-5.

[110] Seyforth, J. A. 2015. Scanning Electron Microscopy (SEM). An introduction to the use of SEM for characterising the surface topology and composition of matter with further applications scanning electron microscopy (SEM). *Experimental Techniques In Condensed Matter Physics*, Vol.30, No.1, pp.779-89.

[111] Shashi, G. M., Laskar, M. A. R., Biswas, H., & Saha, A. K. 2017. A brief review of additive manufacturing with applications. *Journal of Mechanics Engineering and Automation*, Vol.4, No.10, pp.138-147.

[112] Singh, S., Sachdeva, A., & Sharma, V. S. 2012. Investigation of dimensional accuracy/mechanical properties of part produced by selective laser sintering. *International Journal of Applied Science and Engineering*, Vol.10, No.1, pp.59-68.

[113] Sinha, N. 2017. Additive manufacturing. *Department of Mechanical Engineering IIT Kanpur*, Vol.5, No.2, pp.1-64.

[114] Stucker, B. 2012. Additive Manufacturing: standards & other international trends. In *Workshop on Measurement and Standards for Metal-based Additive Manufacturing*. Retrieved from https://www.nist.gov/system/files/documents/el/isd/Plenary_Stucker.pdf. (Accessed on 22/03/2021).

[115] Test procedure for laser diffraction particle size distribution. 1999. *Analyzer TxDOT Designation*, Vol.238, No.100, pp.1-7.

[116] Udroiu, R., & Braga, I. C. 2017. PolyJet technology applications for rapid tooling. *MATEC Web of Conferences*, Vol.112, No.2017, pp.3011-3017.

[117] Vaupotic, B., Brezocnik, M., & Balic, J. 2006. Use of PolyJet technology in manufacture of new product. *Journal of Achievements in Materials and Manufacturing Engineering*, Vol.18, No.1-2, pp.319-322.

[118] Vogl, O. 1999. Polypropylene: An introduction. *Polymers*, Vol.1, No.2, pp.1547-1559.

[119] Vohlídal, J. 2009. Glossary of class names of polymers based on chemical structure and molecular architecture. *Pure & Applied Chemistry*, Vol.81, No.6, pp.2-9.

[120] Wegner, A., & Ünlü, T. 2016. Powder life cycle analyses for a new polypropylene laser sintering material. *Solid Freeform Fabrication Symposium–an Additive Manufacturing Conf*erence, Vol.27, No.1, pp.834-846.

[121] Wegner, A., Mielicki, C., Grimm, T., Gronhoff, B., Witt, G., & Wortberg, J. 2014. Determination of robust material qualities and processing conditions for laser sintering of polyamide 12. *Polymer Engineering & Science*, Vol.54, No.7, pp.1540-1554.

[122] Wilkie, C. A., & McKinney, M. A. 2004. Thermal properties of thermoplastics. *Plastics Flammability Handbook*, Vol.1, No.2, pp.58-76.

[123] Wohlers, T., & Gornet, T. 2014. History of additive manufacturing. *Wohlers Report*, Vol.24, No.2014, pp.118-152.

[124] Wong, K. V., & Hernandez, A. 2012. A review of additive manufacturing. *ISRN Mechanical Engineering*, Vol.5, No.3, pp.3-17.

[125] Wudy, K & Drummer, D, 2016. Aging behaviour of polyamide 12, interrelation between bulk characteristics and part properties. *Solid Freeform Fabrication Symposium—an Additive Manufacturing Conference*, Vol.2016, No.27, pp.770-781.

[126] Wudy, K., & Drummer, D. 2016. Aging behavior of polyamide 12: interrelation between bulk characteristics and part properties. *Solid Freeform Fabrication Symposium—an Additive Manufacturing Conference*, Vol.2016, No.27, pp.770-781.

[127] Wudy, K., Drummer, D. & Drexler, M. 2014. Selective laser melting of polyamide 12–A holistic approach for modelling of the ageing behaviour. *Proceedings of the 5th International Conference on Additive Technologies,* Vol.14, No.5, pp.216-221.

[128] Wudy, K., Drummer, D., Kühnlein, F., & Drexler, M. 2014. Influence of degradation behaviour of polyamide 12 powders in laser sintering process on produced parts. *AIP Conference Proceedings*, Vol.1593, No.1, pp.691-695.

[129] Wypych, G. 2012. Handbook of polymers. ChemTec Publishing, Toronto.

[130] Yamauchi, Y., Kigure, T., & Niino, T. 2016. Low temperature laser sintering of PA powder using fiber laser. *Annual International Solid Freeform Fabrication Symposium*, Vol.27, No.1, pp.2204-2216.

[131] Yamauchi, Y., Niino, T., & Kigure, T. 2017. Influence of process time and geometry on part quality of low-temperature laser sintering. *Solid Freeform Fabrication Symposium*, Vol.28, No.1, pp.1495-1506.

[132] Yordem, O. S., Simanke, A. G., & Lesser, A. J. 2011. Reinforcing and toughening of polypropylene with self-assembled low molar mass additives. *Polymer Engineering & Science*, Vol.51, No.3, pp.550-558.

[133] Zaborski, A. (n.d.). *Adam Zaborski – handouts for Afghans*. Retrieved from https://docplayer.net/23884535-Adam-zaborski-handouts-for-afghans.html. (Accessed on 08/03/2021).

[134] Zeus. 2005. Thermal degradation of plastics. *Zeus Technical Whitepaper*, Vol.1, No.2, pp.1-8.

[135] Zhang, H., & LeBlanc, S. 2018. Processing parameters for selective laser sintering or melting of oxide ceramics. *Additive Manufacturing of High-performance Metals and Alloys-Modeling and Optimization*, Vol.10, No.57, pp.1-44.

[136] Zhou, W., Apkarian, R., Wang, Z. L., & Joy, D. 2007. Fundamentals of scanning electron microscopy (SEM). *Scanning Microscopy for Nanotechnology: Techniques and Applications*, Vol.10, No.2, pp.1-40.